Influencing Parameters on Tire–Pavement Interaction Noise: Review, Experiments, and Design Considerations

Tan Li [1,2]

1   Department of Mechanical Engineering, Virginia Tech, Blacksburg, VA 24061, USA; L@vt.edu or tli@maxxis.com
2   Maxxis Technology Center, Suwanee, GA 30024, USA

Abstract: Tire–pavement interaction noise (TPIN) is dominant for passenger vehicles above 40 km/h and 70 km/h for trucks. In order to reduce TPIN, numerous investigations have been conducted to reveal the influencing parameters. In this work, the influencing parameters on TPIN were reviewed and divided into five categories: driver influence parameters, tire related parameters, tread pattern parameters, pavement related parameters, and environmental parameters. The experimental setup on analyzing and insights into optimizing those parameters are given. At the end, summary tables are presented to compare all the parameters discussed, including the pertinent frequency, potential noise influence, physical mechanism, etc. As such, this review article can also serve as a reference tool for new researchers on this topic. This work covers references from 1950s till present, aiming to distribute key knowledge in both classic and recent studies.

Keywords: tire–pavement interaction noise; influencing parameter; driving condition; tread pattern; environmental parameter

1. Introduction

Tire–Pavement Interaction Noise (TPIN) is also known as tire road interaction noise, tire–pavement noise, tire road noise, or tire noise, which is defined as the noise emitted from a rolling tire as a result of the interaction between the tire and road surface (Sandberg and Ejsmont, 2002 [1]). Its modeling (Li et al., 2018 [2]) and measurement techniques (Li, 2018 [3]) have been extensively investigated since the 1970s, with the former focusing on the theoretical part and the latter on the experimental part.

As noise from engine and wind turbulence reduces, TPIN becomes the dominant source of noise for passenger vehicles above 40 km/h and 70 km/h for trucks. TPIN might become more dominant in the electric vehicles (EV) with internal combustion engine (ICE) removed. In addition, the sound spectral shape of EV is very different from that of ICE vehicles. Usually EV shows worse sound quality especially at higher frequencies over 1000 Hz due to the electric motor generating total noise and without the sound masking of ICE at lower frequencies. The dominant frequency range of TPIN from 800 to 1200 Hz might deteriorate the sound quality of EV. On the other hand, some countries start to put forth regulations on the minimum sound generated from EV at low speed considering the safety of pedestrians. Therefore, the TPIN control or modification in the future might become an art: (1) increasing TPIN at low speed while decreasing at high speed; (2) shifting the spectral contents to lower frequencies that would be more pleasant to humans.

In order to reduce/increase or tune the TPIN (Li, 2018 [4]), its influencing parameters need to be investigated. Different parameters affect TPIN to different degrees, as shown in Table 1 (Sandberg and Ejsmont, 2002 [1]).

Table 1. Overview of parameters affecting Tire–Pavement Interaction Noise (TPIN) (summarized from Sandberg and Ejsmont, 2002 [1]).

Parameters	Potential Noise Variation [dB]	
Speed	25	
Pavement	10	
Tire	10	
Studs in Tire	8	
Load and Inflation	5	
Road Condition	5	
Temperature	4	
Wheel Torque	3	
Category	Cars	Trucks
Due to Vehicles	7	12
Due to Pavements	9	6

Generally, the types of vehicles play major roles in the tire–pavement interaction noise (TPIN), such as heavy commercial vehicle (HCV), bus, light commercial vehicle (LCV), car, auto-rickshaw (AR), and two-wheeler (2W). Overall noise level increases with increase in size of the vehicles. That is, the noise produced by heavy commercial vehicle and bus is 10 dB higher than that produced by a two-wheeler when all these vehicles were driven at 70 km/h (Syamkumar et al., 2013 [5]). There are also some vehicle construction related parameters that might influence TPIN (Sandberg and Ejsmont, 2002 [1]), such as vehicle geometry, rim effect, wheel housing and underbody screening, but these vehicular parameters are not of interest in this work. Instead, it is assumed that the tested vehicle is of the same type or at least similar.

Some other parameters, such as the geometry of the vehicle and wheel shielding, exterior absorption fender around the tire (Sorenson and Jorro, 2012 [6]) and sound absorbing body undershields (Bückers and Stöckert, 2012 [7]), might have some influence, but only marginally. Biermann and Viehofer (2012) [8] researched on development of cars specified for tire-road noise measurement to reduce vehicle noise other than TPIN and avoid variations due to vehicle. Kim (2015) [9] developed a wheel guard to reduce the high frequency (500–4000 Hz) road noise by 0.5~1 dB.

In this work, the influencing parameters are divided into five categories: driver influence parameters, tire related parameters, tread pattern parameters, pavement related parameters, and environmental parameters. Extensive experimental studies are included, which might be of interest and help to automotive/tire/pavement industries in designing their products. The pertinent frequency, relation with tire noise, potential noise contribution, measurement equipment and relevant mechanism of each parameter are listed in the summary tables at the end.

2. Driver Influence Parameters

Driver influence parameters are those that can be changed by drivers after tire/pavement combination has been determined. A lot of parameters of this type are difficult to quantify, such as steering speed. A few most important factors are discussed below.

2.1. Speed

Speed is the most important single parameter in terms of TPIN levels, so nearly all TPIN models include it (Li et al., 2016 [10]). As the vehicle speed and the number of tire revolutions per unit time increase, the speed with which the tire comes in contact with the pavement surface increases resulting in higher tire/pavement impact and also an increased pumping in and out of air from the contact edge (Syamkumar et al., 2013 [5]).

As shown in Table 1, no other single factor has such a prominent influence on TPIN as does speed. The influence of speed is large but not very interesting (Sandberg, 2001 [11]), since the speed can be

easily changed and the range is wide. The approximate relationship between TPIN and speed is shown in Equation (1) (Dare and Bernhard, 2013 [12]).

$$L_p = 10n \log_{10}(v) + b \qquad (1)$$

where L_p is sound pressure level, n is speed exponent, v is vehicle speed, and b is a speed coefficient. It is noted that different mechanism has different speed exponent, shown in Table 2. The tread/texture impact mechanism is also called shock mechanism, which is the sudden impulse contact between tire tread and pavement texture. Stick/slip describes the phenomenon that, as the rubber tread element enters the contact patch, it will be deformed and stick with the pavement due to the normal tire force, but also periodically slip once tangential force reaches the critical limit. Stick/snap mechanism occurs when tread blocks stick to the pavement due to adhesion bonding or vacuum and then are pulled away and released at the trailing edge of the contact patch. Air pumping noise occurs when the air is squeezed out or sucked in the tread grooves as the tire and pavement roll together. Air turbulence is potentially caused by the tire displacing air when it rotates and moves forward. Pipe resonance refers to the longitudinal groove channel amplifying noise at selective frequencies. Helmholtz resonance is a mass-spring vibration effect occurring when the tread lifts off the pavement, a narrow channel forms and connects to the cavity where the air is trapped and enclosed by the tread grove and the pavement. Unfortunately, the present author did not find any references with strong evidence for how the values of speed exponents given in Table 2 are derived. Possibly these are just based on experience and reasonable engineering judgement.

It might be instructive to develop a relevant method to differentiate mechanisms at different frequencies. A speed exponent of zero means the corresponding mechanisms are independent of speed, such as pipe resonance and Helmholtz resonance. However, it should be pointed out that these two mechanisms are amplification mechanisms rather than generation mechanisms, which means the corresponding amplifying factors for the two mechanisms are independent of speed. The speed exponent for each frequency ranges was reported by Beckenbauer and Kuijpers (2001) [13], as shown in Figure 1. The overall speed exponent is around 4, however, we can see a clear drop around 500–800 Hz for normal tires.

Table 2. Speed exponents for different TPIN mechanisms (modified from Kuijpers and van Blokland, 2001 [14], Figure 1).

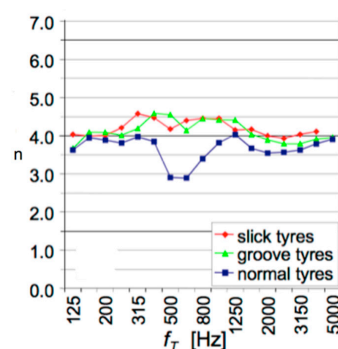| TPIN Mechanism	Speed Exponent
Tread Impact	2.0–3.0
Texture Impact	3.0–3.5
Stick/Slip (Friction)	3.0–5.0
Stick/Snap	3.0–5.0
Air Pumping	4.0–5.0
Air Turbulence	5.0–6.0
Pipe Resonance	0.0
Helmholtz Resonance	0.0

Figure 1. Speed exponent in 1/3 octave band (n is speed exponent; f_T is the center frequency of 1/3 octave band) (source from Beckenbauer and Kuijpers, 2001 [13], Figure 4; reprinted under fair use provision).

In practice, a more general and easier equation is used (Sandberg and Ejsmont, 2002 [1]).

$$L = A + B \cdot \log(V) \tag{2}$$

where L is the sound pressure level (SPL) in [dB], A and B are speed coefficients (constants), and V is speed in [km/h]. A and B vary with different measurement specifications, as shown in Table 3. However, it is shown that A and B are not independent of each other. A decreases as B increases. It should be noted that extrapolation is not recommended since tire–pavement interaction is not the main source of noise at lower speeds (Mogrovejo et al., 2013 [15]).

Table 3. Coefficients in relationship between speed and TPIN level (source from Sandberg and Ejsmont, 2002 [1], Table 9.1; reprinted with permission from Dr. Ulf Sandberg of VTI, Sweden).

Reference	Author	Year	A	B	Method	Notes
[16]	Ejsmont	1982	$=98.2 - 1.95B$	27–46	CPX and DR	Passenger car tires
[17]	Landers	1976	N/A	40	CPX	Passenger car tires
[18]	Nilsson	1976	$=77 - 1.95B$	14–32	CB	Incl. wet road
[19]	Anonymous	1971	24.1	30.5	CB	Truck, rib
			9.3	41.6		Truck, lug
[20]	Corcoran	1972	N/A	40	CB	Truck tires
[21]	Walker and Williams	1979	N/A	30–40	CB	Passenger car tires
				33		Truck tires
[22]	Tetlow	1968	N/A	36.5	CB	Truck, rib
				30		Truck, lug
				20		Wet road
[23]	Hamet	1988	N/A	26–41	CB	Car tires; power levels
[24]	Köhler and Liedl	1981	N/A	30–45	CB	Dry road
				20–40		Wet road
[25]	Steven and Pauls	1990	26.2	32.9	CPX	Porous AC 0/5
			27.3	33.5		Porous AC 0/8
			23.4	37.3		ISO-S
			24.4	36.9		SMA 0/5
			24.6	37.2		Surface dressing
			21.9	39.9		PCC
			27.9	35.5		AC 0/11
			27.1	36.7		Asphalt 0/11
[26]	Ivannikov et al.	1998	7.1	37.6	CB	Average of 10 truck tires, ISO surface
			11.8	36.3		Average of 10 truck tires, SMA surface
			10.7	36.8		Average of 10 truck tires, porous surface
[27]	Steven et al.	2000	30.6	34.9	CPX	AC 0/16 with chippings spread on surface
			33.5	33		SMA 0/4
			34.2	32.6		SMA 0/6
			30.4	34.9		SMA 0/8
			27.8	37		Surface dressing 5/8
			39.5	29.2		Porous AC 6/16
			37.1	29		Porous AC 4/8+11/16 double layer
			34.4	29.2		Porous AC 2/4+11/16 double layer
			38.9	30.9		Gussasphalt 0/11+2/5+5/8
			20.3	42		Cement concrete transversely brushed
			32.7	34.2		Cement concrete with epoxy-durop 3/4
			24.3	37.8		Cement concrete burlap drag
			27.6	36.9		Cement concrete exposed aggregate

A similar equation is often used to normalize TPIN to a specified speed,

$$L_{norm} = L_{meas} + B \cdot \log\left(\frac{V_{ref}}{V}\right) \tag{3}$$

where L_{norm} is the normalized TPIN level at reference speed V_{ref}, L_{meas} is the measured level at actual speed V, B is speed coefficient. B is taken as 35 in CPX measurements (Steven et al., 2000 [28]).

The speed has an influence on the TPIN spectrum as it affects the tire eigenfrequencies (Lopez Arteaga, 2011 [29]). There are three effects: (1) The stiffening due to the rotation leads to slightly higher eigenfrequencies; (2) the Coriolis acceleration leads to the so-called 'bifurcation' effect, where the speed

of waves propagating in opposite circumferential directions with the same wavelength are different even when observed in the Lagrangian reference system (tire-fixed) (Kim and Bolton, 2004 [30]; Huang and Soedel, 1987 [31]; Huang and Soedel, 1988 [32]); (3) the Doppler-shift, which appears when the tire is observed from an Eulerian (vehicle-fixed) reference system. Following one particular particle is the Lagrangian description and looking at a particular location in the ambient space is the Eulerian description of motion.

Schuhmacher (2015) [33] investigated the effect of vehicle speed on spectrogram of tire noise, as shown in Figure 2. It can be seen that some of the spectral content (e.g., around 400–500 Hz) does not change with speed, but some of it does indeed change with speed.
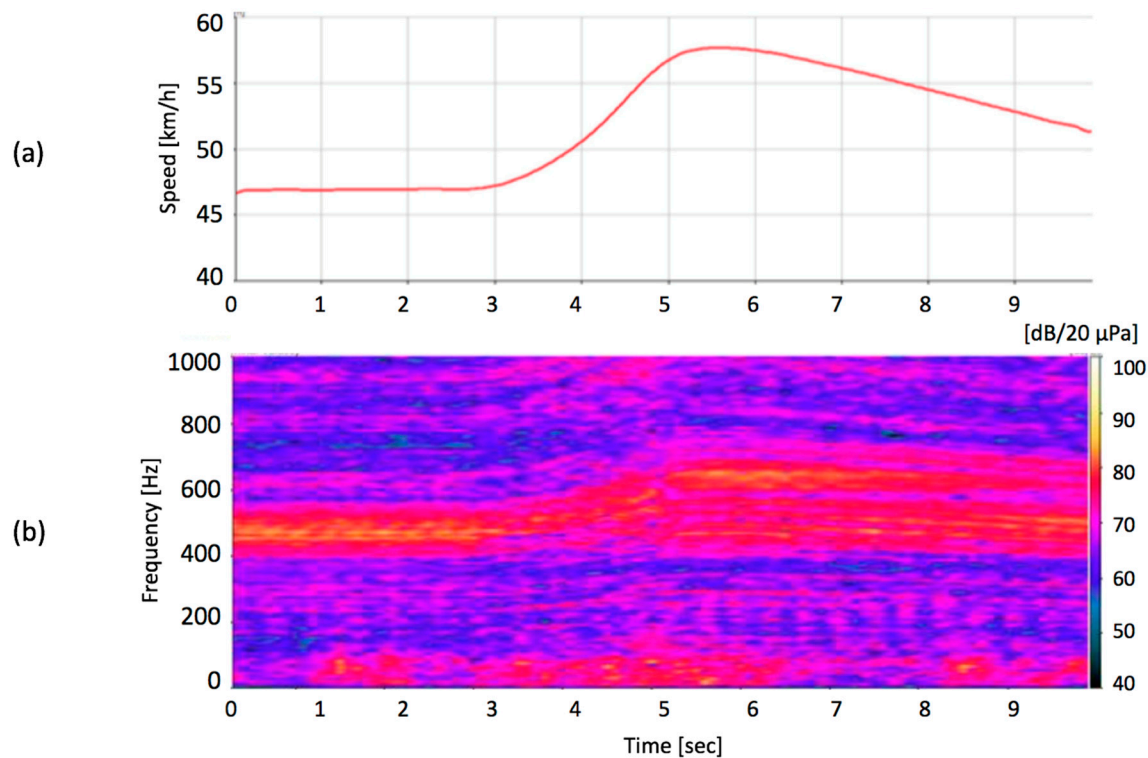
Figure 2. (**a**) Top figure is vehicle speed versus time; (**b**) bottom figure is tire noise spectrum versus time (modified from Schuhmacher, 2015 [33], Figure 12).

Ulrich (1984) [34] reported that the sound power P has the relationship with tire rolling speed V as $P \propto V^n$ where $n = 3{\sim}4$.

2.2. Longitudinal Force/Slip

During accelerating (driving condition) and decelerating (braking condition), extra longitudinal force/slip is generated leading to greater stick/slip and increasing TPIN. Driving/breaking torque and slide/skid ratio (slip ratio) are also physically equal to longitudinal force/slip.

However, the magnitude of this effect is highly dependent on the type of tires. Some tires such as high performance sporty tires are marginally affected, while TPIN levels for some tires vary by 9 dB using OBSI method (Donavan, 1993 [35]). It is found that the dominant frequency range is from 800 Hz to 1.6 kHz, which is similar to that of the vertical tire load (Iwao and Yamazaki, 1996 [36]).

The driving torque effect on TPIN is also dependent on inflation pressure. Generally, the higher the inflation is, the greater the effect will be, as shown in Figure 3.

TPIN measurement in driving conditions is standardized in ISO 362-1 (2015) [37,38].

The acceleration effect depends on the type of tires, as show in Figure 4 (Donavan et al., 1998 [39]). It can be seen the noise from Tire A is completely independent of acceleration.
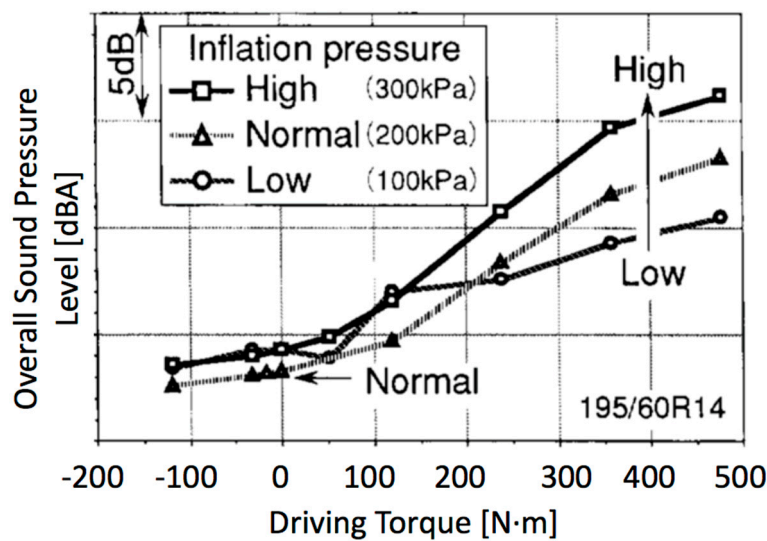
Figure 3. Changes of TPIN due to driving torque and inflation pressure (modified from Iwao and Yamazaki, 1996 [36], Figure 7).
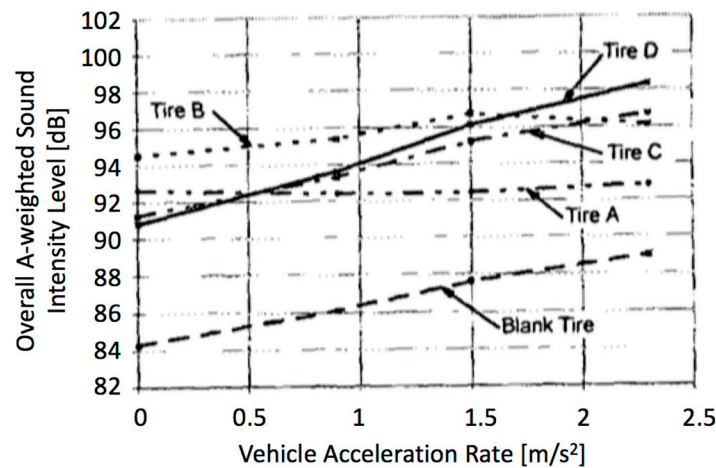

Figure 4. The effect of vehicle acceleration rate on tire noise as measured with on-board sound intensity (source from Donavan et al., 1998 [39], Figure 2; reprinted with permission from AIP Publishing LLC).

2.3. Lateral Force/Slip

In practical driving conditions, the lateral acceleration distribution is around 60% for <0.5 m/s^2, 30% for 0.5–1.5 m/s^2, and 10% for 1.5–2.5 m/s^2 (Yamazaki et al., 1989 [40]). Under the 10% of conditions (cornering speed 40–60 km/h with radius R = 100 m), the lateral force will be around 4–8 kN and the slip angle will be 1–2°. In addition, the slip angle is also caused by road crossfall and wheel alignment toe angle, but is relatively small. Commonly, 2% crossfall leads to 0.1° slip angle, and normal toe angle leads to 0–0.5° slip angle. Ejsmont (1990) [41] reported that there was a sharp increase of noise and rolling resistance with a slip angle above only 0.5°. Donavan (1982) [42] also indicated that tire noise was higher under a curved path than under a straight path.

In cornering, SPL essentially increases equally much up to 1 kHz, but creates higher increases with up to 10dB at 5–8 kHz [1], and so it was found that the non-patterned tire is most sensitive to this effect. It is interesting to compare the outside tire (increased load) and inside tire (decreased load) in terms of TPIN spectrum during cornering. It was shown that for the outside tire (increased load), the TPIN level is larger at high frequencies (>2 kHz) but smaller at low frequencies (<1 kHz) than inside tire (decreased load). The larger level at high frequencies (>2 kHz) is due to the increased stick/slip

phenomenon; while the smaller level at low frequencies (<1 kHz) is probably due to the movement difficulty of tread elements under large load.

Squeal phenomenon is often observed when cornering (Senda et al., 1984 [43]; Trivisonno et al., 1968 [44]); for example, very pronounced peaks at frequencies 1.2 kHz and 2.5 kHz were shown in a replica drum test. The squeal characteristics were independent on the tread patterns but highly dependent on the pavements.

Tread compound properties have major influence here. Stiffer rubber can reduce this cornering effect by reducing stick/slip. It also explains why tire squeal is more common in summer than in winter, which is probably because the hot weather in summer makes the tire rubber softer. However, under non-slip conditions, stiffer rubber is not preferable from the point of view of noise reduction.

It is noteworthy that it is very difficult to quantify this effect, due to the transient characteristics of cornering/steering. The tangential force generally includes longitudinal force and lateral force, which both influence TPIN at high frequencies.

2.4. Tire Load

Tire load could affect several different TPIN mechanisms. Sidewall vibrations increased with load (Reiter and Eberhardt, 1974 [45]). Tread/texture impact could be enlarged as loading changes the shape of the tire near the contact patch [5]. More deformation of air pockets in the contact patch increased air pumping (Dare, 2012 [46]). Generally, for passenger car radial tires TPIN increased by 1 to 2 dBA per doubling of wheel load when inflation pressure was adjusted to the load; by 0.7 to 1.5 dBA if inflation pressure was not adjusted (Taryma, 1982 [47]). For truck tires TPIN increased 8–15 dB per tripling of the load on each tire (Leasure and Bender, 1975 [48]). Results from other researchers are listed in Table 4 (Sandberg and Ejsmont, 2002 [1]). It was shown that tire load has a much larger influence on crossbar tires than ribbed tires.

It should be noted that heavy trucks might emit similar or even lower TPIN than some cars (Sandberg, 2001 [11]) despite that tires of trucks carry a load 5–7 times that of car tires (Sandberg, 2003 [49]). One research found heavy trucks carrying 10–20 tons gross vehicle weight (GVW) emitted lower TPIN than some high-performance cars with wide tires (Sandberg, 2001 [11]). This unexpected phenomenon might be due to the fact that the peak for truck tires is shifted to lower frequencies, which will be greatly reduced after A-weighting filtering. It may also be due to the less pronounced peak character resulting from higher belt stiffness and larger contact patch in the tire/pavement interface (Sandberg, 2003 [49]).

Tong et al. (2013) [50] concluded that TPIN increases as vertical load increases, but the variation is marginal. It was also shown that the sound pressure level tends to show a peak value at a certain value of vertical tire load (3000 N, shown in Figure 5) as the tire speed increases (Iwao and Yamazaki, 1996 [36]).
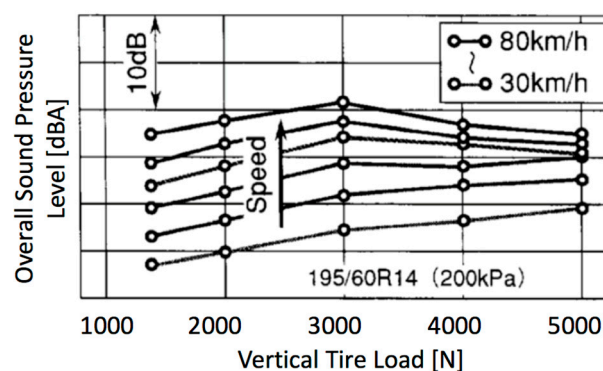

Figure 5. Changes of tire noise due to tire load and speed (modified from Iwao and Yamazaki, 1996 [36], Figure 6).

Table 4. Influence of tire load on TPIN (summarized from Sandberg and Ejsmont, 2002 [1]).

Reference	Author	Year	Results (Increase per Doubling of Load)	Tire
[19]	Anon	1971	5 dBA Some tenths of 1 dBA	Cross-ply truck tires with lugged pattern Cross-ply truck tires with rib pattern
[51]	Leasure et al.	1972	3–6 dBA 0–2.5 dBA	Cross-bar and pocket tread truck tires Ribbed truck tires
[52]	Kilmer	1976	2–3 dBA Negligible	Cross-ply truck tires with crossbar pattern Cross-ply truck tires with ribbed pattern
[53]	Kilmer	1979	5 dBA 1 dBA	Cross-ply truck tires with crossbar pattern Cross-ply truck tires with ribbed pattern
[54,55]	Underwood	1980 1984	6.5 dBA 0.5 dBA	Cross-ply truck tires with crossbar pattern Cross-ply truck tires with ribbed pattern
[56]	Walker	1981	Does not change appreciably	Cross-ply truck tires
[57]	Köllman	1993	2.4 dBA	More than 100 car tires
[58]	Wolf et al.	1992	1–1.5 dBA 5 dBA 4.4 dBA	Trucks and buses Traction truck tires Ribbed truck tires
[59]	von Meier	1992	3.8 dBA between 70% and 100% max load 1.2 dBA between 70% and 100% max load	Traction truck tires Ribbed truck tires
[1]	Sandberg and Ejsmont	2003	ISO Surface (Smooth) GRB-R Surface (Rough) Slick Tire 2.4 dBA 0.5 dBA Summer Tire 1.4 dBA −0.1 dBA Winter Tire 1.4 dBA 0.9 dBA Average 1.7 dBA 0.4 dBA	

Heckl (1986) [60] indicated that sound power increases as the 1/3 power of the tire load. Tire load can influence the size, shape and pressure distribution of contact patch. It was generally agreed that the larger the contact patch, the greater the tire noise. The vehicle load also has marginal influence on the tire acoustic cavity (Bharadwaja and Siva, 2013 [61]) and interior noise (Beniguel and Pen, 2012 [62]). Similarly, it has very small influence on the eigenfrequency (Lopez Arteaga, 2011 [29]).

Ulrich (1984) [34] reported that the sound power P has the relationship with tire static load p_L as $P \propto p_L^{1/3}$.

2.5. Inflation Pressure

Inflation pressure could affect the same mechanisms as tire load because tire deflection is dependent on both inflation pressure and tire load [46]. Increased inflation could stiffen the tire carcass and change vibration characteristics such as structural resonance frequencies. It could also influence the size and shape of contact patch, and affect air pumping by changing how the air pockets deform.

Although inflation pressure is usually included as a parameter in TPIN models (Kropp et al., 2001 [63]; Keltie, 1982 [64]), few studies have investigated its effect (Tong et al., 2013 [65]). There seems to be no clear or at least no linear dependence between inflation pressure and the vibration patterns of a tire (Bolton et al., 1998 [66]). It was reported that TPIN increased slightly with the increase of tire inflation pressure (Bremner et al., 1997 [67]). Heckl (1986) [60] indicated that the sound power increases as the square root of inflation pressure. However, Donavan (1998) [39] and Samuels (1979) [68] reported the opposite results. Muthukrishnan (1996) [69] noted that the noise levels increased with the increase of inflation pressure under lighter tire load, but the trend reversed under higher load.

Keltie (1982) [64] (for truck tires) demonstrated that acoustic power spectrum is shifted towards higher frequency as the inflation pressure increases from 60 psi to 80 psi. It was also reported that the acoustic power generated decreases significantly with the increase of inflation pressure (0.6 dB/psi) while at sufficiently high pressure (above 70 psi) the acoustic power is insensitive to further pressure increases.

Generally, inflation pressure affects TPIN and tire acoustic cavity (Bharadwaja and Siva, 2013 [61]), but the variation is marginal (Tong et al., 2013 [50]). However, with driving torque, TPIN rises with the inflation pressure (Iwao and Yamazaki, 1996 [36]), as shown in Figure 3. Increased inflation also increases the tire eigenfrequenicies (Kostial et al., 2013 [70]) and the cut-on frequencies for propagating

vibration modes (Bolton et al., 1998 [66]). However, TPIN from lug type truck tires was shown to decrease as inflation increased, especially for pressure in the range of 200–400 kPa (EPA, 1980 [71]).

Bremner et al. (1997) [67] indicated that the effect of increasing inflation pressure is to increase the tire stiffness at lower frequencies without increasing the mass, resulting in the increase of wavespeed and decrease of modal wavenumbers. Kindt et al. (2007) [72] found that as the inflation pressure increases, the vibration spectrum shows in general a higher amplitude and a positive frequency shift at the structural resonances, which is due to the tire structure stiffening (both tread band and sidewall), shown in Figure 6. The transfer of tire vibrations to the rim is also improved with the sidewall stiffening. However, the acoustic resonance frequencies are not affected, because they are dependent on the geometry of the air cavity and the velocity of sound (Kindt et al., 2006 [73]). The velocity of sound for ideal gas is determined by

$$c = \sqrt{\gamma \frac{p}{\rho}} = \sqrt{\gamma R T} \tag{4}$$

where c is speed of sound, γ is adiabatic index (1.402 for air), p is pressure, ρ is air density, R is gas constant and T is temperature (constant). As such, the velocity of sound is constant and geometry of the air cavity also doesn't change significantly with inflation pressure, so the acoustic resonance frequencies do not change much, except when the pressure change leads to the change of tire deflection on the contact patch.
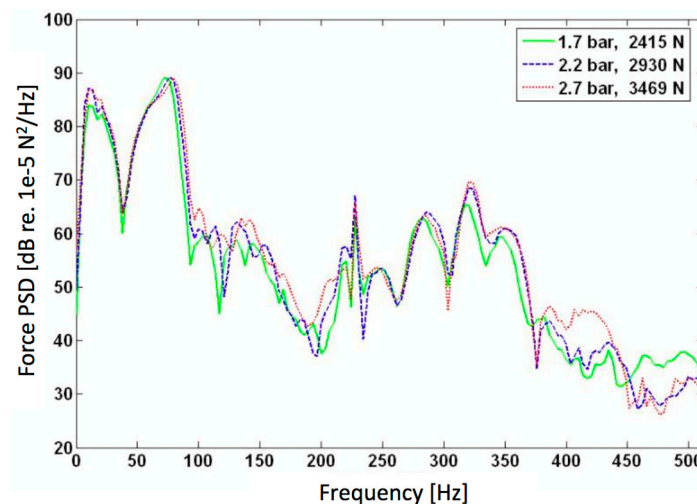

Figure 6. Vertical spindle force spectrum at different inflation pressures; driving over 5 mm high semi-circular cleat at speed of 22.6 km/h (modified from Kindt et al., 2007 [72], Figure 8).

Inflation pressure is sometimes or more often considered as a tire-related parameter. However, the present author includes it in the driver influence parameter, because the driver can easily change it.

Ulrich (1984) [34] reported that the sound power P has the relationship with tire inflation pressure p_s as $P \propto p_s^{1/2}$.

2.6. Tire Camber Angle

Camber angle is the angle between the vertical axis of the wheel and the vertical axis of the vehicle when viewed from the front or rear. It is one of the parameters indicating wheel/tire alignment (others include caster angle and toe angle). The positive camber angle is where the top of the wheel tilts outwards from the vehicle.

Camber angle was found to have larger influence on TPIN for asymmetric tire on smooth surface at negative camber angles for middle range of speeds (50–90 km/h) (Wozniak et al., 2015 [74]). TPIN increases by about 5 dB with camber angle from +3° to −6° at 90 km/h. Impact mechanism and

stick/slip mechanism were thought to contribute most to this change. Change of camber angle can change the cross-section of the tire, footprint, and load distribution. The change of footprint geometry leads to the change of channels between the tread elements, thus influences air pumping and pipe resonance mechanism. Also, at negative camber angles, two additional "horns" occur near the leading edge and trailing edge directed with their outlets outwards, which somewhat explains why negative camber angle increases TPIN.

It should be noted that the proper camber angle for testing using laboratory drum method (DR) or close-proximity trailer method (CPX) should be 0°, but no formal requirements are indicated in the standards. However, when experiments are conducted using CPX method, the camber angle is usually in the range from −1.5° to −0.5° due to a compromise between good traction performance (0°) and cornering grip (−3° to −2°), so the TPIN measurement might be influenced by this angle (Wozniak et al., 2015 [74]).

3. Tire Related Parameters

Tire properties have major influence on TPIN emission, especially for truck tires (Reinink et al., 2005 [75]). The spread between the noisiest and the quietest tire might be 10 dB, irrespective of pavement type (Sandberg and Ejsmont, 2000 [76]).

The relationships between tire parameters and TPIN from a single tire are presented in this subsection. TPIN from multiple tires (Takahashi et al., 1995 [77]; Mioduszewski, 1995 [78]) in the vehicle is not discussed here.

3.1. Tire Type/Construction

It is not easy to identify which type of tire is noisiest/quietest. One study found that on the same pavement, the maximum TPIN occurs on winter tire, followed by slick tire, and the minimum TPIN occurs on summer tire (Chang, 2012 [79]). However, another research claimed that winter tires (not studded) appear to be somewhat less "noisy" than the tires for summer use (Sandberg and Ejsmont, 2000 [76]). It might be reasonable to argue that nowadays the overall TPIN levels from summer tires and winter tires are similar (VTI, 2006 [80]). Having said that, the TPIN spectrum of these two types of tires is still different (Tanizaki et al., 2013 [81]).

The influence of tire construction on tire stiffness is limited since roughly 90% of the tire stiffness originates from the air pressure inside the tire-rim cavity (Bekke et al., 2013 [82]). A maximum influence of tire construction including changing from summer to winter compound was found to be just around 3 dBA (Seamenn, 2008 [83]). It was shown that tires with different sidewall filler height all produce similar overall sound pressure level and frequency spectra for a specific test surface (Bernhard, 2003 [84]). Whether the tire has cap ply or not doesn't influence the results either. It was also indicated that angle of cord either in the carcass or the belt does not have much influence.

For the same types of tread design and rolling speed on the same pavement, the TPIN of radial tire is lower than that of bias tire. It is often assumed the difference is about 2 dBA in favor of radial tires (Sandberg and Ejsmont, 2002 [1]). Leasure and Bender (1975) [48] indicated that radial tires are 1–3 dB quieter than bias-ply tires. A more important benefit of radial tire is 20–30% reduction of rolling resistance (Ejsmont, 1990 [41]). The difference between radial tire and bias tire is the crown angle (90° for radial tire), which is the angle between the ply cord and the circumferential tire centerline. In general, smaller crown angle leads to better cornering performance but harsher ride (El-Gindy et al., 1999 [85]). Most tires in the market right now are radial tires due to low energy dissipation (60% of that of bias tire) and long durability (twice as long as that of bias tire) (Moore, 1975 [86]).

Different tire components (including apex, bead, belt coat, belt wedge, belt wire, cap ply coat, cap ply cord, chafer, liner, ply coat, ply cord, rimstrip, sidewall, tread and undertread) have different influence on structure-borne TPIN (Aboutorabi and Kung, 2012 [87]). The stiffness and mass of tread were found to be the most importance for the tire mode frequencies and generalized mass. Ejsmont

(1990) [41] reported that the reinforcement material and tread material in radial tires do not have much influence on TPIN.

Leasure and Bender [48] (1975), and Staadt (1974) [88] indicted that truck tire noise was a major contributor to traffic noise. Fong (1998) [89] reported that the contact pressure for truck tires are usually a magnitude higher than passenger car tire due to higher tread rubber stiffness and inflation pressure. It was also indicated that truck tires radiated greater noise below 100 Hz up to 10 dBA than passenger tires, as well as above 1000 Hz, but similar noise levels between 100 to 1000 Hz.

Bremner et al. (1997) [67] reported that the increase of tire damping loss factor reduces noise above 300 Hz. Bremner et al. also indicated that the increase of tread thickness will increase its mass per unit area as well as the bending stiffness, resulting in the increase of power input from the pavement and noise radiation especially at the higher frequencies. The increase of the equivalent isotropic modulus of the rubber/fabric matrix was reported to increase noise radiation. Adding the steel belting was shown to increase the tread mass, leading to two contradictory effects, i.e., the increase of input power from impact mechanism but decrease of radiation coupling. The total effect is a small decrease in the noise radiation. Adding the radial ply stiffness with lightweight materials such as Kevlar crossply was reported to increase noise radiation.

Pei et al. (2015) [90] investigated the Influence of tread structure design parameters on tire vibration noise using boundary element method (BEM) and modal acoustic transfer vector (MATV). It was found that the contact force spectrum is flat between 0–5000 Hz. It was observed that there is no clear trend for influence of the ratio of radial contact force between belt and carcass to inflation pressure on the tire vibrations, but there seems to be an optimized point.

3.2. Tire Size

The conventional naming for tire size of passenger car tires is like 215/60R16: 215 is tire section width is mm; 60 is aspect ratio (section height divided by section width) in percentage; 16 is rim diameter in inch.

There seems to be a persistent trend for tires to be wider and wider over time, especially for sports cars (Dimitri, 2012 [91]), as is shown in Figure 7 (Sandberg and Ejsmont, 2002 [1]). Survey showed that in the last 15 years of the 20th century, the average tire width of cars on market increased from 165 to 195 mm (Sandberg and Ejsmont, 2002 [1]). However, it might not be a good practice from the perspective of noise reduction.

As the tire width increases, the tread/texture impact becomes more extensive leading to greater vibrations. Stick/slip and stick/snap phenomena are also amplified. A tire with a wider section involves greater displacement of air within the tire-road interface, amplifying both air pumping and air turbulence. In addition, horn shape and Helmholtz resonator are easier to occur with greater tire width (Kumar et al., 2011 [92]).

Generally, wider tire section generates greater TPIN (Sandberg and Ejsmont, 1998 [93]), especially in the low frequency band from 500 to 1000 Hz (Yang et al., 2013 [94]). As such, tire noise regulations usually have step limits for different range of tire width. It was found that TPIN on smooth pavement at the speed of 70 km/h increased by around 0.3–0.4 dB per 10 mm of width increase (Storeheier and Sandberg, 1990 [95]), as shown in Figure 8. The width influence may also be expressed as an increase of 4 dB per doubling of width (Sandberg and Ejsmont, 2002 [1]). Ulrich (1984) [34] reported that the sound power P has the relationship with tire width b as $P \propto b^{3/2}$.
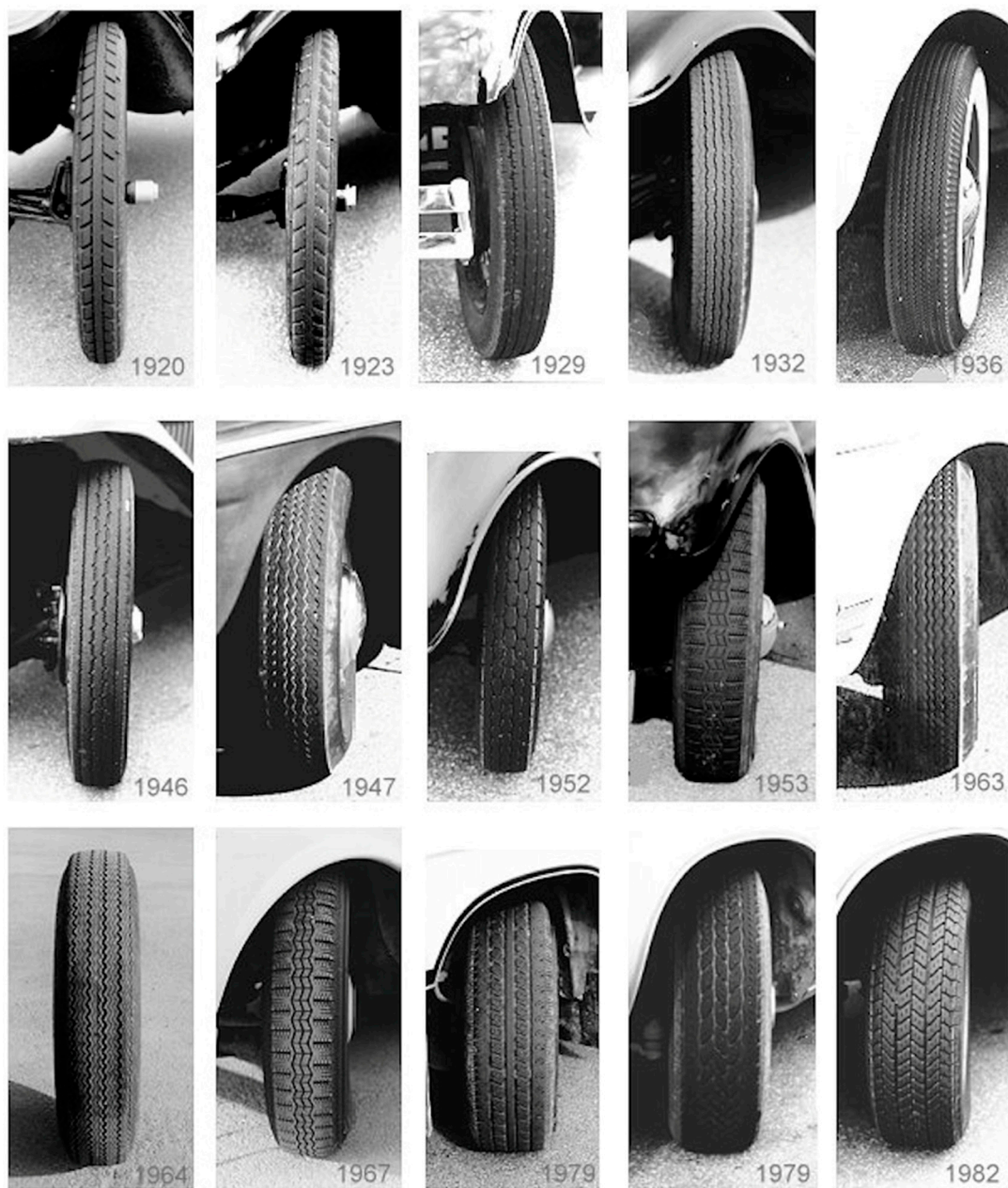
Figure 7. Common tires with year indicated (source from Sandberg and Ejsmont, 2002 [1], Figure 6.5; reprinted with permission from Dr. Ulf Sandberg of VTI, Sweden).
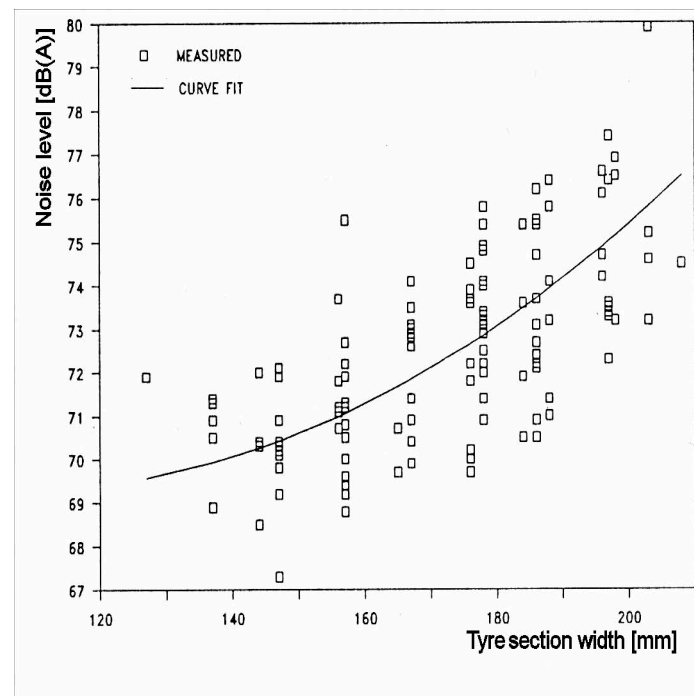
Figure 8. Relation between TPIN level and tire width (data based on measurements 1981–1987 on radial car tires in Germany, Sweden and Norway) (source from Storeheier and Sandberg, 1990 [95]; reprinted with permission from Dr. Ulf Sandberg of VTI, Sweden. Dr. Sandberg also informed that the measurements were made on tires which were modern about 30 years ago, and they were different also in other ways than width; thus, caution in interpreting the data in today's situation is advised).

However, it was found that the influence of tire width is not linear or consistent, and becomes insignificant when it exceeds 200 mm (Yang et al., 2013 [94]), which contradicts with the results shown in Figure 8. Only a weak correlation (R^2 = 0.38) was found in a set of 276 tires of different widths (Sandberg, 2001 [11]). Actually, it was shown that for the same speeds and number of tires, TPIN of truck tires is only slightly higher than that of car tires, despite the greater widths and much higher loads (Sandberg, 2001 [11]).

Tire width has a small influence on the radial natural frequency but it also depends on the tire diameter which will be discussed below (Kostial et al., 2013 [70]).

It was shown that TPIN decreases with increase in overall tire diameter (Kumar et al., 2011 [92]). As tire diameter increases, the attack angle decreases, as shown in Figure 9, leading to less pronounced and abrupt tread/texture impact. On the other hand, the decreased attack angle amplifies the horn effect. Increased tire diameter will reduce the tire cavity resonant frequency (Mohamed and Wang, 2015 [96]). Ulrich (1984) [34] reported that the sound power P has the relationship with tire radius a as $P \propto 1/a^3$. Pei et al. (2015) [90] found that the increase of the radius of the belt layer or the radius of tire tread will reduce the tire vibrations.
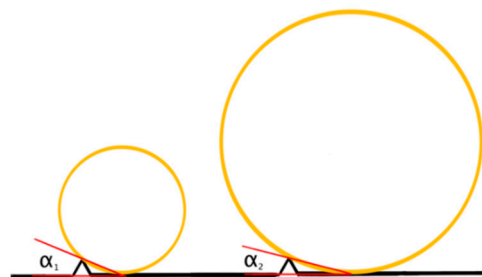

Figure 9. Attack angles of tires with different tire diameters ($\alpha_1 > \alpha_2$).

Tire aspect ratio is another important dimensional parameter, defined as the section height divided by the nominal section width multiplied by 100 (expressed as a percentage), but it is not an interesting aspect in TPIN analysis. However, it worth noting that the aspect ratio has decreased from 0.8 to 0.4 over the last three decades (Tanaka et al., 2016 [97]) in order to improve the vehicle stability at high speed.

3.3. Belt Stiffness

Belt stiffness also refers to belt bending stiffness or the stiffness of tread band (Wolfgang et al., 1998 [98]). The bending stiffness of a plate is also called flexural rigidity representing the moment per unit length per unit of curvature, given by

$$D = \frac{Eh_e^3}{12(1 - v^2)} \tag{5}$$

where D is flexural rigidity in [Pa·m^3] or [N·m], E is Young's Modulus, h_e is elastic thickness and v is Poisson's ratio (Landau and Lifshitz, 1986 [99]). The normal values of standard tires are in the order of 2–5 N·m for circumferential bending stiffness and 1–3 N·m for lateral bending stiffness. When it comes to belt stiffness, it usually refers to circumferential bending stiffness. O'Boy and Dowling, 2009 [100] reported that for the tire belt without the layer of tread rubber, the equivalent bending stiffness is 7.6 N·m with an area density of 14 kg/m^2, while for the tire belt with the layer of tread rubber, the equivalent bending stiffness is 13.6 N·m with an area density of 21.8 kg/m^2.

The radial belt bending stiffness can also be measured by the following method. The non-inflated tire tread was deflected by a spherically shaped narrow bar. The force required to produce a certain deflection of the tread area was considered the radial belt bending stiffness with the unit of kN/mm (Sandberg and Ejsmont, 2002 [1]). It generally depends on the construction of tread, such as the number of layer and materials.

It was found that the increased carcass stiffness reduces the shoulder tread vibration and the TPIN (Ejsmont, 1982 [16]; Watanabe et al., 1988 [101]). Increasing tread belt stiffness will reduce air pumping (Plotkin and Stusnick, 1981 [102]). It was also indicated that tire with a high tension at the shoulder and/or a lower belt tension at the center of the tread reduces TPIN by up to 2 dB (Doan, 1996 [103]). Bremner et al. (1997) [67] reported that increasing damping or adding steel belts would decrease tire noise. However, increasing bending stiffness of the belt will result in the increase of its mass, which is not good from the dynamics perspective (Kropp et al., 1998 [98]). Wolfgang et al., 1998 [98] indicated that the radial driving point mobility decreases with the increase of belt bending stiffness, resulting in the decrease of velocity amplitude. However, the radiated sound does not change much, because the radiation efficiency increases with the increase of belt bending stiffness. It was pointed out the to avoid this compensation, the surface density (mass per square meter of the belt) should be increased at the same time. It should be noted that large numbers of studies on such construction parameters as belt stiffness, belt angle are proprietary to tire companies and have not been published. However, it is reasonable to assume these parameters have much smaller influence on TPIN than tire dynamics.

Belt stiffness can also refer to circumferential stiffness, lateral stiffness, and torsional stiffness (Kostial et al., 2013 [70]). Generally, they all have similar effect on TPIN as radial stiffness, but to different degrees.

However, Keltie (1982) [64] demonstrated that for truck tires, the sound power is dominated by in-plane or membrane effects rather than bending effects. As such, bending stiffness has little effects on the tire noise (less than 1 dB when doubling the bending stiffness). In addition, it was also shown that as the inflation pressure increases, the effects of the bending stiffness on the radiated sound power decrease.

3.4. Damping (Loss Factor)

The damping effect is usually combined with Young's modulus *E* to form a complex Young's modulus *E* with bar above, as given by

$$\overline{E} = E(1 + j\delta_E) \tag{6}$$

where *j* is imaginary unit, δ_E is loss factor.

The damping is shown to have very small effect on the radiated sound power, indicating that the tire vibration is a forced acoustic radiation problem below acoustic coincidence (Keltie, 1982 [64]). It was reported that only the bands between 250 and 500 Hz show an appreciable (1–2 dB) decrease as the loss factor is increased from 0.7 to 1.05. The decrease for overall sound power level is only about 0.6 dB.

3.5. Non-Uniformity

Tire non-uniformity or unbalance could result in large self-generated resonant vibrations and a dramatic modulation of low frequencies below 100 Hz (Eberhardt, 1979 [104]). A study on truck tires found that the modulation frequency depended on tire rotation speed (a circumferce of 3.3 m corresponded to 3.8 Hz at 50 km/h). This increased the 200 Hz third-octave band by 15–20 dB and increased the axle vibration amplitude by 1 mm (Ivannikov et al., 1998 [26]). Another study on car tires found that then non-uniformity increased the 80 Hz third-octave band by 7 dB and increased the radial force variation from 70 N to 180 N (Ejsmont, 1982 [16]). However, due to the A-weighting on these frequencies, the overall TPIN increase was only around 1dB. While negligible for exterior noise, it causes major low frequency noise and infrasound inside vehicle, which is not neutral to human health and feeling.

3.6. Rubber Hardness

In general, rubber hardness has a positive correlation with TPIN (R^2 = 0.3) (Sandberg and Ejsmont, 2000 [76]), especially at high frequencies and on rough road surface (Sandberg and Ejsmont, 2007 [105]). If the types of pavement are categorized, the coefficient of determination is much higher with R^2 = 0.68~0.98 (Ho et al., 2013 [28]).

A cross-bar truck tire with a tread rubber hardness of 59 Shore A tested on a drum facility was shown to be 5–8 dB noisier than a tire with softer rubber (40 Shore A). However it should be noted that in practice such soft rubber as 40 Shore A (rubber hardness unit according to ISO 868 [106], also in ASTM D2240-05 (2010) [107]) is not suitable for truck tires due to the deterioration of other parameters such as wear resistance (Watanabe et al., 1998 [101]) and steering/handling performance. In general, TPIN increases by 1–2.5 dB per 10 unit increase in Shore A hardness (Sandberg and Ejsmont, 2007 [105]). Similarly, Oddershede and Kragh (2014) [108] found that noise levels using Close Proximity method (CPX) increase by approximately 0.09 dB per Shore A for SRTT (Standard Reference Test Tire) with tread hardness ranging from 62–74 Shore A, as shown in Figure 10 where it also demonstrates that rubber hardness does not significantly influence the TPIN spectral shape in that hardness range. They also found that tire rubber hardness increases with the tire age (2006–2012), called rubber hardening.

The rubber hardness influences TPIN mostly in the frequency range of 1–3 kHz (Sandberg and Ejsmont, 2002 [1]). For the aggressive tread, the influence around 2–2.5 kHz might be 10 dB. It is reasonable to speculate that increased hardness amplifies the stick/slip motions.

A study attempted to explain the hardness effect by modeling is Wullens and Kropp, 2001 [109]. The frequency range of 400–700 Hz and 1300–1400 Hz was found to match the measurements best (Wullens, 2002 [110]).
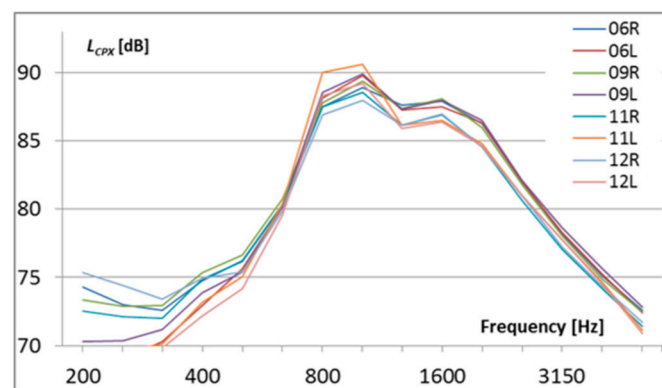
Figure 10. Frequency spectra measured at each individual tire on the ISO test track (the numbers in the legend indicate year) (source from Oddershede and Kragh, 2014 [108], Figure 6; reprinted with permission from Mr. Jens Oddershede of Vejdirektoratet, Denmark).

Parameters physically similar to tire hardness is the stiffness and storage moduli (Bekke et al., 2013 [82]). The tread compound stiffness (E' or called elastic modulus) measures how much force needed to deform the tire to a certain distance. The loss modulus (E'') measures the compound's hysteresis reducing the travelling distance of vibrational waves. Their respective ratio ($\tan\delta = E''/E'$) is often used as a design parameter in rubber compounding. It was shown that a higher $\tan\delta$ reduces the TPIN and a maximum effect is around 1.5 dB(A). It means a smaller elastic modulus and a higher loss modulus are in favor of noise reduction. However, the loss modulus should not be too large, because higher hysteresis often increases rolling resistance (Saemann, 2008 [111]).

Compared to sidewall modulus, Muthukrishnan (1996) [69] concluded that tread modulus has a much larger influence on TPIN but they have to be taken into consideration together. Other properties of tread material also have influence on TPIN but the effect is complicated. It was shown high-hysteresis rubber (Ishige et al., 2008 [112]) increased TPIN on rough pavements but decreased TPIN on smooth pavement (Underwood and Nelson, 1984 [55]) (the present author questions this remark). Bremner et al. (1997) [67] reported that increasing tread thickness (tread depth) and rubber stiffness would increase noise.

Rochoux and Biesse (2010) [113] found that soft rubber has better noise performance at high frequencies, which leads to a paradox: it should give higher air compression because of its higher deformation, since at high texture frequencies, a deeper road cavity is better because it results in better air drainage which reduces air compression, thus cavity air pumping noise, as illustrated in Figure 11. This might suggest that the air pumping mechanism is insignificant for the tire tested. Rochoux and Biesse (2010) [113] also observed that the decrease of rubber viscosity (hysteretic behavior) will increase the vibrations from texture impact on the tire rubber, especially at the contact center and the trailing edge.

Swieczko-Zurek et al. (2015) [114] showed 0.15 dB/Shore A for SRTT and 0.19 dB/Shore A for Avon AV4 tires on ISO road surface while Buehlmann et al. (2013) [115] showed up to 0.3 dB/Shore A.

Schubert et al. (2016) [116] reported that the values are in the range from -0.03 to 0.14 dB/Shore A depending on the tire and pavement, indicating Shore hardness of the tires is not able to sufficiently describe the acoustically relevant properties of tires. Therefore, the mechanical admittance (mobility) or its inverse (i.e., mechanical impedance) is used instead since it is a direct descriptor for the vibrational behavior of the tire. The study was conducted on 11 CPX tires (six Uniroyal SRTT tires and five Avon AV4 tires) manufactured between 14th week in 2014 and 42th week of 2006.
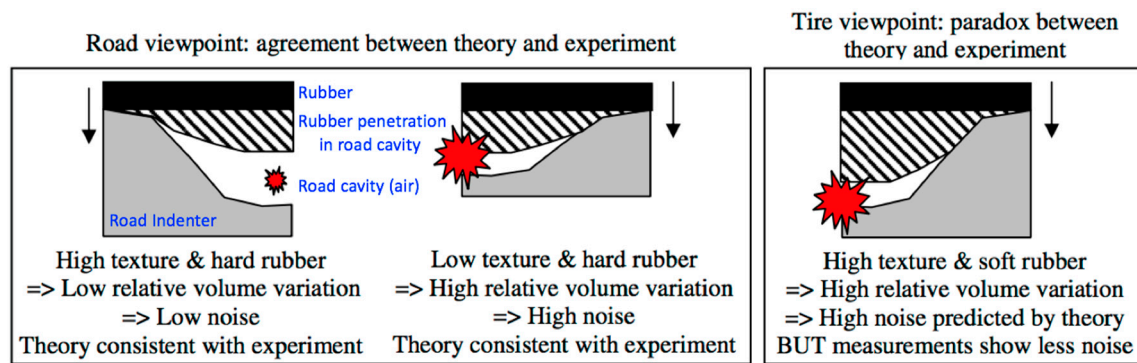
Figure 11. Commonly proposed air pumping mechanism: disagreement with measurements from the tire's point of view (modified from Rochoux and Biesse, 2010 [113], Figure 1; reprinted under fair use provision).

The tires inflated at 200 kPa were mounted on rims suspended by a hub without any load, so the vibrations could propagate unaffected. The shaker was preloaded at 2 kg against the center of the tread. The excitation signal was a band-limited white noise (15 Hz to 4 kHz). The exemplary results of the tire mobility measurements are shown in Figure 12.
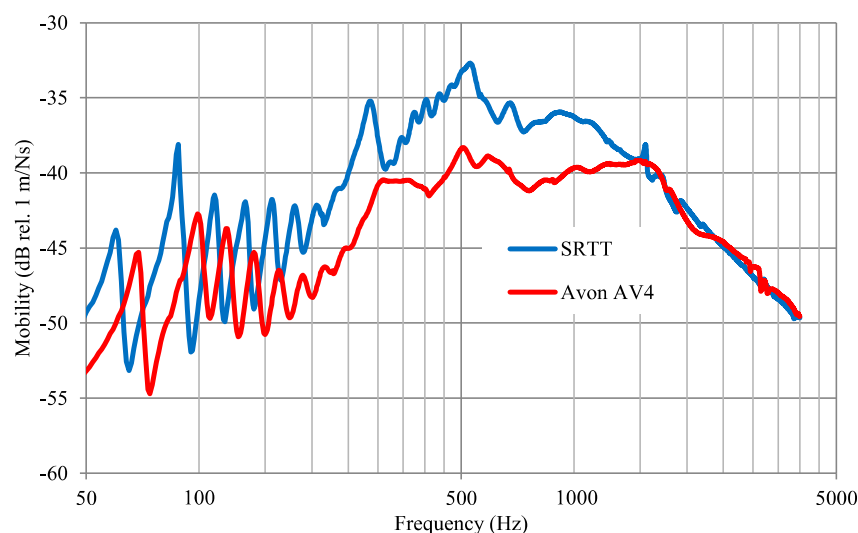
Figure 12. Example for mobility measurements results (source from Schubert et al., 2016 [116], Figure 5; reprinted with permission from Mr. Manuel Männel of Müller-BBM GmbH, Germany).

As shown in Figure 13, aging (or hardening) generally causes a decrease of the tire mobility and a slightly increase of the mode frequencies, based on which Schubert et al. (2016) [116] suggested an adjustment of the Young's modulus of the tread layer (−20% for a younger tire and +50% for an older tire), and of the stiffness of the additional contact springs (−5% for a younger tire, +10% for an older tire).

The tire degradations include mechanical wear and chemical ageing. Langwieder et al. (2001) [117] reported that 2–5% of tires in actual use had a tread depth of less than the legal minimum 1.6 mm and that 1–4% of the tires were "over-aged". The age effect is the effect which occurs when a tire is stored in a way in which its tread rubber compound undergoes changes due to exposure to moderate or high temperatures, or to certain substances and gasses in the air, for example, oxygen diffusing through the tire composite and reacting with the internal components (Sandberg and Ejsmont, 2007 [105]). Gothié (2001) [118] reported that the ageing effect is around 1 Shore A/year; however, larger the first years and lower in later years. Even though the tire is stored in a professional way (dark and in a relatively

cool place), the ageing effect still exists. However, a temperature of −10 °C is able to suppress the aging effect well (Gothié, 2005 [119]).
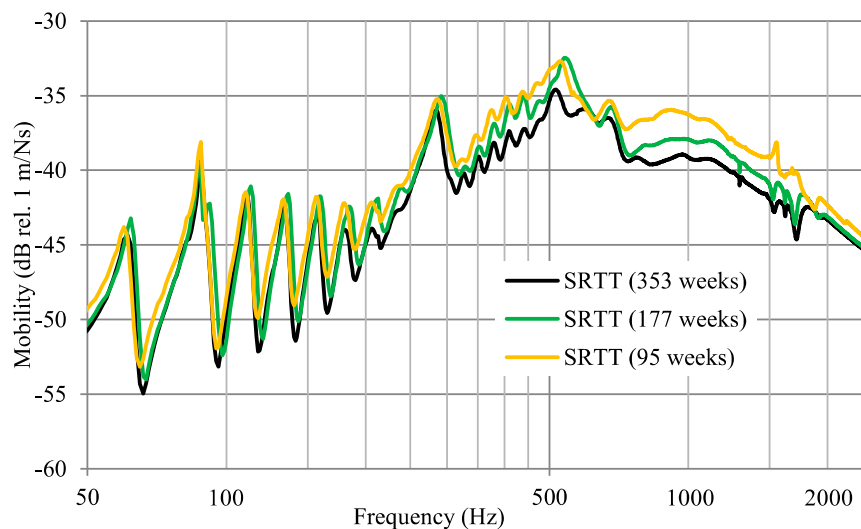

Figure 13. Comparison of measured mobility spectra for SRTT tires of different age (source from Schubert et al., 2016 [116], Figure 8; reprinted with permission from Mr. Manuel Männel of Müller-BBM GmbH, Germany).

Sandberg and Ejsmont (2007) [105] reported that the rubber hardness of individual tires may increase by up to 15 Shore A in its lifetime, which is an equally large range as new tires may differ in hardness due to construction and material design differences. The summer tires seem to age approximately as winter tires do, but they take longer time to do so, given the same high temperature exposure, which is logical since summer tires are optimized for higher temperatures. The hardness increase usually results in a noise emission increase, mainly at high frequencies; often as high as 0.2–0.25 dB(A)/Shore A in overall noise level (Li et al., 2017 [120]). Hardness is one of the most influential parameters in low-noise tires design. It was also noted that tire noise is generally more closely related to hardness for rough than for very smooth road surfaces.

However, Sandberg and Ejsmont (2002) [1] reported that when running tires with substantial side forces, a totally contrary effect of tread rubber hardness occurred, namely that the softer tread gave higher noise levels above 1 kHz.

3.7. Wear/Aging

Tire wear and aging can be affected by tire storage, tire mounting and vehicle maintenance (ETRTO, 2002 [121]). Thiriez and Subramanian (2001) [122] reported that nine percent of vehicles had at least one tire that was bald (tread depth of 2/32^{nds} of an inch or less).

Tire wear might be the most important single tire-related parameter in terms of TPIN (Tong et al., 2013 [50]). Leasure and Bender (1975) [48] reported that tire noise often increases then decreases with wear due to initial flattening of tire curvature and edges, then tread depth reduction.

When a tire in operation or in storage ages due to oxidization, the rubber hardness both in the tread and the sidewall increases. The aging effect is around 6 Shore A per year (Ho et al., 2013 [28]). The TPIN level increases by 0.08–0.48 dB(A) per shore A value increase, depending on the pavement. Thus, TPIN increases by 0.5–2.5 dB(A) per year due to this effect.

Tire wear/aging not only leads to hardness increase, but also results in cracks in the rubber due to cyclic deflection and kneading, which will affect the carcass vibrational characteristics. In addition, most importantly, there is a loss of tread rubber, leading to a thinner tread and smaller tread depth. As a result, the wear influence on TPIN is very complicated. Generally, TPIN increases with tire wear then decreases, which means the peak occurs when the tire is half worn for both truck tires

(Walker and Major, 1974 [123]; Walker, 1975 [124]; Flanagan, 1972 [125]) and car tires (Hillquist and Carpenter, 1973 [126]). It was suggested that changes to tread curvature (crown radius) due to tire wear might explain the TPIN increase (Tetlow, 1971 [127]). It was also found that this effect is more pronounced on smooth pavement than rough pavement (Underwood and Nelson, 1984 [112]). The latter decreased TPIN for further wear might be due to the thinner and smoother tread, especially on smooth surface. However, this effect was not easy to be observed on rough pavement, probably because the thinner rubber layer reduced dynamic stiffness and made the tread band vibrate more easily due to the tread/texture impact (Iwao and Yamazaki, 1996 [36]).

In practice, the wear is seldom even around the tire resulting in tire unbalance, which will cause the problems discussed in the Section 3.5 Non-uniformity. The Archard wear theory (Archard, 1953 [128]) could be used to model and calculate the sliding/adhesive tire wear (Tong et al., 2013 [65]; Tong et al., 2014 [129]). The fundamental equation is as follows.

$$V = K \frac{F_N}{H} L \tag{7}$$

where V is the total volume of wear amount, K is the wear coefficient, F_N is the normal load of contact pair, H is the hardness of the softer material in the contact pair, L is the slip distance. The ratio of wear volume $\dot{h}$ for a tire (Tong et al., 2013 [65]) is

$$\dot{h} = \frac{\frac{K}{H} \sum\limits_{i=1}^{N} P_i \gamma_i T_i}{\sum\limits_{i=1}^{N} A_i} \tag{8}$$

where subscript i is the node index, P_i is normal contact pressure at node i, γ_i is the slip ratio, T_i is the width of contact node, A_i is the contact area near node i.

3.8. Retreaded

Retreading is the process of replacing the worn-out tread with a new one. The same carcass might be retreaded several times because the life span of tire carcass largely exceeds the tread. Roughly half of the truck tires in Europe are retreaded (FEHRL, 2001 [130]). High quality retreading meets certain national criteria (such as tire balance and randomized pattern), which guarantees no compromise for safety. However, there exists a prejudice regarding retreaded tires, that they are noisier than the corresponding brand-new tires.

A study on 20 truck tires using CPX method revealed that retreaded tires were equally quiet or noisy as "ordinary" new tires (Sandberg, 1991 [131]). The TPIN level differences were within ±1 dB. It was also shown that retreaded tires were less noisy than new tires on the rough pavement but noisier on the smooth pavement. It is probably because the retreaded patterns are often more aggressive and the rubber is softer. Another study on 11 retreaded car tires through the Trailer Coast-By (TCB) method, also showed the same results (Köllman, 1993 [57]).

3.9. Studded

Many winter tires (snow tire) are fitted with studs (steel or aluminum pins) into the tread to enhance traction performance. However, this generally makes studded tire the noisiest tire. It is very easy to identify studded tires based on the tire noise characteristics (higher levels and more annoying than non-studded winter tires and summer tires). At low speed, the sound is a clatter originating from the metal pin impacting the pavement; at higher speed (above 50 km/h), the individual impacting sound turns into a high frequency hissing sound (Sandberg and Ejsmont, 2002 [1]).

TPIN above 5000 Hz largely increased, probably due to the impact and the associated scratching (when tangential movement occurs) of the pin on the pavement. Studs also produce more noise in the

middle frequency range of 400–3000 Hz, which is likely to be caused by the rubber being pressed-in by the studs, thus causing the tire vibrations (Sandberg and Ejsmont, 2002 [1]). Sandberg and Ejsmont (2000) [76] indicated that on average the studded winter tires are about 2 dBA louder than summer tires and about 3 dBA louder than the non-studded winter tires. The studded tire is limited in Japan and Norway, but mostly due to dust generation and pavement damage rather than noise issues (Sandberg, 2001 [132]).

Johnsson and Nykänen (2013) [133] developed a model to predict/auralize the tire stud noise in the vehicle compartment based on the stud pattern and stud/tire response at any desired speed. A typical stud pattern is illustrated in Figure 14 (Johnsson and Nykänen, 2013 [133]). It was also indicated that even though annoyance (human perception) has strong correlation ($R^2 = 0.81$) with loudness (analytical quantity), listening test is still preferred to evaluate the stud effects.
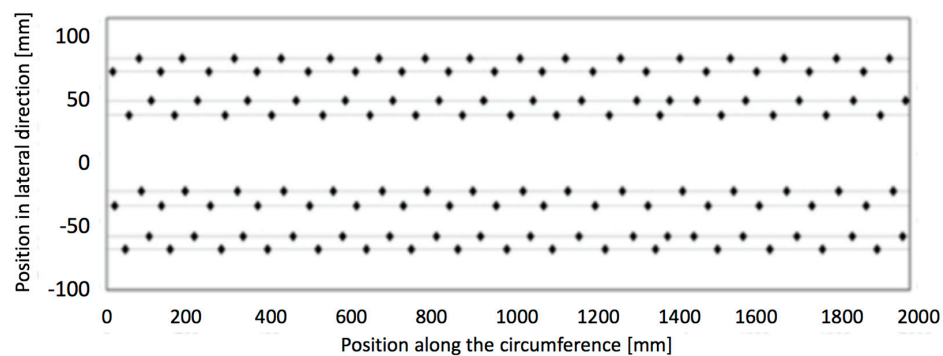
Figure 14. A typical stud pattern (8 stud lines with 16 stud on each line, 128 studs in total) (modified from Johnsson and Nykänen, 2013 [133], Figure 3).

3.10. Tread Porosity

Just as porous pavement as a quiet pavement, porous rubber has been used as one of the changes in prototype quiet tires (Nilsson, 1982 [134]). Rubber granules bound with polyurethane are used in the tread to create a porous structure with interconnecting air voids (Sandberg et al., 2005 [135]). This will mitigate air pumping and the horn effect by sound absorption.

Swedish research found that porous rubber tires reduce TPIN by about 7 dBA on rough pavements. On smoother pavements, this reduction is a bit lower. Besides, rolling resistance was not compromised by the porous rubber, but wet friction performance was poorer (Sandberg et al., 2005 [135]).

3.11. Tire Cavity Content

As discussed above, multiple attempts have been successful to mitigate the cavity acoustic resonance by filling the tire with extra materials. For example, filling the test tire with soft dense rubber reduces TPIN by some 8 dB over a frequency range from about 400 to about 1100 Hz (Pottinger et al., 1986 [136]). Results from foam-filled cavities are similar. However, even though vibration amplitudes were reduced, TPIN did not seem to be reduced.

Another method is to fill the cavity with other gases than air such as nitrogen or helium (Wang et al., 2014 [137]). It did shift the resonant frequency a bit, it was shown that acoustic resonances do not affect vibration and the cavity content changes do not affect TPIN very much (Bolton et al., 1998 [66]).

It should be pointed out that changing tire cavity content is definitely not common practice due to cost and durability issues.

3.12. Rolling Resistance

TPIN and tire rolling resistance (corresponding to fuel consumption and exhaust emission) are two of the most important environmental problems in beginning the 21st century (Ejsmont et al., 2012 [138]).

Results from many studies indicated that there is only weak positive correlation ($R^2 = 0.08$ [76]) between TPIN and tire rolling resistance (Sandberg and Ejsmont, 2000 [76]; Ejsmont et al., 2012 [138]; Stenschke and Vietzke, 2000 [139]; Hoever and Kropp, 2012 [140]). It means it is possible to reduce TPIN and rolling resistance at the same time without compromising each other, as shown in Table 5.

Table 5. General influences of different parameters on TPIN and tire rolling resistance (modified from Ejsmont et al., 2012 [138], Table 1) (↑ denotes large increase; ↗ denotes small increase; • denotes no influence; ↘ denotes small decrease; ↓ denotes large decrease).

	Relation with TPIN (↑↗•↘↓)	Relation with Rolling Resistance (↑↗•↘↓)
Speed	↑	↗
Tire Load	↗	↑
Inflation Pressure	•	↓
Rubber Hardness	↗	↘
Wear/Aging	↗	↘
Studded	↑	↗
Surface Rating (IRI)	•	↗
Porosity	↓	•
Stiffness (Impedance)	↗	N/A
MTD/MPD/Texture	↑	↗
Wetness	↑	↑

The method for measuring rolling resistance is standardized in ISO 18164 (2015) [141] combining three individual standards ISO 8767 (1992) [142], ISO 9948 (1992) [143], and ISO 13327 (1998) [144].

3.13. Reference Tire

A form of reference tires are desired in many studies, such as comparing performances of different vehicles and/or pavements, constructing reference pavement [145]. A reference tire should have well documented specifications, be commercially available over time and represent common tires in market. A previous reference tire was Goodyear Aquatred III (Rasmussen, 2009 [146]). Currently, the P225/60R16 97S Radial Standard Reference Test Tire (SRTT) is the commonly accepted referenced tire described in ASTM F2493 (2014) [147]. Besides noise tests, the SRTT is also used as a reference tire for braking and wear performance. The sole source of supply of SRTT known to the author at this time is Michelin Passenger and Light Truck Tire Manufacturing (P225/60R16 97S SRTT Uniroyal Tiger Paw AWP) (2014) [147]. The tread pattern is shown in Figure 15. The previous SRTT in 1990s' used to be Uniroyal Tiger Paw XTM P195/75R14 (Ruhala, 1999 [148]), with footprint illustrated in Figure 16. It had 56 circumferential tread elements with 9 varied sizes as shown in Table 6. The sequence of the 56 tread elements is below starting from left to right, top to bottom. This means the full tread is assembled by the 56 tread elements covering 9 different element lengths.

1, 2, 4, 6, 8, 8, 6, 4,
2, 2, 4, 6, 6, 4, 2, 1,
2, 4, 6, 8, 9, 8, 6, 4,
4, 6, 6, 4, 3, 5, 7, 5,
3, 5, 7, 9, 9, 7, 5, 3,
1, 1, 3, 5, 7, 5, 3, 1,
3, 5, 7, 9, 7, 5, 3, 1.

Even though the reference tire has strict specifications, there still exist variations from test to test (Donavan and Lodico, 2013 [149]). The variation for a single new SRTT tested on the same pavement for multiple times might be 0.7 dB. The variation for multiple new SRTT's tested on the same pavement for multiple times is 1.1 dB on average. Another issue is the variation in TPIN for one tire over time, i.e., wear/aging. TPIN of the older tires was shown to be 0.5 dB higher than the new tires when averaged for all pavements. As a result, a strategy for deciding when test tires should be retired is needed based on the rubber hardness, reduced tread depth, accumulated mileage, and in-service years (Donavan and Lodico, 2013 [149]).

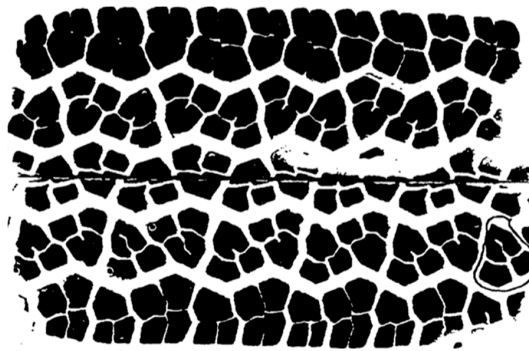**Figure 15.** Tread pattern of SRTT (tread surface is white painted).

Figure 16. Footprint of old Uniroyal SRTT (4410 N in load, 19 cm in length, 13 cm in width) (source from Ruhala, 1999 [148], Figure 5.2; reprinted with permission from Dr. Richard J. Ruhala of Kennesaw State University).

Table 6. Tread element number and length for old SRTT (modified from Ruhala, 1999 [148]).

Element Number	Element Length [inch]
1	1.152
2	1.224
3	1.297
4	1.368
5	1.439
6	1.513
7	1.584
8	1.655
9	1.727

4. Tread Pattern Parameters

Tread pattern is considered to be the most important tire parameter that influences TPIN, and it is also the one that is easiest to modify. Pope and Reynolds (1976) [150] have correlated the tread pattern with tire noise below 1 kHz; Li et al. (2016, 2017) [151,152] correlated the tread pattern spectrum with the tread pattern noise spectrum.

It is believed among general public that TPIN comes mainly from the effect of tread pattern impact on the pavement (Cao et al., 2008 [153]) and the non-patterned tire is the quietest tire. However, this is not the case. In fact, non-patterned tire might be the noisiest tire if tested on the rough pavement (FEHRL, 2001 [130]). Fong (1998) [89] found that the sound levels from smooth tires (P175/70R13) were slightly greater than the patterned tire over all the chipseal pavements. Generally, for the same tire construction and rolling speed, the lowest TPIN is produced by a rib tread design (FEHRL, 2001 [130]). Having said that, tread pattern is an important factor that is easy to modify for TPIN reduction. It affects nearly all mechanisms, especially on smooth pavement (Sandberg and Ejsmont, 2002 [1]). In addition, it was found that the noise spectra from slick tire and standard patterned tire were different, especially around 1000 Hz, as shown in Figures 17 and 18 (Alt et al., 2006, [154]).
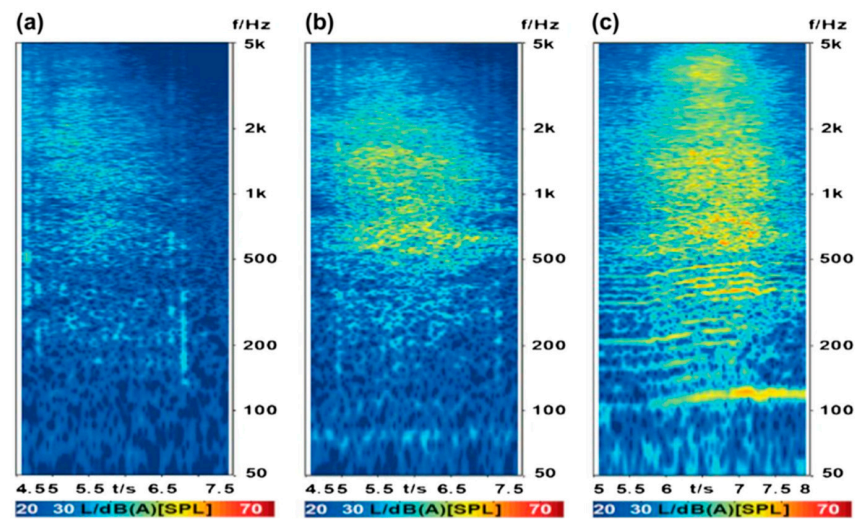
Figure 17. Colourmap plots of different pass-by noise tests: (**a**) engine switched off and slick tires; (**b**) engine switched off with standard tires; (**c**) ISO 362 acceleration test (source from Braun et al., 2013 [155], Figure 7; original from Alt et al., 2006, [154]; reprinted with permission from Elsevier).
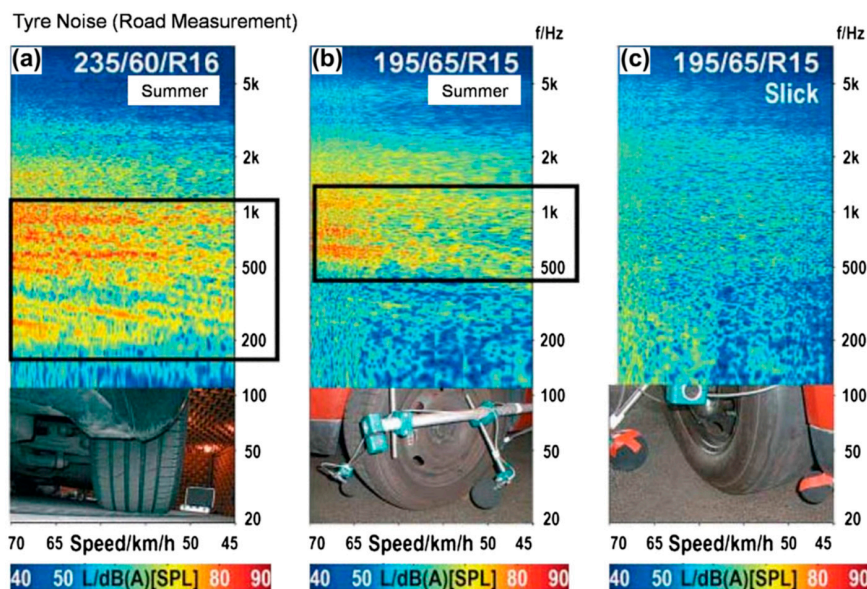

Figure 18. Waterfall plots of tire/road noise measured on the road with three different tire types: (**a**) wide summer tire; (**b**) regular summer tire; (**c**) slick tire (source from Braun et al., 2013 [155], Figure 20; original from Alt et al., 2006, [154]; reprinted with permission from Elsevier).

There are approximately 16,000 different tire tread patterns used on tires (Hanson et al., 2004 [156]). It is not an easy task to parameterize the tread pattern. A lot of parameters are just qualitative, as shown in Table 7 (Sandberg and Ejsmont, 2002 [1]), making the results questionable in some sense. An alternative and smart method to parameterize 2D tread pattern is through image processing (Che et al., 2012 [157]). The drawback of 2D tread pattern is the loss of tread/groove depth information. Ge et al. (2004) [158] found that sound pressure level increased by 10 dBA as the groove depth increased from 0 to 12 mm for a single groove tire. As such, the 3D tread profile is an alternative, and often applied with 3D laser scanner (CTWIST).

The tread patterns under investigation were usually hand-cut from slick tires, so it might not represent the industrious tires on the market, for example unwanted reduction of dynamic stiffness of the tread might occur (Iwao and Yamazaki, 1996 [36]).

Tire tread pattern design is a compromise between traction, handling, ride, noise, safety and tire longevity (Hanson et al., 2004 [156]). Example of a tread design with low noise characteristics is shown in Figure 19 (Saemann, 2005 [159]). Xie (2003) [160] presented a method to design a tread unit that may be repeated in succession about the circumference of a tire to produce an acoustically acceptable tread pattern, mainly focusing on impact mechanism.

Table 7. General influence of tread pattern on TPIN (source from Sandberg and Ejsmont, 2002 [1], Table 10.3; reprinted with permission from Dr. Ulf Sandberg of VTI, Sweden) (↑ denotes increase; • denotes no influence; ↓ denotes decrease).
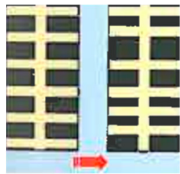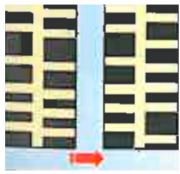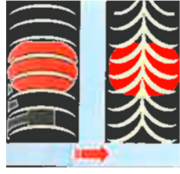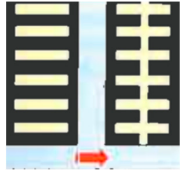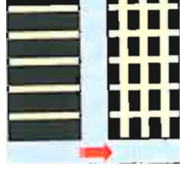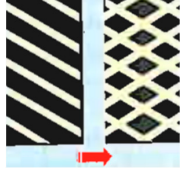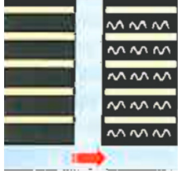
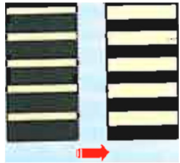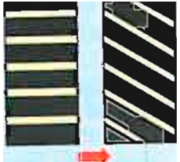|	Changes in Tread Pattern	A-Weighted SPL	Low to Mid Frequency (Tread Impact)	Mid to High Frequency (Air Resonance)	Highest Frequency (4–16 kHz)
Randomization	Tread randomization	↓	↓	•	•
	Introduction of an "offset" between left and right side of the tread or introduction of asynchronous randomization	↓	↓	↓	•
	Elimination of grooves that coincide with the contour of the tire footprint	↓	↓	•	•
Ventilation	Ventilation of air pockets	↓	•	↓	↓
	Addition of circumferential grooves to a transverse groove pattern	↓	•	↓	↓
	Addition of "mirror Image" grooves	•	•	•	↓
	Addition of lamellae	↓•	↓	•	•

Table 7. *Cont.*

Changes in Tread Pattern		A-Weighted SPL	Low to Mid Frequency (Tread Impact)	Mid to High Frequency (Air Resonance)	Highest Frequency (4–16 kHz)
	Increasedo of groove width 2 → 9 mm 9 → 12 mm	↑ ↓	↑ ↓	↑ •	↓ ↓
Tread Segment	Increase of groove angle (relative to lateral axis) ([161,162]) 0 → 20° 20 → 90°	↓ •	↓ ↓	↓ •	• •

Figure 19. Example of a tread design with low TPIN characteristics (modified from Saemann, 2005 [159]; reprinted under fair use provision).

A study applied weighting functions to the grooves and blocks in the contact patch using particle swarm algorithm to correlate tread patterns with TPIN, where the average errors were found to be within 2.5 dB (Chiu and Tu, 2015 [163]).

In addition, tread pattern design is a compromise between several tire performance requirements, as shown in Table 8 (Liljegren, 2008 [164]). Tread pattern design is not only a science but also a creative art (Williams, 1995 [165]).

Table 8. Tread pattern design requirements (modified from Liljegren, 2008 [164], Figure 46) (↑ denotes positive influence; • denotes no influence; ↓ denotes negative influence).

	Dry Handling	Dry Braking	Track Performance	Noise and Comfort	Wet Performance	Regular Wear	Rolling Resistance	Mileage
Priority (A is highest)	A	A	A	B	B	B	C	C
Large Shoulder Groove Angle	↓	↓	↑	↑	↑	•	↑	•
Large Number of Sipes	↓	↓	↑	↑	•	↓	↓	↓
Large Shifts	•	•	↑	↑	•	↑	↑	•
Randomization	•	•	•	↑	•	↓	•	↓
Wide Blocks	↑	↑	↑	↑	↓	•	↓	↓
Large Part Horizontal Void	↑	↑	↓	↓	↓	•	↓	↓

4.1. Randomization

The randomization process is also called "pitch sequencing" (Bandel et al., 1994 [166]; Williams, 1995 [165]). Tread pattern is comprised of sequence of tread segments (or elements) around the tire circumference. That is to say, usually the tread pattern is randomized, but not completely; the tread pattern segments follow a specific sequence with limited number of elements (3~9).

The tread segment is a combination of the block/lug and the groove/sipe in between. Before 1960's, the tread segments were identical with constant pitch. This resulted in a very objectionable tonal noise. One of the solutions is to vary the segment pitches (patented Michelin in 1929). Usually the segments are stretched or compressed circumferentially to form two to four different lengths. The next step is to spread different pitches around the tire, which is called tread randomization. This process was done manually in earlier years then taken over by computer programs. The latter have been doing a better job. Purely random spacing (within given limits) seems to be not as good as the optimized spacing (found by trial and error) on good commercial tires (Heckl, 1986 [60]). It should be noted that randomization often does not reduce overall TPIN levels, but it distributes the spectrum energy to a larger range and makes the sound more pleasant (ISO, 2007 [167]), or pushes the spectral contents to higher frequencies to avoid the coincidence with vehicle resonant frequencies. For a car with speed of 56 km/h, the sound corresponding to the first-order component (excites the side wall having low dynamic stiffness) of the pattern with a central frequency of 500 Hz is dispersed into the frequency range from 400 Hz to 600 Hz, and the sound corresponding to the second-order component (excites the tread surface) of the pattern with a central frequency of 1000 Hz is dispersed into the frequency range from 800 Hz to 1.2 kHz (Iwao and Yamazaki, 1996 [36]).

The different layouts of tire segments and principles of randomization are shown in Table 9 (Sandberg and Ejsmont, 2002 [1]).

An optimized randomization (such as asynchronous randomization in Table 9) can also be favorable to the uniform distribution of mass and hardness around the tire. A smooth rib or groove is often placed in the central part to avoid segment conflicts between two sides of the tire tread.

Tread randomization might often increase the cost of tire molds, especially more different pitches, or continuous variation of pitch and changing pattern along the circumference are needed.

Another practice to reduce structure-borne TPIN is to avoid abrupt and coherent tread impact over a large part of the tire width (Sandberg and Ejsmont, 2002 [1]). It means the shape of tread pattern should not coincide with the contour of contact patch, which is to say the contour of the tread elements should be longitudinal at the center area but transversal near the shoulder.

Specific pitch sequences were usually proprietary of tire companies and not released to public. Many of those were patented, the earliest one of which dates back to 1935 (Ewart, 1935 [168]). Varterasian (1969) [169] developed a mathematical method based on mechanical frequency modulation to optimize the tread spacings.

Pitch sequencing has been investigated to reduce tire noise since the 1930s. All tire tread element pitch sequences can be defined with five basic parameters: (1) total number of pitches which roughly determines the average pitch size; (2) actual pitch arrangement usually determined by a computer program that uses mathematical algorithms to determine the best possible order; (3) number of different pitch sizes determining the complexity of a pitch sequence; (4) ratio for each pitch size with the largest pitch divided by the smallest pitch usually ranging from 1.4 to 1.6; (5) total pitches of each size (Williams, 1995 [165]). Table 10 shows the progression of pitch sequencing techniques in historical perspective.

Table 9. Different layouts of tire segments and principles of randomization (source from Sandberg and Ejsmont, 2002 [1], Table 10.2; reprinted with permission from Dr. Ulf Sandberg of VTI, Sweden).

Category	Type	Meaning	Illustration
Randomization	Constant Pitch	All segments are of the same length (no randomization)	
	Synchronous	Segments differ in length, but the order of their placement is the same on the left and right side	
	Asynchronous	Segment differ in length and their order is different on left and right side of the tire	
Symmetry	Symmetric	Segments on the left side of the tire are identical to segments on the right side (but there is an offset in this case)	
	Asymmetric	Segments on the left side have different pattern in relation to right side	
Directivity	Bi-directional	Segments on the left side of the tire are rotated 180° in relation to segments on the right side	
	Directional	Segments on the right side are mirror images of the segments on the left side. Other special properties possible, for example tilted lamellae.	

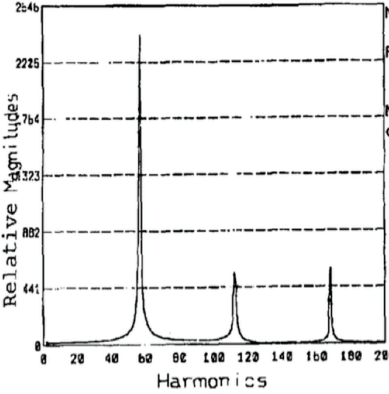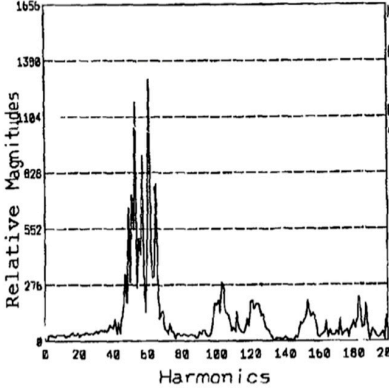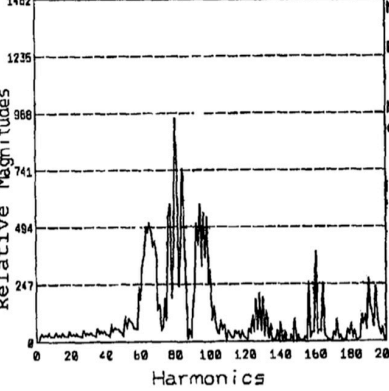**Table 10.** Progression of pitch sequencing techniques in historical perspective (Williams, 1995 [165]).
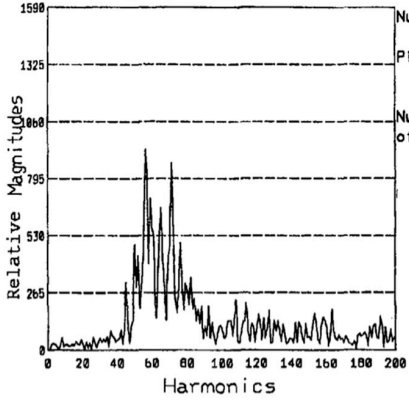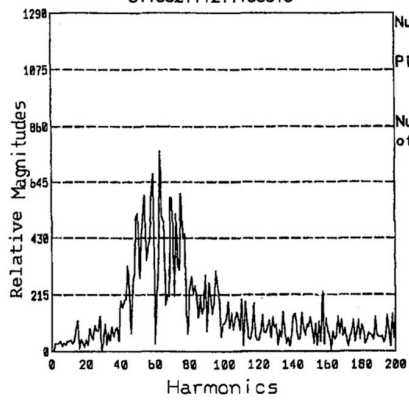
No.	Reference	Tread Pattern Harmonic Spectrum Distribution	Notes
1	Mono-space sequence		A mono-space sequence would actually be very noisy. A good example of the sound made would be a car going over a metal bridge grating.
2	Ewart, 1935 [168] (US Patent 2006197)		A pitch sequence typically provides an improvement if it can lower the overall magnitude and spread the Fourier spectrum over a broader bandwidth. Mr. Ewart's basic approach is relatively simple. The tire is divided into 8 main sections that are each separated by a small 7-degree section. The main sections are composed of pitch lengths of the same sizes arranged so that the main sections have different lengths. The sequence is further constrained to vary from small to medium to large pitches and back down. This basic concept of cycling from small to medium to large and back down is still in use today, 60 years later (1995).
3	Buddenhagen, 1952 [170] (US Patent 2612928)		Mr. Buddenhagen again used a division of the tire into 8 segments. In this technique, each segment comprises 45 degrees of the tire circumference. Each segment is however made up of different pitch lengths. There are 2 "A" segments made up of eight large pitches, 4 "B" segments made up of ten medium segments and 2 "C" segments made up of twelve small pitches.

Table 10. *Cont.*

No.	Reference	Tread Pattern Harmonic Spectrum Distribution	Notes
4	Landers, 1982 [171] (US Patent 4327792)		Mr. Landers makes a major change in the pitch sequencing process by breaking the segments into groupings of the same size pitch that in turn make up segments of the tire circumference that are different sizes.
5	Williams, 1994 [172] (US Patent 5314551)		One of the primary departures of this technique from the previous examples is the consistency of the previous techniques to always progress from a small pitch to a medium and then to a large before progressing back down to a small. The General Tire patent in fact encourages going directly from a small pitch to a large pitch. The patent defines any change between two pitches as a transition. The patent claims that the best frequency distribution is obtained when between 15 to 30 percent of the total transitions between pitches are between a small and a large pitch.

Wei et al. (2016) [173] indicated that the relative phase of the tread pattern pitch, or the offset of the two halves of tire molds, plays a great role in tire noise reduction up to 0.7 dB. The Michelin Primacy 3 ST tires are "Silence Tuned" (ST) to be extra quiet by having tread blocks of varying sizes [174].

4.2. Rotation Direction/Side Asymmetry

Asymmetric tread pattern becomes more and more popular due to many reasons (Sandberg and Ejsmont, 2002 [1]). It can optimize traction, braking, handling and safety at the same time. For example, good traction performance is desired for inboard side while handling is valued for outboard side where more side force is carried. As a result, the outboard side needs more rigid blocks or ribs with less lamellae than inboard side (Sandberg and Ejsmont, 2002 [1]).

From the perspective of TPIN reduction, quieter pattern is preferred for outboard side in terms of noise emission. TPIN from inboard side is better damped by vehicle underbody screening or pavement absorption. As a result, the direction of rotation of asymmetric patterned tire matters, especially on smooth pavement.

4.3. Ventilation

Air pumping and air resonance contribute largely to TPIN. Good ventilation can keep acoustic pressure from building up or resonating, so it is good practice to avoid closed pockets (air pumping), cavities with narrow outlets and long grooves without ventilated side channels (pipe resonance) (Sandberg and Ejsmont, 2002 [1]). This is also favorable to water drainage (Dong et al., 2010 [175]; Oshino et al., 1999 [176]) and anti-skid (Wang et al., 2013 [177]) properties of tire tread.

A shorter groove might increase the TPIN level at higher frequency, but it is still preferred as long as it avoids the concentration around 1000 Hz. Another way to reduce pipe resonance is to block the grooves using "groove fence" developed by Bridgestone (Sandberg and Ejsmont, 2002 [1]).

Wei et al. (2016) [173] suggested that the long longitudinal groove across the tire circumference has little contribution to the overall tire noise (<1 dB), because no air volume change is caused. On the other hand, the lateral groove can increase the tire noise by over 4 dB and the wider the groove is, the larger the increase. Wei et al. (2016) [173] observed that the time signal for the lateral groove air pumping occurring at the leading edge and trailing edge is damped sinusoidal, as illustrated in Figure 20.
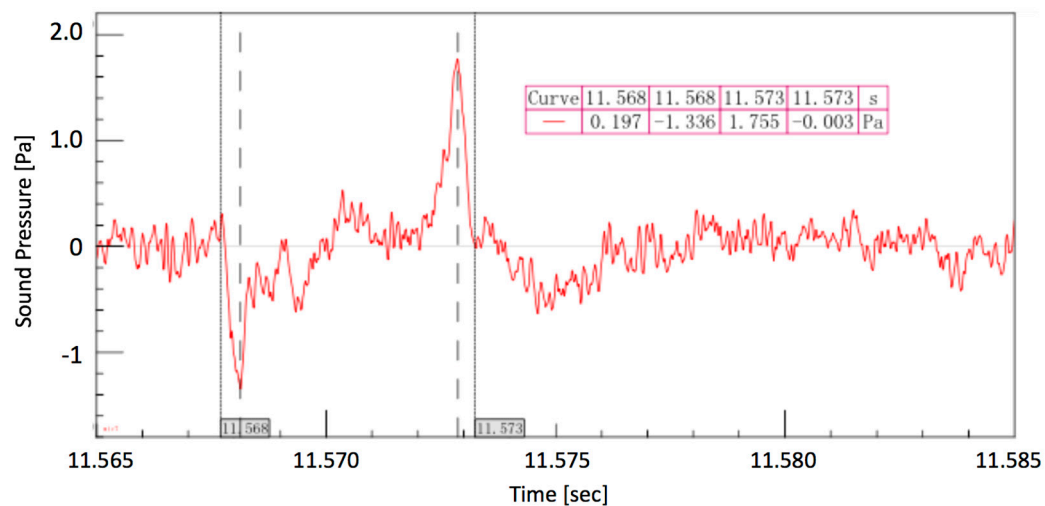

Figure 20. Noise characteristics in the time domain when lateral groove contacts ground (modified from Wei et al., 2016 [173], Figure 3).

4.4. Tread Segment

Most of the parameters about tread pattern discussed above are layout or sequence of tread segments, which are difficult to quantify. For tread segment parameterization, the quantification process is easier. The most important factors are block/groove width, block/groove depth, block/groove length, and block/groove angle (relative to the lateral axis).

It was shown that as groove width increases, TPIN increases due to increased air cavity between blocks. However, after the groove width reaches beyond 9 mm, TPIN decreases, likely due to the tread stiffness reduction (Sandberg and Ejsmont, 2002 [1]).

Increased groove depth also increased air pumping. It was indicated that groove depth is more important than groove width (Zhou, 2013 [178]).

Increased groove length reduces the frequency of pipe resonance but will usually cause higher amplitude due to the coincidence with the impact frequency (Ejsmont et al., 1984 [179]).

TPIN decreases with the increased groove angle, because it avoids simultaneous impact over the tread width. However, it cannot explain why TPIN is not sensitive to groove angle after it is over 20°. There was another study showing that the lowest TPIN occurred when the groove angle is 0°. The groove angle was shown to be the least important parameter (Zhou, 2013 [178]).

Tread pattern redistributes structural stiffness and mass concentration that affect the vibration characteristics of tire (Ih and Oey, 2012 [180]). The groove structure behaves as filter that mitigates some vibration energy components and causes delay. It takes some time to dissipate the vibration and to excite the adjacent block after one block is excited.

5. Pavement Related Parameters

The requirements of pavement have been changed from traffic load support only to multiple aspects, including structural (bearing capacity), environmental (noise and vibration generation, water

pollution), safety (friction, aquaplaning, water spray, durability), and hydrological (surface water discharge) (Domenichini et al., 1999 [181]). As such, different criteria need to be accounted for during pavement design.

As mentioned above, pavement parameter might be more important than tire parameters (Sandberg and Ejsmont, 2002 [1]) in terms of tire noise. As a matter of fact, two thirds of the literature focus on the pavement effects while only one third focus on the tire effects (Sandberg and Ejsmont, 2002 [1]). Fong (1998) [89] indicated that the texture dominated in noise generation for chipseal surfaces. Different parameters affect different generation and propagation mechanisms.

Generally, pavement can be categorized into two major types: cement concrete pavement and asphalt concrete pavement. The illustrations of different types of pavements are displayed in Table 11 (NZ Transport Agency, 2014 [182]). Different types of pavements have different acoustic performance (Donavan, 2005 [183]), as shown in Figure 21 (Mcghee, 2012 [184]). TPIN levels on cement concrete pavements were found to be 2 dB higher than TPIN levels on asphalt pavements (Syamkumar et al., 2013 [5]). The high frequency noise (over 1 kHz) and low frequency noise (below 250 Hz) was found to be much higher on the cement concrete pavements than on the asphalt pavements (Sandberg et al., 1990 [185]). Asphalt pavements characteristics are affected largely by the mixture design whereas for concrete pavements, the texturing pattern is the key contributor (Rasmussen, 2009 [146]).

Table 11. Illustrations of different types of pavements (modified from NZ Transport Agency, 2014 [182], Figures 1.6–1.19; reprinted with permission from Ms. Helen Lane on behalf of NZ Transport Agency).
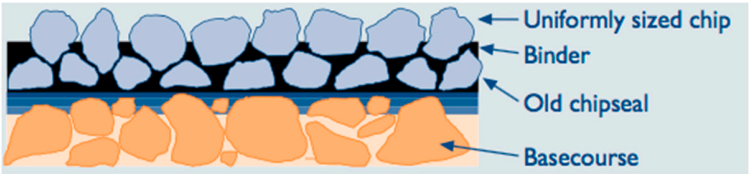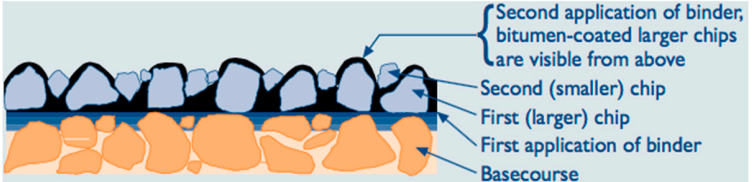
Pavement Type	Sub-Type	Illustration
Traditional	Gravel	
	Chipseal	
Asphalt Concrete (AC)	Single Coat Seal	
	Reseal	
	Two-coat Seal	

Table 11. *Cont.*
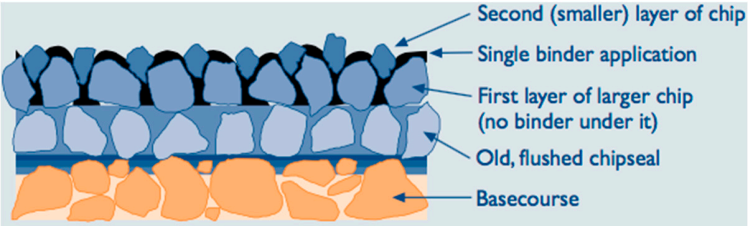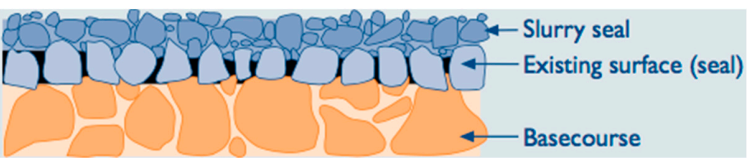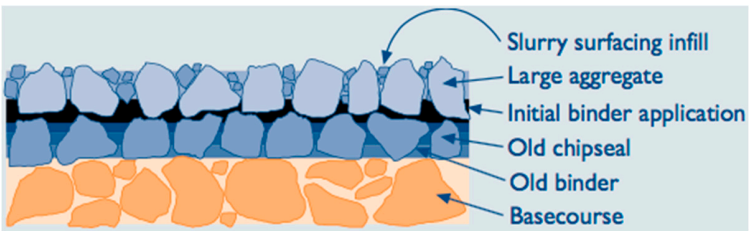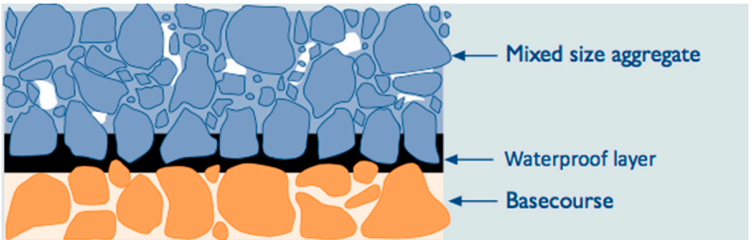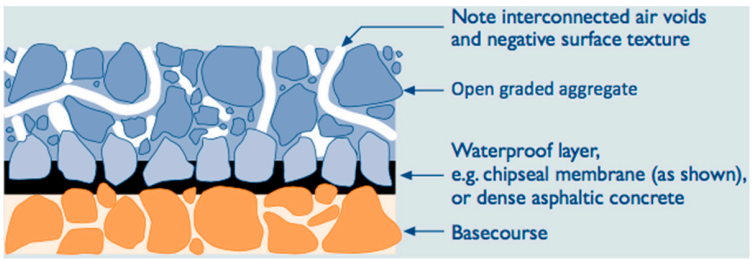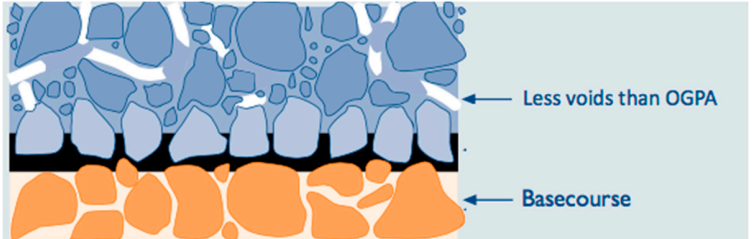
Pavement Type	Sub-Type	Illustration
	Racked-in Seal	
	Sandwich Seal	
	Slurry Seal	
	Cape Seal	
	Asphaltic Concrete	
	Open Graded Porous Asphalt (OGPA)	
	Stone Mastic Asphalt (SMA)	

Table 11. *Cont.*
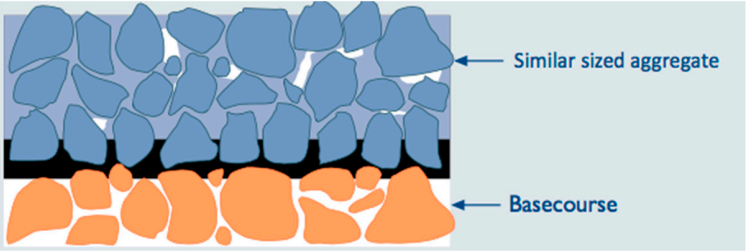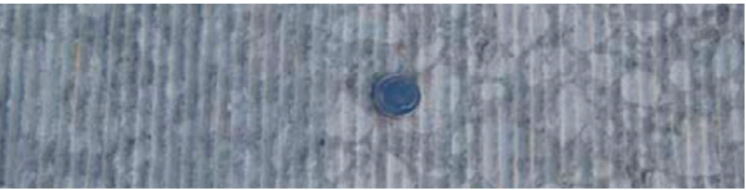
Pavement Type	Sub-Type	Illustration
	Macadam	
Cement Concrete (CC)	Transvers Grooves	
	Longitudinal Grooves	
	Artificial Turf Drag	
	Burlap Drag	
	Diamond Grinding	
	Exposed Aggregate	

Figure 21. Acoustic performances of typical pavements in Virginia (modified from McGhee, 2012 [184], Page 14; reprinted under fair use provision).

The pavement related parameters could be categorized into primary parameters, secondary parameters and tertiary parameters. The primary parameters are those for pavement design or mixture properties, such as grading size distribution, content of binder and thickness; the secondary parameters are characteristics that show up and remain relatively constant after the pavement is built, such as porosity, texture and impedance (Li et al., 2009 [186]); the tertiary parameters are those that might change with time, such as wetness, wear/age, and surface rating.

5.1. Texture

The pavement texture is acknowledged to have a significant influence on tire–pavement interaction noise where the tread pattern is not too aggressive (Klein and Cesbron, 2016 [187]; Li, 2017 [188]).
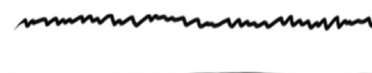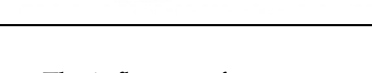
Pavement texture is defined as "the deviation of a pavement surface from a true planar surface" within a specific wavelength range (ISO, 1997 [189]). Among the pavement related parameters, pavement texture has the greatest influence on TPIN (Huschek, 1996 [190]) and is included in nearly all TPIN models. However, texture cannot be described using one single metric. It is divided into a group of parameters representing different aspects of texture based on the wavelength of the texture. They have different impacts on TPIN and other tire characteristics, as shown in Table 12 (Dimitri, 2012 [91]; Wayson, 1998 [191]).

Table 12. Texture parameters and influence on tire/pavement characteristics (red ↑ indicates increase, green ↓ indicates decrease and blue ● indicates complex) (modified from Dimitri, 2012 [91]; Wayson, 1998 [191]).

	Micro-Texture	Macro-Texture	Mega-Texture	Unevenness	Topographical Undulations
Wavelength	<0.5 mm	0.5–50 mm	50–500 mm	0.5–50 m	>50 m
Road Roughness			↑	↑ ↑	↑ ↑
Rolling Resistance		↑ ↑	↑ ↑	↑	
Tire Road Friction	↑ ↑	↑ ↑	↓ ↓		
Adhesion	↓ ↓				
Drainage		↑ ↑			
Water Skid Resistance	↑ ↑	↑ ↑			
Ride Comfort				↓ ↓ ↓	
Optical Property		● ●			
Road Hold				↑ ↑ ↑	
Splash and Spray		↓ ↓			
Dynamic Loads				↑ ↑ ↑	
Tire Wear	↑ ↑				
Vehicle Wear				↑ ↑	
TPIN		↑	↑ ↑		
Interior Noise			↑ ↑		

The common pavement textures are shown in Table 13 (Thrasher et al., 1976 [192]).

Table 13. Examples of different pavement textures (modified from Thrasher et al., 1976 [192]).

Pavement Texture	Macro-Texture (Roughness/Smoothness)	Micro-Texture (Harshness/Polishedness)	Dominant Mechanism
	High (rough)	High (harsh)	Impact and stick/slip
	High (rough)	Low (polished)	Impact
	Low (smooth)	High (harsh)	Stick/slip
	Low (smooth)	Low (polished)	Stick/snap

The influence of pavement texture on TPIN is shown in Figure 22 (Sandberg and Ejsmont, 2002 [1]). It shows that TPIN at low frequencies (below 1000 Hz) increases with texture amplitude within the texture wavelength range of 10–500 mm. TPIN at high frequencies (above 1000 Hz) decreases with texture amplitude within the texture wavelength range of 0.5–10 mm. Li et al. (2015) [193] reported the similar trends. However, Domenichini et al. (1999) (Domenichini et al., 1999 [181]) reported that the effect TPIN above 1000 Hz decreases with texture amplitude centered on 5 mm only when the total texture spectral line of 4, 5 and 6.3 mm is less than 200. It should be pointed out that the correlation between TPIN and pavement texture of short wavelengths is still uncovered. Many researchers failed to measure texture levels with enough precision at such short wavelengths, so the results were usually debatable (Fong, 1998 [89]).
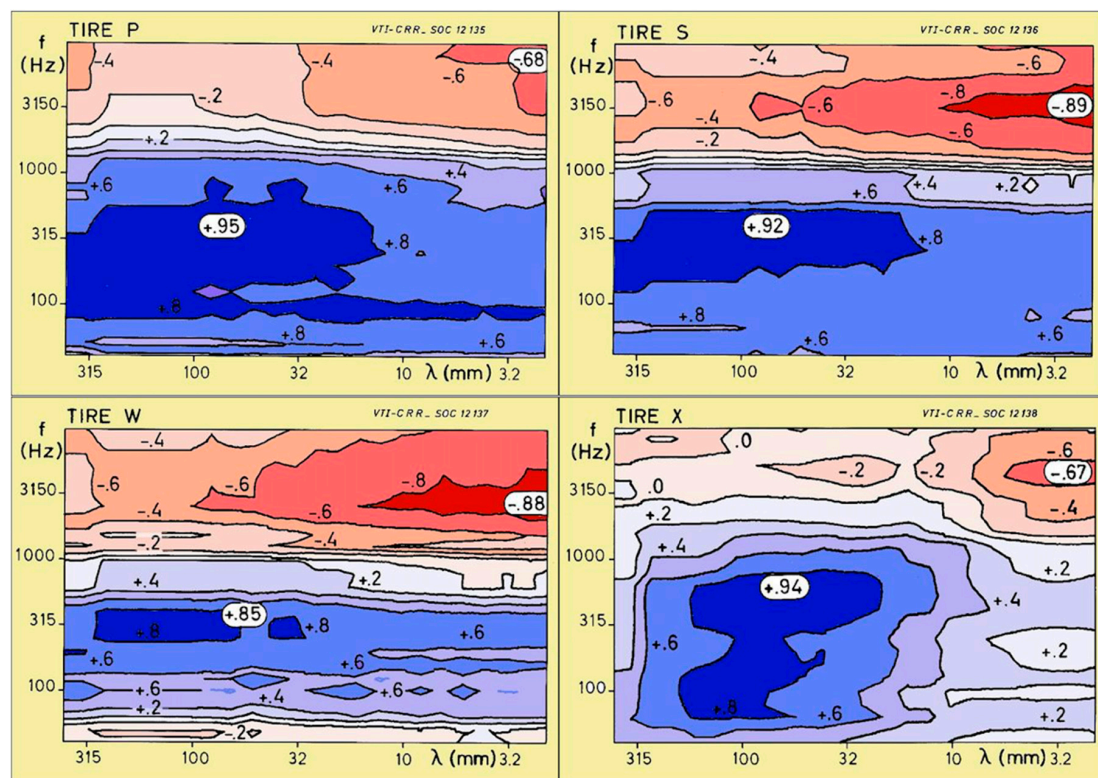
Figure 22. Contour lines of the correlation coefficient between TPIN levels (at 80 km/h) and pavement texture levels for four different tires (source from Sandberg and Ejsmont, 2002 [1], Figure 11.6; reprinted with permission from Dr. Ulf Sandberg of VTI, Sweden).

It means TPIN has different sensitivities to the different components of texture spectrum, and certain range of spectrum might be ignored or cannot be recognized by the tire (Biermann et al.,

2007 [194]). Most of the cases, power spectrum of the texture is used, which will lose the phase information. However, Hamet and Klein (2000) [195] claimed that two pavements with identical power spectrum or amplitude spectrum of the texture do not necessarily show the same acoustical behavior. Both the amplitude and phase information should be considered.

Concrete pavements texturing is conducted while the concrete is still in fresh (plastic) state. There are basically three techniques: (1) Burlap drag; (2) rake tining; (3) diamond grinding (Rasmussen, 2009 [146]). Different pavement textures or finishes often result from different approaches of paving, leading to different TPIN performance. For example, it was shown that astro-drag pavements are quieter than tined and diamond ground pavements (Hanson and Waller, 2005 [196]).

There are different texture modeling for tire–pavement interaction including friction, vibration and TPIN (Pinnington, 2012 [197]; Pinnington, 2013 [198]). Particles of different orders of magnitude, e.g., atoms, crystals, and stones, are arranged in what are called roughness orders representing a size distribution of the particles. An eight-term truncated Fourier series describes the particle shapes and the envelope of particle peaks [197]. Texture spectrum analysis (He and Wang, 1991 [199]; Lee et al., 1998 [200]; Wang and He, 1990 [201]) can also be applied to pavement texture investigations standardized in ISO/TS 13473-4 (2008) [202].

Texture profile can be measured using a laser profiler standardized in ISO 13473 (2002) [203]. Multiple lasers are used to measure the depth of the pavements at regularly spaced points along the direction of travel to collect three-dimensional texture data for all wavelengths (Dubois et al., 2013 [204]). An alternative method for texture measurement is the Circular Track Meter (CTM) or Circular Texture Meter standardized in ASTM E2157 (2009) [205]. It is a portable device and much cheaper than laser-based device but only applicable for macro-texture measurements. 2D profile can also be used to if it is sufficient enough to represent pavement texture characteristics (Hamet and Klein, 2001 [206]).

The power spectral density of texture levels Φ^2, as shown in Figure 23, can be typically expressed as (Bremner et al., 1997 [67])

$$\Phi^2(k) = 0.0001 \cdot k^{-4} \tag{9}$$

where k spatial roughness wavenumber defined by

$$k = \frac{\omega}{V} \tag{10}$$

where ω is temporal frequency of vibration, V is the tire rolling speed. Figure 23 also shows a typical tread profile spectrum, which explains why the noise from patterned tire is usually higher than the smooth tire mainly from 300 to 1000 Hz.
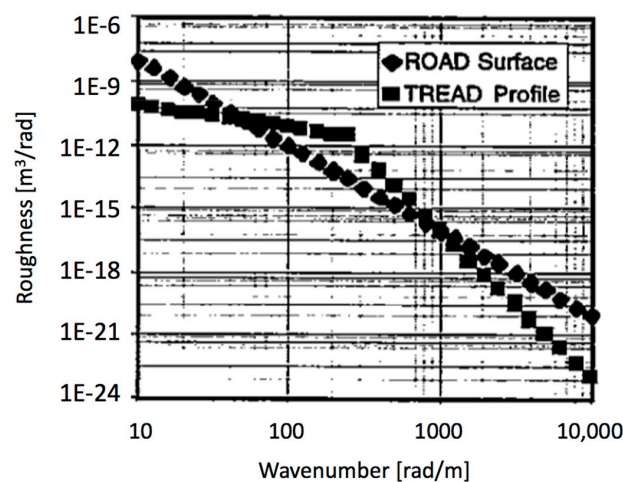
Figure 23. Pavement texture PSD (Power Spectral Density) and tread profile PSD (modified from Bremner et al., 1997 [67], Figure 21).

Typical surface texture levels are shown in Figure 24 (Li et al., 2015 [193]).
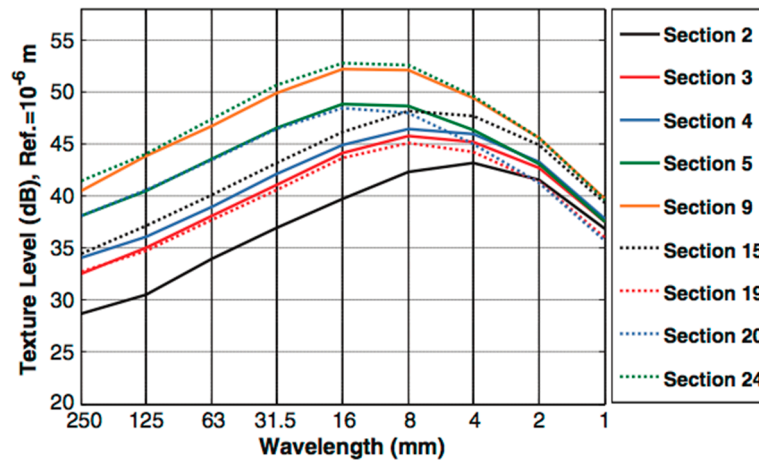
Figure 24. Surface texture levels for the thin-layer surfacing sections (source from Li et al., 2015 [193], Figure 3; reprinted with permission from American Society of Civil Engineers).

5.1.1. Micro-Texture (below 0.5 mm)

Pavement micro-texture is defined as "a deviation of a pavement surface from a true planar surface with characteristic dimensions along the surface of less than 0.5 mm" (Mcdaniel et al., 2014 [207]). It is a function of the surface texture of the aggregate particles. High micro-texture provides high frictional resistance and water skid resistance by disrupting the continuity of the water film. It can be analogous to sand paper with a gritty surface.

Higher micro-texture increases stick/slip (friction) noise generation mechanism but decreases stick/snap generation mechanism. These conflicting changes might explain why it is difficult to find clear relations between micro-texture and TPIN (Sandberg and Ejsmont, 2002 [1]). Micro-texture was shown to influence TPIN above 1000 Hz (Dare and Bernhard, 2009 [208]; Sandberg and Ejsmont, 1998 [209]).

5.1.2. Macro-Texture (0.5–50 mm)

Macro-texture is in the same order of size as coarse aggregate or tire tread elements, with spatial wavelengths between 0.5 mm and 50 mm. Indentations made into the tire tread surface generate fluctuating force (Fong, 1998 [89]). Macro-texture represents the overall properties of the pavement surface and has the greatest influence on TPIN among texture characteristics. It depends on the type of asphalt surface (e.g., dense versus porous), the gradation of the aggregates in the mixture, and presence of air voids at the surface (Mcdaniel et al., 2014 [207]). Higher macro-texture reduces hydroplaning by providing channels at the surface through which water can travel away from the contact area.

Higher macro-texture (10–50 mm) increases texture impact TPIN generation mechanism. It also influences the air pumping generation mechanism by changing the volume of air cavities in the pavement. It has certain influence on the stick/slip, pipe resonance and Helmholtz resonance mechanism. Macro-texture was shown to affect TPIN levels in the range of 630–1000 Hz (Rasmussen et al., 2006 [210]). However, higher macro-texture (0.5–10 mm) was reported to decrease TPIN levels (FHWA, 2005 [211]).

The engineering applications of macro-texture are to measure pavement skid resistance relating to crash rate on rainy days (Henry, 2000 [212]), and to evaluate construction segregation or non-uniformity relating to pavement condition rating (Flintsch et al., 2003 [213]). An alternative metric for macro-texture is Mean Profile Depth (MPD), which will be discussed later.

The macro-texture can be measured manually or automatically. The former corresponds to sand patch method (ASTM, 2006 [214]), the outflow meter, and the circular texture meter (Flintsch et al., 2003 [213]). The latter corresponds to vehicle-mounted laser profilometer (ASTM, 2009 [215]).

5.1.3. Mega-Texture (50–500 mm)

Generally, mega-texture has little influence on TPIN, except in cases of extreme roughness such as potholes, joints and bumps. However, higher mega-texture normally increases interior noise (FHWA, 2005 [211]). High mega-texture usually indicates construction defect or the end of pavement service life. The determination of pavement mega-texture is standardized in ISO 13473-5 (2009) [216].

5.1.4. Unevenness (0.5–50 m)

Pavement texture of higher wavelengths such as unevenness (0.5–50 m) and topographical undulations (>50 m) is considered to have no influence on TPIN. However, it was found TPIN increased with unevenness in the range 0.5–0.8 m (Domenichini et al., 1999 [181]). The same study also reported that TPIN in the frequency range of 200–1500 Hz decreased with increasing unevenness in the 10–80 m wavelength range (Domenichini et al., 1999 [181]), which was highly questionable because only 11 surfaces were tested.

Unevenness does have great influence on the traffic induced vibrations according to unevenness classification standard ISO 8608 (1995) [217], as shown in Figure 25. The classification is based on the power spectral density (PSD) of the pavement profile with reference to the special frequency value of 0.1 cycle/m or at the wavelength of 10 m. The evenness is classified in eight classes, from A (the best) to H (the worst).
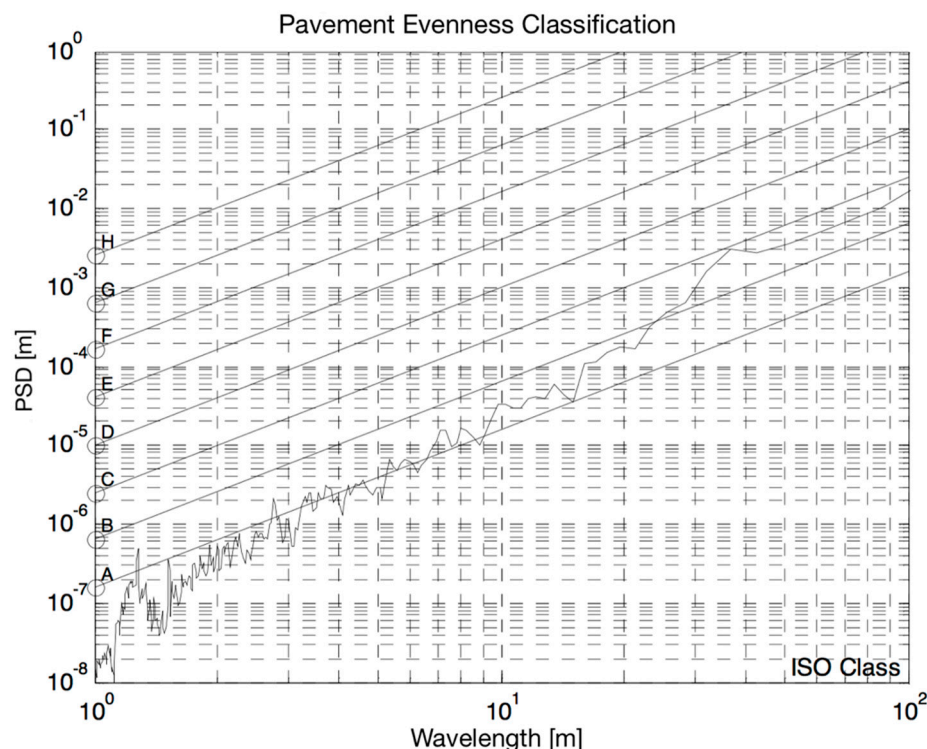
Figure 25. Evenness classification according to ISO 8608 (1995) [217] (modified from Barbosa, 2011 [218], Figure 8; reprinted under CC BY-NC 4.0 suggested by Dr. Francisco Ricardo Cunha, Editor-in-Chief of the J. Braz. Soc. Mech. Sci and Engn).

The unevenness also has great correlation with International Roughness Index (IRI), which will be discussed later.

5.2. MPD/MTD/Texture

Mean profile depth (MPD) is defined as the average depth of a section of pavement and indicates the pavement texture (mainly macro-texture). MPD is evaluated based on the pavement profiles mostly measured by laser profilometers according to ASTM E1845 (2009) [215] and ISO 13473-1 (1997) [189]. It is related to wet friction of tire pavement interaction, and the severity of segregation, which will lead to pavement distress such as raveling (Stroup-Gardiner and Brown, 2000 [219]). High MPD means rough pavement and low pavement condition index (PCI, $R^2 = 0.99$ [220]). It has almost the same influence on TPIN as macro-texture. TPIN has good correlation with MPD and correlation increases with vehicle speed (Saykin, 2011 [221]). However, some researchers claimed that the correlation is weak, because MPD filters out the spectral contents of short wavelengths and cannot be representative of texture characteristics.

A similar term, mean texture depth (MTD) is traditionally measured and calculated with Sand Patch Method, which is standardized in ASTM E965 (2006) [214]. In the test, a known volume of sand is spread out and allowed to infiltrate the surface. The diameter of the patch is measured to calculate the MPD or mean texture depth (MTD) using the equation below.

$$MPD = \frac{4V}{\pi D^2} \tag{11}$$

where V is the sampling volume, D is the diameter of the area covered by sand. MTD has strong correlations with MPD ($R^2 \approx 0.95$ [181]), and usually they are indicating the same thing (sometimes they are just called texture).

The MPD is shown to have strong relation ($R^2 = 0.85$) with the root mean square (RMS) of the pavement texture, which describes the roughness of the pavement surface or the texture height deviation from the true plane (Reyes and Harvey, 2011 [222]).

5.3. International Roughness Index (IRI)

The International Roughness Index (IRI) is the roughness index and a measure of ride and comfort quality calculated from longitudinal pavement profile. A quarter-car vehicle math model is used to yield a roughness index with units of slope (m/km). Most of the texture is in the wavelength range of 1.25–30 m, which represents the pavement unevenness. It was shown IRI has marginal correlation with TPIN (Kohler, 2010 [223]).

IRI is measured with profilometers, which is standardized in ASTM E1926 (2008) [224] and ASTM E1364 (2012) [225]. The standardization work was originally conducted by the World Bank Group (WBG, specification WB TP 46) to determine how to compare or convert data obtained from different countries initiated by The United States National Cooperative Highway Research Program (NCHRP) in the 1980's (Sayers et al., 1986 [226]).

5.4. Positive versus Negative Texture

Positive texture is texture features projected above the mean pavement level such as chip seal. Negative texture is texture features with channels or air voids below the mean pavement level such as fine graded asphalt mixture. Positive texture increases impact and friction mechanisms while negative texture reduces air pumping and resonance mechanisms.

It was shown two pavements with identical texture spectra, but one with primarily positive texture and the other with negative texture, have different TPIN levels (Beckenbauer and Kuijpers, 2001 [13]). Positive and negative textures can be addressed by envelopment process where negative texture features can be filtered out.

Texture skewness is often used to quantify positive/negative textures (Rasmussen, 2009 [146]), using the equation below according to ASME B46.1 (2009) [227].

$$\gamma = \frac{1}{N\sigma^3} \sum_{n=1}^{N} z_n^3 \tag{12}$$

where γ is the texture skewness, N is the number of samples along the longitudinal texture line measured, z_n is the texture height at sample point n (the mean value of z_n is 0), σ is the standard deviation of z_n. Most of the pavements have negative skewness, indicating that most of the texture is negative (Dare, 2012 [46]).

5.5. Transverse Texture

When speaking of pavement texture, it usually means longitudinal texture. However, transverse texture is also important (Wullens et al., 2004 [228]), especially on cement concrete or grooved asphalt pavements. Transverse texture allows coincident impact between tire and pavement along the contact patch width, resulting in high TPIN levels.

Tined transverse texture can be uniformly spaced or randomly spaced (Rasmussen et al., 2008 [229]). The former can also produce high tonal noise (Hamet and Klein, 2001 [206]).

5.6. Anisotropic Texture

Texture on conventional asphalt surfaces without grooving is typically isotropic, but most concrete pavement textures are anisotropic/orientated, which means the texture is different in the longitudinal and transverse directions (Rasmussen et al., 2008 [229]).

Anisotropic texture is often in the form of periodic features, such as peaks and grooves. If they are transverse, it will be transverse texture mentioned above and increase impact mechanism. If they are longitudinal, it will increase the air displacement mechanism and pipe resonance. Generally, transverse textures shall be avoided from the perspective of TPIN reduction.

5.7. Joints

Contraction joints between slabs are often used on Portland cement concrete (PCC) pavements to control cracking caused by the curing process, temperature fluctuations, and vehicle loading (Kane, 1990 [230]). However, the joints will usually cause high tonal "clap" sound called wheel-slap noise or joint-slap noise (Dare and Bernhard, 2013 [12]), increasing the TPIN level by up to 3 dB concentrated in the 800–1000 Hz at highway speed (Donavan, 2004 [231]; Meiarashi et al., 1998 [232]). The joint had little impact on TPIN frequencies above 1600 Hz and below 500 Hz. The wheel-slap noise usually decays within 15 ms (Dare et al., 2011 [233]).

The noise was found to be related to the structural vibration induced by the joints (Dare and Bernhard, 2013 [12]). However, the speed coefficient of increased noise cannot be well explained, since the frequency of excess noise did not depend on vehicle speed. In addition, the wave speed of the vibration induced wave was found to be around 1.7 m/s, which is not efficient sound radiator (Bolton et al., 1998 [66]).

Therefore, increased tread/texture vibration is not a major cause of increased noise at contraction joints, and other mechanisms have been proposed (Dare and Bernhard, 2013 [12]). (1) The contraction joint changes the loading condition at the contact patch and the vibration characteristics. (2) Air is forced out from the joint, i.e., air pumping mechanism. (3) A pipe-like structure is formed as tire rolls over the joint, i.e., pipe resonance, which is shown for slick tires but not significant for treaded tires (Dare and Bernhard, 2010 [234]).

Even though these mechanisms have not been proved by direct experiments, empirical relationships between joint parameters such as width (typically 8 mm) and depth have been found (Dare et al., 2011 [233]). Dare et al., 2011 [233] did a comprehensive investigation on the influences of contraction joint parameters. It was shown that the wheel-slap noise increases by 0.5 dB/mm ($R^2 = 0.95$~0.98) as the joint width increases from 5 to 24 mm at speed range of 16–48 km/h. The silicone sealant in the joint can reduce the noise substantially for wide joints, but only marginally for

narrow joints. The SPL increases by 1.7 dB/mm as the step-down faulting increases from 0 to 6 mm, while the SPL increases by 2.2 dB/mm as the step-up faulting increases from 0 to 6 mm (R^2 = 0.89~0.99). The beveled joint has similar effect to the standard joint with the same width at the top of the bevel.

Contraction joint is also called Modular Expansion Joint (MEJ) in Canada (Marriner and Wakefield, 2011 [235]). For general traffic with speed of 100 km/h, the dominant MEJ emission frequency was found to be centered at the 630 Hz one-third octave band in 73% of cases. For heavier vehicles, MEJ emission levels were increased by 3.2 to 8.7 dB (Marriner and Wakefield, 2011 [235]).

For the directionality of the joint noise, the MEJ emission level 100 m behind the test vehicle was 8.6 dBA higher than 100 m ahead of the vehicle, but the joint emission level received 7 m behind the vehicle was approximately the same as that received 7 m ahead (Marriner and Wakefield, 2011 [235]).

There are also other common types of faults in road: joint is negative texture and speed bump is positive texture. It was shown that for a bump of height 0.04 m, the peak noise level is increased by 1 to 14 dBA depending on the vehicle speed (20–60 km/h) (Behzad et al., 2007 [236]).

The joints also occur between a road and a bridge, sometimes increasing the overall TPIN by about 10 dBA (Sexton, 2011 [237]; Glaeser et al., 2011 [238]; Wakefield and Marriner, 2011 [239]). It is worth mentioning that the bridge deck surfaces made of open grid steel structures also produce great vibration and noise (Tournour and Cuschieri, 1994 [240]; Cuschieri et al., 1996 [241]; Meggers, 2016 [242]).

Kindt et al. (2007) [72] investigated the cleat height effect on the tire vibrations. The tire stiffness decreases with the increase of cleat height due to Payne effect where increasing deformation amplitude leads to the decrease of the number of physical bonds in the filler network decreases, resulting in a decrease of stiffness and increase of vibrations (Payne and Scott, 1960 [243]).

5.8. Porosity (Air Void Content)

High pavement porosity can greatly reduce TPIN levels, which might explain why porous asphalt pavement with porosity exceeding 20% is quietest pavement. Porous pavements (a.k.a. drainage asphalt or pervious macadam) have been widely used in Europe and are increasingly used in the United States to mitigate TPIN and improve safety. Donavan (2014) [244] reported that the open-graded asphalt concrete (OGAC, a porous pavement) in the U.S. Highway 101 reduced the traffic noise by over 10 dB.

Pavement porosity can reduce nearly all TPIN generation and amplification mechanisms as sound pressure energy can be absorbed and dissipated through fluid friction within these tortuous channels. Air pumping, pipe resonance, Helmholtz resonance and horn effect are mitigated by interconnected voids providing channels for air pressure to travel away. It also reduces the contact area between the tire and pavement, leading to less stick/slip and stick/snap. It reduces TPIN in the middle and high frequencies but might increase TPIN at low frequencies such as below 1000 Hz due to higher macro-texture (Bernhard et al., 2003 [84]).

A measure of pavement porosity is air void content, including the air voids at the surface and interconnected voids within the mixture. The pores are generated due to the discontinuous granular formulation (Bérengier et al., 1997 [245]). As such, pavement porosity or air void content is largely dependent on the type of mixture such as the size of aggregates. The bigger the aggregates are, the larger the pore size and porosity are. For example, open-graded mixtures tend to have more interconnected voids than dense-graded mixtures. Reyes and Harvey (2011) [222] found that air void content has a positive relation (R^2 = 0.64) with mean profile depth (MPD) which also increases as the size of aggregates increase.

The measurement of the air void content is standardized in ASTM D7063/D7063M (2011) [246] and can be calculated using the pavement core sample with the equation below.

$$V_A = \frac{G_{mm} - G_{mb}}{G_{mm}} \times 100\% \tag{13}$$

where V_A is air void content, G_{mm} is theoretical maximum specific gravity standardized in AASHTO T 209 (2011) [247], G_{mb} is the bulk specific gravity standardized in AASHTO T 331 (2010) [248]. Asphalt

pavement can be divided into three categories based on the air void content: dense asphalt (<10%), semi-porous asphalt (10–15%), and porous asphalt (>15%). The effect of air void content is dependent on the type of pavements. Ongel and Harvey (2010) [249] reported that sound intensity levels decrease as V_A increases from 5% to 15% for dense-graded asphalt concrete mixes (DGAC) and gap-graded rubberized asphalt concrete mixes (RAC-G), while sound intensity levels increase as V_A increases from 10% to 20% for conventional open-graded mixes (OGAC) and open-graded rubberized asphalt concrete mixes (RAC-O).

Cement concrete pavement can also be porous, such as modified Portland cement concrete with porosity of 15%–25% (Neithalath et al., 2005 [250]). Two methods have been explored, one using non-aggregate component of the mixture resulting in Enhanced Porosity Concrete (EPC), and the other using soft inclusions in the matrix (Neithalath et al., 2005 [250]).

The porosity can also be expressed as:

$$\Omega = 1 - \frac{\rho_p}{\rho_a} \tag{14}$$

where ρ_p is the average density of the pavement, ρ_a is the average density of the aggregate. However, in most cases the empirical expression below will be more practical (De Roo and Gerretsen, 2000 [251])

$$\Omega(\text{in \%}) = 0.26 \cdot (100 - s_\% - f_\%) + 2.5 \cdot \frac{\Delta d_{st}}{d_{average}} - 9 \cdot \left(1 - e^{-0.00001 b_\%^5}\right) \tag{15}$$

where $s_\%$ is percentage of sand, $f_\%$ is percentage of filler, $b_\%$ is percentage of binder, Δd_{st} is difference between maximum and minimum grain size of the aggregate, $d_{average}$ is average grain size of the aggregate. The deviations between predicted and measured values range from −9% to +13%, which is pretty accurate.

Another term describing porosity is tortuosity (Olek et al., 2003 [252]). It should be noted that porosity is in conflict with the mechanical strength and durability (Sandberg and Ejsmont, 2002 [1]). High quality binders are often used when designing high porosity pavements. The structure factor measuring the tortuosity of the pores can only be assessed theoretically for idealized geometries [251]. For perpendicular uniform channels, the value can be set to 1. For diffusely oriented uniform channels, a value of 3 would be valid. In granular materials the structure factor appears to be an approximate function of the porosity, as shown below (De Roo and Gerretsen, 2000 [251]).

$$s_f \simeq \Omega^{-1} \tag{16}$$

where s_f is the structure factor, and Ω is the porosity. However, until now, many assumptions and simplifications still exist due to the complexity of the sound wave propagating in the porous media.

The air void content associated with porous pavement is just a measure of the proportion, but does not consider how much the pores are interconnected, which is more acoustically relevant. Airflow resistance accounts for this effect, which will be discussed later.

5.9. Sound Absorption

Sound absorption is highly correlated with porosity. Generally, sound absorption is determined using impedance tube with either standing wave ratio method standardized in ISO 10534-1 (1996) [253] or transfer function method standardized in ISO 10534-2 (1998) [254]. However, core samples need to be extracted from the pavement. A Similar measurement standard in lab for pavement sound absorption is described in ASTM E1050 (2012) [255].

In-situ measurement allows non-destructive tests of absorption standardized in ISO 13472-1 (2002) [256] and ISO 13472-2 (2010) [257], in which diameter and length of the impedance tube within close tolerances are specified and procedure to seal between the pavement and the impedance tube is provided. Sound absorption data are usually reported as narrow-band spectra. However,

absorption data are valid only up to approximately 1600 Hz for the most common size of pavement specimen tested. The sound absorption is usually reported in one-third octave bands from 500–1600 Hz. Different types of pavements have absorption spectra of different shapes. Some have low absorption with maximum below 0.1 across all frequencies while porous asphalt has absorption coefficient of 0.5–0.6 for all frequencies. Some pavement has a sharp peak at 800 Hz (Dare, 2012 [46]).

Sound absorption is a function of the acoustic impedance, as shown below (De Roo and Gerretsen, 2000 [251]).

$$\alpha(\phi_0) = 1 - \left| \frac{Z'(\phi_0) \cos \phi_0 - 1}{Z'(\phi_0) \cos \phi_0 + 1} \right|^2 \tag{17}$$

where Z' is acoustic impedance, ϕ_0 is the angle of incidence. Acoustic impedance Z' is considered to be a function of the layer thickness, the porosity of the layer, the specific flow resistance of the material and the structure factor, which is a measure for the tortuosity of the pores (De Roo and Gerretsen, 2000 [251]).

Typical sound absorption coefficients for thin-layer surfacing is shown in Figure 26 (Li et al., 2015 [193]). In the same study, Li et al., 2015 [193] presented the correlation coefficient between noise levels and sound absorption coefficient, both in frequency domain, as illustrated in Figure 27. As expected, sound absorption reduces tire noise maximally when the frequencies of both coincide, especially around 800 Hz and 2000 Hz.
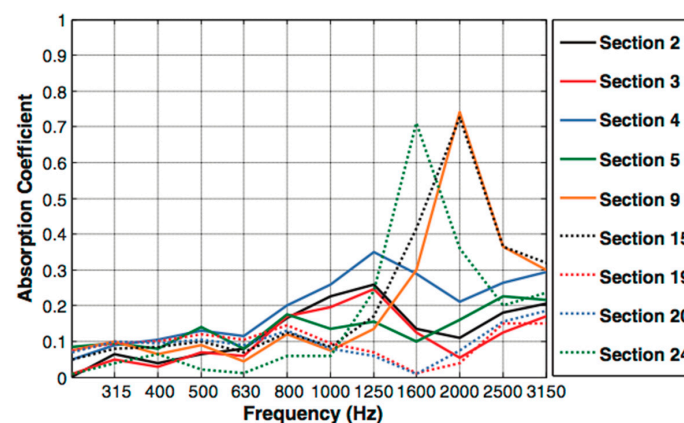
Figure 26. Sound absorption coefficients for the thin-layer surfacing sections (source from Li et al., 2015 [193], Figure 4; reprinted with permission from American Society of Civil Engineers).

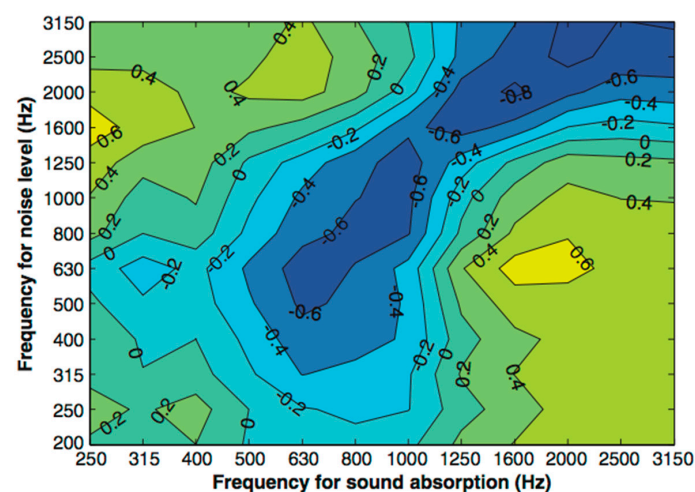**Figure 27.** Contour lines of the correlation coefficient between noise level (passenger car tire at 80 km/h) and sound absorption coefficient (source from Li et al., 2015 [193], Figure 6; reprinted with permission from American Society of Civil Engineers).

5.10. Airflow Resistance

Airflow resistance is considered to be a more relevant measure of absorption, because it is measured at a shallow angle rather than perpendicular to the pavement surface (Rasmussen et al., 2007 [258]). It indicates how difficult it is for air to flow through a pavement. According to ISO 9053 (1991) [259] and ANSI/ASA S1.18 (2010) [260], air is forced through a pavement sample, the pressure difference and flow rate are both measured, and airflow resistance is then calculated.

Airflow resistance as acoustic impedance is related to TPIN air pumping and resonance mechanisms. The specific flow resistance of a granular material may be expressed as (De Roo and Gerretsen, 2000 [251])

$$\sigma = \frac{C}{\langle d^2 \rangle} \left(\frac{1}{\Omega} - 1 \right)^2 \tag{18}$$

where C is a constant (2.8×10^4 in the literature to best fit the measurement), d is the effective diameter of the aggregate granules (in mm), Ω is the porosity. Nevertheless, the errors between prediction and measurements are fairly large. However, flow resistance is not very important for calculation of sound absorption, variations up to a factor of 2 may be acceptable.

Another expression for specific airflow resistance is

$$R_f = \frac{\Delta p}{u} \tag{19}$$

where R_f is specific airflow resistance, Δp is the difference of pressure across the specimen, and u is the flow velocity (Reyes and Harvey, 2011 [222]). The specific airflow resistance has strong negative relation with air void content. Reyes and Harvey (2011) [222] found that specific airflow resistance of 2000 Pa·s/Pa corresponds to 15% air void content for porous asphalt pavement. It was also found that airflow resistance has good negative relation with water permeability.

A porous pavement with low airflow resistance implies that the airflow generated at the tire–pavement interaction due to air pumping is able to penetrate the pavement without much resistance, leading to the noise reduction from the airborne mechanisms. In contrast, if the airflow resistance is high, the airflow will not pass easily, leading to the increase of the turbulent flow at the contact path and noise increase (Reyes and Harvey, 2011 [222]).

5.11. Thickness of Layer

For porous pavement, sound absorption has positive correlation ($R^2 = 0.74$ [1]) with the product of layer thickness and air void content (Sandberg and Ejsmont, 2002 [1]). Ren and Gao (2009) [261] reported that void content and pavement depth are the main contributing factors to the noise reduction. The frequency at the peak absorption is related to the thickness of the pavement, which can be used to calculate the optimal thickness based on the frequency of interest (Neithalath et al., 2005 [250]). However, Mogrovejo et al. (2014) [262] reported that the thickness was effective up to a certain degree, but declining benefits then occurred.

The thickness of layer can influence both acoustic impedance and mechanical impedance to be discussed below.

5.12. Stiffness (Mechanical Impedance)

The pavement stiffness or modulus has a profound impact on the structural strength of the pavement. It also influences TPIN levels by affecting impact mechanism and discharging high frequency tire vibrations into pavement. Rigid pavements are generally louder than flexible pavements (Berge and Storeheier, 1936 [263]), especially around 630–1600 Hz (Li et al., 2012 [264]). For example, Poro-Elastic Road Surface (PERS) containing epoxy-bound shredded rubber was shown to be quieter than conventional pavements (Sandberg and Goubert, 2011 [265]; Storeheier, 1987 [266]; Nilsson and Sylwan, 2003 [267]; Sandberg and Goubert, 2011 [268]; Swieczko-Zurek, 2013 [269]). It is analogous to

the running shoes on a flexible running track. Bilawchuk (2005) [270] reported that noise levels on asphalt pavement constructed using crumb rubber binder were lower than normal asphalt pavement when test vehicle was driven at relatively higher speeds. Ponniah et al. (2010) [271] observed that addition of rubber to open graded mixes reduced TPIN by 2 dBA. Beckenbauer (2001) [272] tested two surfaces (one glued with sandpaper on top, one inserted a rubber sheet between the sandpaper and pavement surface), and found that the latter is 3dBA lower than the former. It is reasonable to argue that softer tire/road contact, with softer tire tread as well as road surface, will have better noise reduction (Sandberg, 2003 [49]).

The stiffness is affected by mixture type, aggregate gradation, mixture volumetrics and binder properties. It was shown that pavement with plastic binder could give 1 dBA TPIN reduction (Stenschke, 1990 [273]). Stiffness changes with temperature and moisture, so the pavement stiffness changes over the course of a day or seasonally, and over the service life due to aging and mixture stiffening (Mcdaniel et al., 2014 [207]). Liao et al. (2015) [274] reported that the stiffness may reduce substantially when pavement temperature increases by 10 °C.

The stiffness/modulus can be measured in lab with Mechanistic–Empirical Pavement Design Guide and the Asphalt Mixture Performance Tester (AMPT), which is standardized in AASHTO T 342 (2011) [275]. It can also be measured in situ with Falling Weight Deflectometer (FWD) (Rao and Von Quintus, 2012 [276]). Stiffness measured is often affected by the loading type, rate, and amount applied in the test, most of the loads used today are impact loads (Li et al., 2012 [264]) described in ASTM C1383 (2010) [277].

Another physically similar and more commonly used parameter is mechanical impedance, defined as the ratio of the driving force to the induced velocity, so it measures the ability of a structure to resist motion when subjected to a given force. It is an overall indicator for the flexibility and energy dissipation properties of the pavement.

Besides the stiffness, mechanical impedance also accounts for the damping properties, which is dependent on the pavement mixture. Biligiri (2013) [278] reported that asphalt rubber friction course (ARFC) mixes provided higher noise-damping response than the conventional dense graded asphalt (DGA) mixes due to the extra binder, higher porosity, rubber inclusions.

5.13. Normal Adhesion

Normal adhesion is correlated with micro-texture. It was shown the pavement sprayed with a layer of anti-adhesion paint has lower TPIN at high frequencies due to less stick/snap (Sandberg and Ejsmont, 2002 [1]).

5.14. Tangential Friction

Pavement friction is highly correlated with micro-texture and often used as a measurement for safety and braking distance. It can also impact TPIN by slip/stick mechanism at high frequencies. However, no statistically significant relationship ($R^2 < 0.3$) was found between noise and wet friction both for optimum slip and blocked wheel (Sandberg and Ejsmont, 2000 [76]; Oshino et al., 2001 [279]).

Friction (or wet skid resistance) can be measured with three methods. (1) Towed skid trailer standardized in ASTM E274/E274M (2011) [280] can be used for field testing but very time consuming. The tested tire can be standard ribbed tire (ASTM E501, 2008 [281]) or standard smooth tire (ASTM E524, 2008 [282]). The skid number (SN), locked wheel longitudinal friction value is reported. (2) Dynamic Friction Tester (DFT) standardized in ASTM E1911 (2009) [283] is a portable device tested in situ. It can be combined with Circular Track Meter (CTM) to calculate the International Friction Index (IFI) standardized in ASTM E1960 (2011) [284]. (3) British Pendulum Tester standardized in ASTM E303 (2013) [285] can be used in lab. The British Pendulum Number (BPN) is reported. The skid number SN_V and British Pendulum Number *BPN* were reported to have relations below (Domenichini et al., 1999 [181]) given the mean texture depth *MTD* and velocity *V*.

$$\begin{cases} SN_0 = -31 + 1.38 \cdot BPN \\ PSNG = 4.1 \cdot \left(\frac{MTD}{0.0254} \right)^{-0.47} \\ SN_V = SN_0 \cdot \exp\left(\frac{-PSNG \cdot V}{100} \right) \end{cases} \qquad (20)$$

where the equations are valid on a wet surface with a nominal water depth of 0.5 mm. In general, skid number SN_V decreases with the increase of velocity V. Khaki et al. (2015) [286] reported that tire noise decreases as BPN increases for both conventional asphalt and porous asphalt.

5.15. Wear/Age

Traffic wear on pavement can change the micro- and macro-texture, resulting in friction and TPIN changes (McDaniel et al., 2010 [287]). Friction initially increases within a few months as traffic wears off the binder film coating the aggregate particles, and then decreases as the particles are further polished (Kowalski, 2010 [288]). For porous asphalt pavement, after a small decrease within the first months of service (Mogrovejo et al., 2014 [262]), TPIN generally increases over year due to the clogging of air voids (Paje, 2007 [289]), and then begins a steady trend (Mogrovejo et al., 2014 [262]). It is a cumulative process whose rate changes depending on porous mixes and locations. An increase of about 0.5 dB per year in CPX measurements for a porous polymer-modified friction course was found (Ng et al., 2009 [290]). Chalupnik (1996) [291] indicated that the age of pavement was more important than the type of pavement in terms of TPIN. For cement concrete pavement, the influence of wear and aging were relatively small (Sandberg et al., 1990 [185]). Longitudinally grooved pavements with significant macro-texture can become quieter as macro-textural features are worn down over time (Dare et al., 2009 [292]).

The amount of wear can be estimated by traffic volume or single axle loads (ESALs). Winter maintenance operations and the impact of cyclic freezing and thawing (weather wear) are also forms of wearing (Neithalath et al., 2005 [250]). Like traffic wear, TPIN generally increase as pavement ages (Bendsten, 2009 [293]). Acoustic longevity describes how well pavement retains its TPIN level over time. For example, the first Next Generation Concrete Surface (NGCS) built by the Washington State Department of Transportation (WSDOT) showed a very short acoustic longevity (Anderson et al., 2014 [294]). On-board sound intensity (OBSI) levels increased from initial levels of 100.6 dBA to 104.4 dBA in 30 months. However, the effects of age were marginal for some other pavements (Hencken, 2012 [295]).

5.16. Surface Rating (SR)

Surface rating (SR) is a measure of the wear or distress on a pavement surface by counting the number of cracks and joint deterioration on a segment of road, and then applying weighting factors (Kay, 1992 [296]; MNDOT, 2003 [297]). The rating is typically highest immediately after construction or rehabilitation and gradually (or sometimes rapidly) decreases due to the accumulation of cracking, rutting, raveling and other types of distress (Mcdaniel et al., 2014 [207]). TPIN increases with the SR dropping as the distress increases the pavement roughness.

Asphalt pavement distress typically includes fatigue (alligator) cracking, block cracking, edge cracks, longitudinal (linear) and transverse cracking, reflection cracking, slippage cracks, corrugations and shoving, rutting, settlement/grade depressions, upheaval/swell, utility cuts/patch failure, pot hole, raveling/weathering, bleeding, polished aggregate, loss of aggregate on surface treatments, and longitudinal/transverse streaking (Miller and Bellinger, 2003 [298]).

5.17. Wetness

As one of the most common pavement conditions, wetness can increase TPIN by up to 3 dBA for heavy commercial vehicles (Syamkumar et al., 2013 [5]). The increase frequency range are found to be above 1000 Hz (Boullosa and Lopez, 1987 [299]; Descornet, 2000 [300]) probably due the water splash

effect. It was also found that TPIN decreases at low and middle frequencies, which might be attributed to less adhesion. The tire vibrations on the wet road are slightly lower than those on a dry road, indicating that there must be a separate noise generating mechanism independent of the tire vibrations (Heckl, 1986 [60]). Bergmann (1980) [301] found a 10 dB increase over 1 kHz on wet pavement and speculated it was due to the acceleration of water particles at the leading edge. Heckl (1986) [60] also indicated that some of the noise on a very wet road does not come from the tire but from the water. The influence to pavement moisture was found to be independent on speed (Descornet, 2000 [300]). Porous pavements are more sensitive to wetness, as the voids can be saturated with moisture in the pavement.

There are some other pavement conditions, such as ice and/or snow. However, few studies address such topics on TPIN. TPIN on snowy surface has more spectral contents at low frequencies (below 1.5 kHz) while TPIN on wet surface has more spectral contents at high frequencies (above 1.5 kHz), as illustrated in Figure 28 (Kongrattanaprasert et al., 2010 [302]).
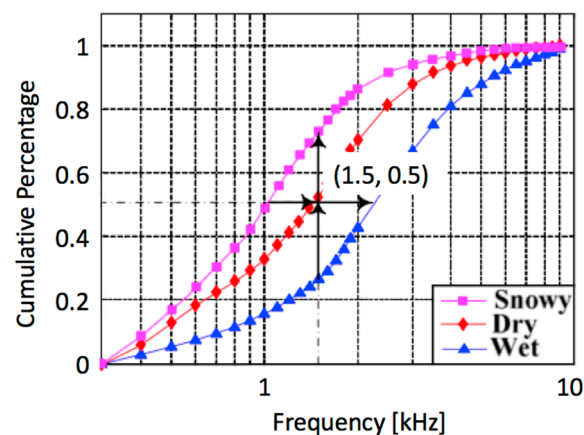
Figure 28. Typical cumulative spectral content of TPIN for different road conditions (modified from Kongrattanaprasert et al., 2010 [302], Figure 1; reprinted under fair use provision).

5.18. Mixture Parameters/Materials

Various pavement parameters discussed above are determined by the mixture parameters such as nominal maximum aggregate sizes, aging conditions, air void contents, binder types, mixture types, aggregates and gradations. It was reported that mixture parameters that had great impact on tire–pavement noise (Kocak and Kutay, 2012 [303]; Biligiri, 2008 [304]).

It was found that voids in the mineral aggregate (VMA) and binder content are in favor of TPIN reduction, while coefficient of uniformity of the aggregate gradation is not (Kocak and Kutay, 2012 [303]).

5.19. Reference Pavement

Standard pavement is required for measuring exterior vehicle noise or TPIN. The current globally accepted standard is ISO 10844 (2014) [145], which is basically a dense asphalt concrete surface with maximum aggregate size of 8 mm. A lot of attempts have been done to improve the repeatability and reproducibility for both on-board and pass-by noise (Sohaney et al., 2012 [305]; Moore, 2011 [306]). Specifications and measurement procedures for texture, roughness, acoustic absorption, planarity, and asphalt mix have been provided in the standard to reduce the variation of noise generation and propagation from track to track. However, it was argued that the ISO surface is too smooth to be representative of general pavements (FEHRL, 2001 [130]). As such, it is of interest to compare the tire ranking on ISO surface with that on normally used roads, or attempt to select more commonly used surface as reference pavement in the future. On the other hand, compared to rougher pavements, the current ISO surface can better distinguish acoustic behavior between tires, providing more accurate acoustic ranking of a tire (Blokland and Leeuwen, 2010 [307]).

Another standard pavement is SAE test surfaces. Donavan et al., 1998 [39] reported that tire noise from SAE test surfaces is larger than ISO surfaces, as shown in Figure 29.
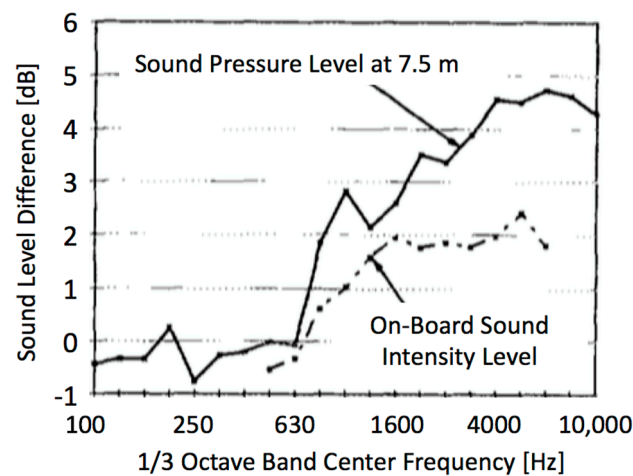
Figure 29. Difference in levels measured on ISO and SAE test surfaces (SAE less ISO) (source from Donavan et al., 1998 [39], Figure 4; reprinted with permission from AIP Publishing LLC).

6. Environmental Parameters

Environmental or atmospheric parameters can influence tire–pavement properties and the characteristics of the transmission path. Therefore, they cannot be neglected and have been included in many TPIN models.

6.1. Temperature

There are three relevant temperatures, i.e., tire temperature, pavement temperature and air temperature. Tire temperature is influenced by pavement temperature via interaction, but it is very difficult to measure when moving and might heat up or cool down over the course of test (Sandberg, 2004 [308]). Tire temperature has less strong correlation with TPIN than pavement temperature or air temperature (Sandberg and Ejsmont, 2002 [1]). Therefore, tire temperature was seldom included in TPIN models. Kindt et al. (2007) [72] investigated the tire temperature effect on the tire structural vertical resonance and found that the resonant frequency decreases by 0.12 Hz/°C with the increase of tire temperature, probably due to the viscoelastic property change of tire materials. It was also suggested that the tire cavity acoustic resonance frequency increases at 0.16%/°C with the increase of temperature.

Pavement temperature is generally highly correlated with air temperature. In general, air temperature equals about 65% of pavement temperature in °C (Kuijpers, 2001 [309]). Liao et al. (2015) [274] reported the following regression equation,

$$T_{pavement} = 1.3591 T_{air} - 2.2902 \tag{21}$$

where $R^2 = 0.9506$. Pavement properties change with pavement temperature. Asphalt exhibits brittle elastic behavior at lower temperatures while at higher temperatures, the material exhibits a significant viscous behavior resulting in TPIN reduction (Syamkumar et al., 2013 [5]).

Pavement temperature is also related to surface color, but it might also be a psychological effect [1]. For example, a black asphalt pavement might easily become 10 °C warmer than a bright cement concrete pavement in sunshine, which corresponds to 1 dBA in TPIN, but black asphalt pavement normally leaves an impression of quiet surface (Sandberg and Ejsmont, 2002 [1]).

Since air temperature is much easier to measure, it is most commonly included. It was shown that TPIN decreases about 0.04–0.1 dBA/°C with the increase of air temperature (Konishi et al.,

1995 [310]; Anfosso-LédéE and Pichaud, 2007 [311]). The temperature coefficient also depends on the tire type and pavement type. The temperature effect is relatively larger for a rough-textured surface than for a smooth-textured surface (Sandberg and Ejsmont, 2002 [1]). Asphalt pavements are more sensitive to temperature than cement concrete because asphalt mixtures are viscoelastic materials whose moduli change with temperature. Liao et al. (2015) [274] investigated four types of asphalt pavements and concluded that air temperature influenced the correlations between noise levels and surface characteristics. They also analyzed the temperature effect on different frequencies and indicated that the effect was most obvious around 2000 Hz for the correlation between sound levels and surface roughness.

It has been found that increased temperature causes TPIN decrease in low-frequency due to the less stiffness of pavement and less hardness of tire rubber, but increase in high-frequency probably due to the more adhesion mechanism (Nilsson, 1980 [312]).

Air temperature or ambient temperature can affect both TPIN generation mechanisms and sound propagation. Therefore, pass-by noise measurements of TPIN are more sensitive to air temperature than near field measurements such as OBSI.

Many TPIN measurement standards provide temperature correction equations to normalize data to a reference temperature (EEC, 2001 [313]; SAE, 2014 [314], AASHTO, 2013 [315]). The On-Board Sound Intensity (OBSI) Standard AASHTO TP 76 (AASHTO, 2013 [315]) provides the following correction for temperature effects.

$$IL_{Normalized} = IL_{Measured} + 0.072 \times (AirTemp - 20) \tag{22}$$

where $IL_{Normalized}$ is the normalized sound intensity level (dBA) for the reference temperature of 20 °C, $IL_{Measured}$ is the measured sound intensity level (dBA) at temperature of *AirTemp* (°C).

Anfosso-LédéE and Pichaud, 2007 [311] reported the following relationship between air temperature, pavement temperature and tire surface temperature.

$$\begin{cases} T_{pavement} = 1.7T_{air} - 4.5(°C) \\ T_{tire} = 1.05T_{air} + 15.8(°C) \end{cases} \tag{23}$$

where both have good correlations ($R^2 = 0.94$). The data were from two normal tires (165/65R13) on seven different pavements using Controlled Pass-By (CPB) method. The temperature coefficients were listed in Table 14. It was indicated that cement concrete pavements have little temperature effect and correlation is not good. It was also shown that the temperature effect is highest in low and high frequency range (below 500 Hz and above 2000 Hz), which can be explained by generating mechanisms rather than propagation. Therefore, temperature has relatively smaller effect on the overall noise level after A-weighting since spectral content in low and high frequencies is reduced.

Table 14. Temperature coefficients of the relationship between pass-by noise level at 90 km/h and air, pavement or tire temperatures, per road pavement category (source from Anfosso-LédéE and Pichaud, 2007 [311], Table 5; reprinted with permission from Elsevier).

Temperature Coefficient	Dense Asphalt	Porous Asphalt (Porosity > 10%)	Cement Concrete
α_{air} (ref. T_{air}) [dBA/°C]	−0.10	−0.06	−0.03
$\alpha_{pavement}$ (ref. $T_{pavement}$) [dBA/°C]	−0.06	−0.04	−0.02
α_{tire} (ref. T_{tire}) [dBA/°C]	−0.09	−0.05	−0.03

The temperature coefficients also depend on the type of tires. Sandberg (2004) [308] reported a positive coefficient has been observed with a specific tire. Jabben and Potma (2013) [316] also reported that α is generally negative but can be positive in some special case, such as for a lug pattern of commercial vehicle tire in frequencies of 315 and 630 Hz.

For different speeds, the temperature coefficient can be also different. Jabben and Potma (2013) [316] reported that for the dense asphalt concrete (DAC), the temperature coefficient for statistical pass-by measurements (SPB) varies from −0.03 to −0.12 dB/°C as the vehicle speed increases from 50 to 140 km/h. The average temperature coefficient for trucks is −0.02 dB/°C. The temperature coefficient used by Dutch standard is −0.05 dB/°C for passenger cars and −0.03 dB/°C for trucks.

Konishi et al. (1995) [310] correlated the temperature coefficient with the elastic modulus change of the tread compound, as given by

$$\begin{aligned}
\alpha \quad &= kr \times \Delta T \times \Delta E30 \\
&= -5.63 \times 1.20 \times \Delta E30 \text{ (Air Temperature)} \\
&= -5.63 \times 0.82 \times \Delta E30 \text{ (Pavement Temperature)}
\end{aligned} \tag{24}$$

where α is temperature coefficient for air or pavement temperature, kr is a coefficient, ΔT is the correction coefficient from air or pavement temperature change to tire temperature change, $\Delta E30$ is the tread rubber elastic modulus change rate at 30 °C (tire temperature).

6.2. Air Humidity

Air humidity or moisture is related to pavement wetness discussed above. Moisture can change the structural strength of unbound materials in the pavement layers. Longitudinal profile can also be affected by subgrade moisture (Bae et al., 2006 [317]). Higher humidity or rainfall may clean the pavement and change the texture (Mcdaniel et al., 2014 [207]). On the other hand, distresses or damages such as potholes, stripping, swelling or depressions may also be caused. In addition, higher air humidity reduces sound propagation.

6.3. Wind

It was shown that even for near-field OBSI measurements with windscreen, some contribution from aerodynamically generated background noise is present mainly at low frequencies (Donavan, 2012 [318]), decreasing the signal to noise ratio (SNR) especially when the vehicle speed is slow. Therefore, many TPIN measurement standards require that wind speed should be less than 5 m/s, e.g., 3.5 m/s in OBSI standard (AASHTO, 2013 [315]).

Besides wind speed, the wind contamination noise is also related to wind direction. The noise levels increased by 1 to 2 dBA when the wind direction is towards the measurement instrument and decreased by 1 to 2 dBA when the wind direction is away from the measurement instrument (Syamkumar et al., 2013 [5]).

7. Summary

The driver influence parameters affecting TPIN are summarized in Table 15. It can be seen that vehicle speed is the most important single parameter influencing TPIN over all frequencies. Accelerating, braking or cornering also largely increases TPIN due to the increase of stick/slip mechanism, especially at higher frequencies. The effects of tire load and inflation pressure are insignificant. Positive camber angle is favorable for TPIN reduction at higher frequencies.

The tire-related parameters affecting TPIN are summarized in Table 16. The tire type (radial/biased) and size can influence TPIN, however, the most important tire parameters are those affecting the contact characteristics between the tire treadband and the pavement, such as tread porosity, embedded stud, wear/aging, and rubber hardness. The parameters that affect the mechanical characteristics of the tire, such as belt stiffness, damping loss factor, non-uniformity, tire cavity content, and rolling resistance, are less influential. The tire width has a greater influence on TPIN than tire diameter.

The tread pattern parameters affecting TPIN are summarized in Table 17. It is shown that appropriate tread pattern optimization is able to reduce TPIN, such as increasing the offset between the tread blocks, and increasing the tread groove ventilation. However, the effects of many other tread pattern design techniques are marginal, such as normal randomization, addition of small sipes. It should be noted that, very few studies have conclusively and quantitatively reported the effect of tread pattern on TPIN, even though the general public considered the tread pattern as an important factor influencing TPIN.

The pavement-related parameters affecting TPIN are summarized in Table 18. It can be seen that the most important factor is the pavement texture, especially the macro- and mega-texture; so are the related or derivative parameters, such as mean profile depth, IRI, positive or transverse or anisotropic texture, joints, wear/age, and surface rating. Some parameters have an effect on the air pumping mechanism, such as porosity, sound absorption, and airflow resistance; some parameters have an effect on the impact mechanism, such as thickness of the pavement layer, and stiffness. However, the normal adhesion or tangential friction of the pavement is shown to be of little influence. In addition, it is widely known that wet pavement is noisier than dry pavement.

The environmental parameters affecting TPIN are summarized in Table 19. The environmental parameters have an influence on the sound propagation and thus on the noise level measured in the far field. However, if these parameters are within the normal range when at least the field tests can be successfully conducted, they can be ignored.

Table 15. Summary of driver influence parameters affecting TPIN.

No.	Parameter	Pertinent Frequency [Hz]	Relation (↑↓)	Potential Noise Variation [dB]	Measurement Equipment	Relevant Mechanism	References
1	Speed	250–8000	↑	25	Speedometer, wheel/axle-mounted encoder, GPS	Various: impact, air pumping	[5,11,12]
2	Longitudinal Force/Slip	800–1600	↑	10	Accelerometer	Stick/slip	[35–38]
3	Lateral Force/Slip	1000–8000	↑	7	Accelerometer, gyroscope	Stick/slip	[1,43,44]
4	Tire Load	800–1600	↑	2	Dynamometer	Impact, air pumping	[51–59]
5	Inflation Pressure	1600–3200	Complex	1	Tire pressure gauge/sensor	Impact, air pumping	[53,319]
6	Tire Camber Angle	1000–3000	↓	5	Protractor	Impact, stick/slip	[74]

Table 16. Summary of tire-related parameters affecting TPIN.

No.	Parameter	Pertinent Frequency [Hz]	Relation (↑↓)	Potential Noise Variation [dB]	Measurement Equipment	Relevant Mechanism	References
1	Tire Type/Construction	N/A	Complex	3	N/A	Various	[80–84]
2	Tire Width	500–1000	↑	3	Measure tape	Various	[94,320]
3	Tire Diameter	N/A	↓	1	Measure tape	Impact, horn	[92,96,320]
4	Belt Stiffness	500–8000	↓	2	Loading test rig with bar	Tire resonance	[16,98,321]
5	Damping (Loss Factor)	250–500	↓	1	N/A	Tire resonance	[64]
6	Non-uniformity	20–200	↑	1	Wheel balancing machines	Tire resonance	[16,26]
7	Rubber Hardness	1000–3000	↑	3	Durometer	Stick/slip	[105,322]
8	Wear/Aging	1000–3000	↑ (then ↓)	5	N/A	Various	[129,323–325]
9	Retreaded	500 and 2000–3000	Complex	2	N/A	Impact	[130,131,326]
10	Studded	400–3000 and above 5000	↑	6	N/A	Impact, stick/slip	[327,328]
11	Tread Porosity	N/A	↓	7	N/A	Air pumping, horn effect	[134,135]
12	Tire Cavity Content	400–1100	Complex (↓)	2	N/A	Cavity resonance	[66,136,137]
13	Rolling Resistance	N/A	↑ (Weak correlation)	0	Dynamometer drum: ISO 18164 [141]	N/A	[76,138–140]

Table 17. Summary of tread pattern parameters affecting TPIN.

No.	Parameter	Pertinent Frequency [Hz]	Relation (↑↓)	Potential Noise Variation [dB]	Measurement Equipment	Relevant Mechanism	References
1	Randomization	600–1000	↓	0 or marginal	N/A	Tread impact	[1,179]
	Elimination of Groove Footprint Coinciding	800–1000	↓	N/A	N/A	Tread impact	[1,179]
	Offset between Left and Right Side	N/A	↓	5	Caliper	Tread impact	[1,179,329]
2	Rotation Direction / Side Asymmetry	N/A	↑	3	N/A	Various	[1,179]
3	Ventilation	800–1000 and 1600–4000	↓	2	N/A	Air pumping, air resonance	[1,130,179]
4	Addition of Mirror Image Grooves	Above 4000	↓	0	N/A	Air pumping, air resonance	[1,179]
	Addition of Lamellae	800–1000	↓	N/A	N/A	Air pumping, air resonance	[1,179]
	Groove Width	800–2000	↑ 9 mm ↓	N/A	Caliper	Air pumping	[1,130,179]
	Groove Angle (Relative to Lateral)	800–2000	↓	N/A	Protractor	Tread impact	[1,130,179]

Table 18. Summary of pavement-related parameters affecting TPIN.

No.	Parameter	Pertinent Frequency [Hz]	Relation (↑↓)	Potential Noise Variation [dB]	Measurement Equipment	Relevant Mechanism	References
1	Micro-texture (below 0.5 mm)	2000–4000	↓	N/A but Marginal	Laser profiler: ISO 13473 [203]; Circular Track Meter (CTM): ASTM E2157 [205] for macro-texture only	Stick/slip, stick/snap	[208,209]
	Macro-texture (0.5–50 mm)	100–1000 and 2000–4000	↓ and (10 mm) ↑	N/A but Significant		Texture impact, air pumping	[207,210,211]
	Mega-texture (50–500 mm)	100–1000	↑	N/A but Significant		Texture impact	[211,216]
	Unevenness (500–800 mm)	N/A	↑	4		N/A	[181]
	Unevenness (10–50 m)	200–1500	↓	1			
2	MPD/MTD/ Texture	N/A	Complex	10	Sand patch method: ASTM E965 [214], ASTM E1845 [215] and ISO 13473-1 [189]	Same as macro-texture	[221]
3	International Roughness Index (IRI)	Same as unevenness	Same as unevenness	Same as unevenness	Profilometer: ASTM E1926 [224] and ASTM E1364 [225]	Same as unevenness	[223]
4	Positive versus Negative Texture	N/A	↑	N/A	Laser profiler	Texture impact, air pumping	[13]
5	Transverse Texture	N/A	↑	N/A	Laser profiler	Texture impact	[228]
6	Anisotropic Texture	N/A	↑	N/A	Laser profiler	Texture impact, air pumping	[229]
7	Joints	800–1000	↑	3	Laser profiler	Texture impact, air pumping	[12,231,233–236]
8	Porosity	500–1600 and 3000	↓	7	Pavement core sample: ASTM D7063/D7063M [246]	Various	[330–333]

Table 18. *Cont*.

No.	Parameter	Pertinent Frequency [Hz]	Relation (↑↓)	Potential Noise Variation [dB]	Measurement Equipment	Relevant Mechanism	References
9	Sound Absorption	Similar to Porosity	Similar to Porosity	Similar to Porosity	Impedance tube: ISO 10534-1 [253] and ISO 13472-1 [256]	Pavement Absorption	[59,334,335]
10	Airflow Resistance	N/A	↑	N/A	Impedance tube: ISO 9053 [259] and ANSI/ASA S1.18 [260]	Air pumping, air resonance	[222,336,337]
11	Thickness of Layer	500–1600	↓	5	Measure tape	Acoustic and mechanical impedance	[1]
12	Stiffness (Mechanical Impedance)	800–1250	↑	1	Impact hammer device: AASHTO T 342 [275]	Vibration Transfer	[265–269]
13	Normal Adhesion	2000–4000	↑	1	N/A	Stick/snap	[1]
14	Tangential Friction	2500–6300	↑	0	Dynamic Friction Tester (DFT): ASTM E1911 [283]	Stick/slip	[76]
15	Wear/Age	1000–4000	↑	2	N/A	Impact, absorption	[250,262,290,293]
16	Surface Rating (SR)	N/A	↓	N/A	N/A	Impact	[296,297]
17	Wetness	Above 1000 Hz	↑	3	N/A	Water splash effect	[5,299,300]
18	Mixture Parameters/Materials	N/A	Complex	Significant	N/A	Various	[303,304]

Table 19. Summary of environmental parameters affecting TPIN.

No.	Parameter	Pertinent Frequency [Hz]	Relation (↑↓)	Potential Noise Variation [dB]	Measurement Equipment	Relevant Mechanism	References
1	Temperature	1000–4000	↓	3	Thermometer	Impact	[310,311]
2	Air Humidity	N/A	↓	1	Air humidity meter	Sound propagation	[317]
3	Wind	300 and 2000	↑	N/A	Wind meter	Air Turbulence	[5,318]

8. Conclusions

In the present paper, the influencing parameters on tire–pavement interaction noise (TPIN) were reviewed. In general, on the same pavement and under the same environmental conditions, the most important parameters are speed, longitudinal force/slip (acceleration), wear/aging, and tread pattern. The tread pattern might not be the most important influencing factor, but it is considered to be the most easily modified property of a tire. The pavement parameters, such as pavement texture, are usually more important than tread pattern and other tire parameters. However, it should be noted that some studies on the influencing parameters were mostly based on the experimental measurements sometimes without reasonable theoretical explanations. In the future, theory development and experimental validation should be more consolidated to reveal the physical mechanisms and the influencing parameters on TPIN. The trend of TPIN control might not only focus on the reduction of the noise level, but also on the tuning of the spectral shape. The sound quality potentially will attract more attention.

Conflicts of Interest: The author declares no conflicts of interest.

References

1. Sandberg, U.; Ejsmont, J.A. *Tyre/Road Noise Reference Book*; INFORMEX: Kisa, Sweden; Harg, Sweden, 2002; ISBN 9789163126109, 9163126109.

2. Li, T.; Burdisso, R.; Sandu, C. Literature review of models on tire-pavement interaction noise. *J. Sound Vib.* **2018**, *420*, 357–445. [CrossRef]

3. Li, T. A state-of-the-art review of measurement techniques on tire–pavement interaction noise. *Meas. J. Int. Meas. Confed.* **2018**, *128*, 325–351. [CrossRef]

4. Li, T. Literature Review of Tire-Pavement Interaction Noise and Reduction Approaches. *J. Vibroeng.* **2018**, *20*, 2424–2452. [CrossRef]

5. Syamkumar, A.; Aditya, K.; Chowdary, V. Development of mode-wise noise prediction models for the noise generated due to tyre-pavement surface interaction. *Adv. Mater. Res.* **2013**, *723*, 50–57. [CrossRef]

6. Sorenson, S.; Jorro, S. Effect of exterior absorption on heavy vehicle tire/surface noise at highway speeds. In Proceedings of the 41st International Congress and Exposition on Noise Control Engineering 2012, INTER-NOISE 2012, New York, NY, USA, 19–22 August 2012; Volume 2, pp. 889–900.

7. Buckers, C.; Stockert, U. Quiet Road Traffic 3—Interdisciplinary approach to reduce the noise emission at the source. In Proceedings of the European Conference on Noise Control, Prague, Czech Republic, 10–13 June 2012; pp. 984–991.

8. Biermann, J.-W.; Viehofer, J. Development of cars specified for tire-road noise measurement. In Proceedings of the 41st International Congress and Exposition on Noise Control Engineering 2012, INTER-NOISE 2012, New York, NY, USA, 19–22 August 2012; Volume 11, pp. 9230–9241.

9. Kim, H. A Study of Wheel Guards for Reduction of High Frequency Road-Noise. *SAE Int. J. Passeng. Cars Mech. Syst.* **2015**, *8*, 46–51. [CrossRef]

10. Li, T.; Feng, J.; Burdisso, R.; Sandu, C. The Effects of Speed on Tire-Pavement Interaction Noise (Tread-Pattern-Related Noise and Non-Tread-Pattern-Related Noise). In Proceedings of the 35th Annual Meeting and Conference on Tire Science and Technology, Akron, OH, USA, 13–14 September 2016.

11. Sandberg, U. Tyre / road noise—Myths and realities. In Proceedings of the 2001 International Congress and Exhibition on Noise Control Engineering, The Hague, The Netherlands, 27–30 August 2001.

12. Dare, T.; Bernhard, R. Accelerometer Measurements of Tire Tread Vibrations and Implications to Wheel-Slap Noise. *Tire Sci. Technol.* **2013**, *41*, 109–126.

13. Beckenbauer, T.; Kuijpers, A. Prediction of pass-by levels depending on road surface parameters by means of a hybrid model. In Proceedings of the Inter-Noise, The Hague, The Netherlands, 27–30 August 2001; pp. 2528–2533.

14. Kuijpers, A.; van Blokland, G. Tyre/road noise models in the last two decades: A critical evaluation. In Proceedings of the Inter-Noise, The Hague, The Netherlands, 27–30 August 2001; p. 2494.

15. Mogrovejo, D.E.; Flintsch, G.W.; de León Izeppi, E.D.; McGhee, K.K. Effect of Air Temperature and Vehicle Speed on Tire/Pavement Noise Measured with On-Board Sound Intensity Methodology. In Proceedings of the 92nd Annual Meeting on Transportation Research Board (TRB), Washington, DC, USA, 13–17 January 2013.

16. Ejsmont, J.A. *Tire/Road Noise: Comparison of Road and Laboratory Measurements and Influence of Some Tire Parameters on Generation of Sound*; VTI Rapport nr 244A; Statens Väg-och Trafikinstitut: Linköping, Sweden, 1982; 47p.

17. Anderson, D.G.; Landers, S.P. On-board passenger tire sound generation study road versus lab wheel. In *SAE Technical Papers*; SAE International: Warrendale, PA, USA, 1976.

18. Nilsson, N.-A. On generating mechanisms for external tire noise. In *SAE Technical Papers*; SAE International: Warrendale, PA, USA, 1976.

19. Anonymous. *Truck Tire Noise*; Rubber Manufacturers Association (RMA): Washington, DC, USA, 1971.

20. Corcoran, D.A. Effects of operating parameters on truck tire sounds. In *SAE Special Publication*; SAE SP-373, Paper 720925; SAE International: Warrendale, PA, USA, 1972.

21. Walker, J.C.; Williams, A.R. The improvement of noise and traction due to road/tire interaction. In Proceedings of the International Tire Noise Conference 1979, Stockholm, Sweden, 29–31 August 1979.

22. Tetlow, D. *Truck Tire Noise—An Initial Survey of Tire Noise Variables*; Report; General Motors Proving Ground: Milford, MI, USA, 1968.

23. Hamet, J.-F. Measurement of power and directivity of tire/road surface noise. In Proceedings of the INTER-NOISE 88, Avignon, France, 30 August–1 September 1988.

24. Köhler, E.; Liedl, W. Grenzen der Beeinflussungdes Reifenabrollgerausches bei nasser Fahrbahn. In *Entwicklungslinien in Kraftfahrzeu-technik und Strassenverkehr, Forschungsbilanz*; TUV Rheinland: Cologne, Germany, 1981.

25. Steven, H.; Pauls, H. *Entwicklung Eines Messverfahrens für das Reifen-Fahrbahn-Geräusch*; Report from FIGE; FIGE: Herzogenrath, Germany, 1990.

26. Ivannikov, A.; Haberkorn, U.; Langenberg, H. *Einflussgrössen auf Riefen/Fahrbahn-Geräusche eines LKW bei unterschiedlichen Fahrbedingunen*; FAT Schriftenreihe Nr. 158; Forschungsvereinigung Automobiltechnik e.v. (FAT): Berlin, Germany, 1998.

27. Steven, H.; Küppers, D.; van Blokland, G.J.; van Houten, M.H.; van Loon, R. *International Validation Test for the Close Proximity (CPX) Method*; TÜV: Albstadt, Germany, 2000.

28. Ho, K.-Y.; Hung, W.-T.; Ng, C.-F.; Lam, Y.-K.; Leung, R.; Kam, E. The effects of road surface and tyre deterioration on tyre/road noise emission. *Appl. Acoust.* **2013**, *74*, 921–925. [CrossRef]

29. Lopez Arteaga, I. Green's functions for a loaded rolling tyre. *Int. J. Solids Struct.* **2011**, *48*, 3462–3470. [CrossRef]

30. Kim, Y.J.; Bolton, J.S. Effects of rotation on the dynamics of a circular cylindrical shell with application to tire vibration. *J. Sound Vib.* **2004**, *275*, 605–621. [CrossRef]

31. Huang, S.C.; Soedel, W. Effects of coriolis acceleration on the free and forced in-plane vibrations of rotating rings on elastic foundation. *J. Sound Vib.* **1987**, *115*, 253–274. [CrossRef]

32. Huang, S.C.; Soedel, W. Effects of Coriolis acceleration on the forced vibration of rotating cylindrical shells. *J. Appl. Mech.* **1988**, *55*, 231–233. [CrossRef]

33. Schuhmacher, A. Blind Source Separation Applied to Indoor Vehicle Pass-By Measurements. *SAE Int. J. Passeng. Cars Mech. Syst.* **2015**, *8*, 1034–1041. [CrossRef]

34. Ulrich, S. *Rollgeräuschmessungen der Bundesanstalt für Strassenwesen an Strassen mit unterschiedlichen Decken und an einem Innentrommelprüfstand (Rolling Noise Measurements of the Federal Highway Research Institute on Roads with Different Ceilings and an Indoor Drum)*; Mitteilung Nr. 57; Institut für Strassen- und Eisenbahn- und Felsbau and der E.T.H.: Zürich, Switzerland, 1984; p. 207.

35. Donavan, P.R. Tire-Pavement Interaction Noise Measurement under Vehicle Operating Conditions of Cruise and Acceleration. In Proceedings of the Noise and Vibration Conference, Traverse City, MI, USA, 10–13 May 1993; Society of Automotive Engineers: Warrendale, PA, USA, 1993.

36.　Iwao, K.; Yamazaki, I. A study on the mechanism of tire/road noise. *JSAE Rev.* **1996**, *17*, 139–144. [CrossRef]

37.　ISO. *Measurement of Noise Emitted by Accelerating Road Vehicles—Engineering Method—Part 1: M and N Categories*; ISO 362-1; ISO: Geneva, Switzerland, 2015.

38.　Moore, D.B. The Revised ISO 362 Standard for Vehicle Exterior Noise Measurement. *Sound Vib.* **2006**, *40*, 19–23.

39.　Donavan, P.R. Assessment of tire/pavement interaction noise under vehicle passby test conditions using sound intensity measurement methods. *J. Acoust. Soc. Am.* **1998**, *103*, 2919. [CrossRef]

40.　Yamazaki, S.; Fujikawa, T.; Hosegawa, A.; Ogasawara, S. Indoor test procedure for evaluation of tire treadwear and influence of suspension alignment. *Tire Sci. Technol.* **1989**, *17*, 236–273. [CrossRef]

41.　Ejsmont, J.A. Tire/road noise and rolling resistance - is there a trade-off? In Proceedings of the International Tire/Road Noise Conference 1990, Gothenburg, Sweden, 8–10 August 1990; pp. 439–452.

42.　Donavan, P.R. *Quantification of Noise Mechanisms for a Straight-Ribbed, HCR Bias-Ply Truck Tire*; Report No. EM-547; General Motors Research Laboratories: Warren, MI, USA, 1982.

43.　Senda, T.; Nakai, M.; Yokoi, M.; Chiba, Y. Tire squeal. *Bull. Jpn. Soc. Mech. Eng. (Japan)* **1984**, *27*, 2016–2023. [CrossRef]

44.　Trivisonno, N.M.; Beatty, J.R.; Miller, R.F. Origin of tire squeal—2. *Rubber Chem. Technol.* **1968**, *41*, 953–976. [CrossRef]

45.　Reiter, W.F.; Eberhardt, A.C. Experimental investigation of truck tire noise generated through tire vibration. In Proceedings of the INTER-NOISE 74, Washington, DC, USA, 30 September–2 October 1974; p. 467.

46.　Dare, T.P. Generation Mechanisms of Tire-Pavement Noise. Ph.D. Thesis, Purdue University, West Lafayette, IN, USA, 2012.

47.　Taryma, J.A.E.S. Halas Opon Samochodow Osobowych Poruszajacych Sie Posuchych Nawierzchniach Asfaltowych I Betonowych (Tire Noise of Cars Moving on the Dry Surfaces of Asphalt and Concrete). Ph.D Thesis, Technical University of Gdansk, Gdansk, Poland, 1982. (In Polish)

48.　Leasure, W.A., Jr.; Bender, E.K. Tire-road interaction noise. *J. Acoust. Soc. Am.* **1975**, *58*, 39–50. [CrossRef]

49.　Sandberg, U.; Kropp, W.; Larsson, K. The multi-coincidence peak around 1kHz in tyre/road noise spectra. *Acta Acust. United Acust.* **2003**, *89*, S84.

50.　Tong, G.; Wang, Q.; Yang, K.; Wang, X.C. An experiment investigation to the radial tire noise. *Adv. Mater. Res.* **2013**, *694–697*, 361–365. [CrossRef]

51.　Leasure, W.A.; Corley, D.M.; Flynn, D.R.; Forrer, J.S. *Truck Noise—I. Peak A-Weighted Sound Levels Due to Truck Tires*; Report No. OST/TST-72-1; National Bureau of Standards, Building Research Division: Washington, DC, USA, 1972.

52.　Kilmer, R.D. Test Procedures for Future Tire Noise Regulations. In Proceedings of the P-70, SAE Highway Tire Noise Symposium, San Francisco, CA, USA, 10–12 November 1976; Society of Automotive Engineers: Warrendale, PA, USA, 1976.

53.　Kilmer, R.D.; Cadoff, M.A.; Mathews, D.E.; Shoemaker, C.O. *Effects of Load, Inflation Pressure and Tire Deflection on Truck Tire Noise Levels*; DOT-HS-803 874; US Department of Transportation: Washington, DC, USA, 1979; 49p.

54.　Underwood, M.C.P. *THe Origins of Tire Noise*; University of Southampton, Institute of Sound and Vibration Research: Southampton, UK, 1980.

55.　Nelson, P.M.; Underwood, M.C.P.; Nelson, P.M. Lorry Tire Noise. In Proceedings of the Vehicle Noise and Vibration, London, UK, 5–7 June 1984.

56.　Walker, J.C. Noise Generated at the Tire-Road Interface. Ph.D. Thesis, TD 1292, Dunlop Ltd., Birmingham, UK, 1981.

57.　Köllman, A. *Ermittlung des Standes der Technik hinsichtlich der Geräuschemission von PKW-Reifen*; Research Report 105 05 144; FIGE GmbH: Herzogenrath, Germany, 1993.

58.　Wolf, A.; Schuh, B.-M.; Krauss, O. *Erfassung des Wissenstandes über Reifen/Fahrbahngeräusche beim Nutzfahrzeug*; FAT Schriftenreihe Nr. 97; Forschungsvereinigung Automobiltechnik e.v. (FAT): Frankfurt, Germany, 1992.

59.　Von Meier, A.; van Bloklan, G.J.; Descornet, G. The influence of texture and sound absorption on the noise of porous road surfaces. In Proceedings of the of the Second International Symposium of Road Surface Characteristics, Technical University of Berlin, Berlin, Germany, 23–26 June 1992.

60.　Heckl, M. Tire noise generation. *Wear* **1986**, *113*, 157–170. [CrossRef]

61.　Bharadwaja, B.V.S.S.; Siva, P.N. A Numerical Study on the Influencing Parameters of Tire-acoustic Cavity. *Appl. Mech. Mater.* **2013**, *459*, 390–395. [CrossRef]

62. Beniguel, J.F.; Le Pen, D. Tire-alone criterion for structure borne road noise performance. In Proceedings of the International Conference on Noise and Vibration Engineering 2012 (ISMA 2012), Leuven, Belgium, 17–19 September 2012; Volum 2, pp. 1527–1539.

63. Kropp, W.; Larsson, K.; Wullens, F.; Andersson, P.; Becot, F.-X.; Beckenbauer, T. The modeling of tyre/road noise—A quasi three-dimensional model. In Proceedings of the INTER-NOISE 01, The Hague, Holland, 27–30 August 2001; p. 2322.

64. Keltie, R.F. Analytical model of the truck tire vibration sound mechanism. *J. Acoust. Soc. Am.* **1982**, *71*, 359. [CrossRef]

65. Tong, G.; Jin, X.; Tian, W.; Yang, K. Simulation on factors affecting radial tire noise. *J. Converg. Inf. Technol. (Korea)* **2013**, *8*, 209–216.

66. Bolton, J.S.; Song, H.J.; Kim, Y.K.; Kang, Y.J. Wave number decomposition approach to the analysis of tire vibration. In Proceedings of the National Conference on Noise Control Engineering, Ypsilanti, MI, USA, 5–8 April 1998; pp. 97–102.

67. Bremner, P.; Huff, J.; Bolton, J.S. A model study of how tire construction and materials affect vibration-radiated noise. In *SAE Technical Papers*; SAE International: Warrendale, PA, USA, 1997.

68. Samuels, S. Recent Australian Tyre/Road Noise Research. In Proceedings of the International Tire Noise Conference; STU-Information No. 168-1980. NUTEK: Stockholm, Sweden, 1979; pp. 1–25.

69. Muthukrishnan, M. Effects of material properties on tire noise. In *SAE Technical Papers*; SAE International: Detroit, MI, USA, 1990.

70. Kostial, P.; Jancikova, Z.; Bakosova, D.; Valicek, J.; Harnicarova, M.; Spicka, I.; Kotial, P.; Bakoova, D.; Picka, I. Artificial Neural Networks Application in Modal Analysis of Tires. *Meas. Sci. Rev.* **2013**, *13*, 273–278. [CrossRef]

71. Anonymous. *Foreign Research in TIre Noise*; Office of Noise Abatement and Control, U.S., Environmental Protection Agency: Washington, DC, USA, 1980.

72. Kindt, P.; De Coninck, F.; Sas, P.; Desmet, W. Analysis of tire/road noise caused by road impact excitations. In *SAE Technical Papers*; SAE International: St. Charles, IL, USA, 2007.

73. Kindt, P.; De Coninck, F.; Sas, P.; Desmet, W. Experimental modal analysis of radial tires under different boundary conditions. In Proceedings of the 13th International Congress on Sound and Vibration 2006, ICSV 2006, Vienna, Austria, 2–6 July 2006; Volume 6, pp. 5111–5118.

74. Wozniak, R.; Taryma, S.; Mioduszewski, P. Tire camber angle influence on tire-pavement noise. *Noise Control Eng. J.* **2015**, *63*, 216–224. [CrossRef]

75. Reinink, H.F.; de Graaff, D.F.; Peeters, A.A.A.; Peeters, H.M. *Tyre/Road Noise Measurements of Truck Tyres*; Report No. M+P.DWW.03.7.1 (5 February 2005); M+P Raadgevende ingenieurs B.V.: Vught, The Netherlands, 2005.

76. Sandberg, U.; Ejsmont, J.A. Noise emission, friction and rolling resistance of car tiressummary of an experimental study. In Proceedings of the NOISE-CON 2000, Newport Beach, CA, USA, 3–8 December 2000.

77. Takahashi, M.; Iimura, K.; Hidaka, Y.; Tachibana, H. Sound power levels of road vehicles measured using a reverberant tunnel—Statistical analysis. In Proceedings of the INTER-NOISE 95, Newport Beach, CA, USA, 10–12 July 1995; pp. 207–210.

78. Mioduszewski, P. Vehicle noise simulation—Computer program. In Proceedings of the EURO/NOISE '95 Symposium, Lyon, France, 21–23 March 1995.

79. Chang, L. Numerical method of evaluating noise from vibrating tyre. *Appl. Mech. Mater.* **2012**, *105–107*, 719–722. [CrossRef]

80. VTI. *Effects of Winter Tyres—State of the Art IN SWEDISH*; VTI Rapport 543; Swedish National Road and Transport Research Institute: Linköping, Sweden, 2006.

81. Tanizaki, T.; Ueda, K.; Murabe, T.; Nomura, H.; Kamakura, T. Discrimination between summer and winter tires using tire/road noises emitted by running vehicles. *IEEJ Trans. Ind. Appl.* **2013**, *133*, 558–565. [CrossRef]

82. Bekke, D.; Wijnant, Y.; Weegerink, T.; De Boer, A. Tire-road noise: An experimental study of tire and road design parameters. In Proceedings of the 42nd International Congress and Exposition on Noise Control Engineering 2013, INTER-NOISE 2013: Noise Control for Quality of Life, Innsbruck, Austria, 15–18 September 2013; Volume 1, pp. 173–180.

83. Seamenn, E.U. Development of low noise tyres in EU project SILENCE. In Proceedings of the Paris Acoustics, Paris, France, 29 June–4 July 2008.

84. Bernhard, R.J.; Thornton, W.D.; Baumann, J. *Effects of Varying the Tire Cap Ply, Sidewall Filler Height and Pavement Surface Texture on Tire/Pavement Noise Generation*; SQDH 2003-1, Final Report; Purdue University: West Lafayette, IN, USA, 2003; p. 90.

85. El-Gindy, M.; Lewis, H.L.; Lewis, A.S. Development of a tire/pavement contact-stress model based on an artificial neural network. In *American Society of Mechanical Engineers, Design Engineering Division (Publication) DE*; ASME: New York, NY, USA, 1999; Volume 101, pp. 25–34.

86. Moore, D.F. *The Friction of Pneumatic Tires*; Elsevier: Amsterdam, The Netherlands, 1975.

87. Aboutorabi, H.M.R.; Kung, L. Application of Coupled Structural Acoustic Analysis and Sensitivity Calculations to a Tire Noise Problem. *Tire Sci. Technol.* **2012**, *40*, 25–41. [CrossRef]

88. Staadt, R.L. *Truck Noise Control*; SAE Publ. SP-386; Society of Automotive Engineers: New York, NY, USA, 1974.

89. Fong, S. Tyre noise predictions from computed road surface texture induced contact pressure. In Proceedings of the INTER-NOISE 98, Christchurch, New Zealand, 16–18 November 1998; pp. 137–140.

90. Pei, X.; Wang, G.; Zhou, H.; Zhao, F.; Yang, J. Influence of tread structure design parameters on tire vibration noise. In Proceedings of the SAE-China Congress 2015: Selected Papers; Society of Automotive Engineers: New York, NY, USA, 2015; Volume 364, pp. 325–338.

91. Saemann, E.-U.; Dimitri, G.; Kindt, P. Tire Requirements for Pavement Surface Characteristics. In Proceedings of the 7th Symposium on Pavement Surface Characteristics: SURF 2012, Norfolk, VA, USA, 19–22 September 2012; pp. 1–33.

92. Kumar, A.; Tandon, A.; Paul, S.; Singla, A.; Kumar, S.; Vijay, P.; Bhangale, U.D. Influence of Tyre's Dimensional Characteristics on Tyre-Pavement Noise Emission. *Phys. Rev. Res. Int.* **2011**, *1*, 124–137.

93. Sandberg, U.; Ejsmont, J. Tire/road noise—A subject of international concern. In Proceedings of the INTER-NOISE 88, Avignon, France, 30 August–1 September 1988; p. 1309.

94. Yang, J.S.; Fwa, T.F.; Ong, G.P.; Chew, C.H. Finite-element analysis of effect of wide-base tire on tire-pavement noise. *Adv. Mater. Res.* **2013**, *723*, 105–112. [CrossRef]

95. Storeheier, S.A.; Sandberg, U. Vehicle Related Parameters Affecting Tyre/Road Noise. In Proceedings of the International Tire/Road Noise Conference, Gothenburg, Sweden, 8–10 August 1990; STU-Information No. 794-1990; NUTEK: Stockholm, Sweden, 1990.

96. Mohamed, Z.; Wang, X. A study of tyre cavity resonance and noise reduction using inner trim. *Mech. Syst. Signal Process.* **2015**, *50–51*, 498–509. [CrossRef]

97. Tanaka, Y.; Horikawa, S.; Murata, S. An evaluation method for measuring SPL and mode shape of tire cavity resonance by using multi-microphone system. *Appl. Acoust.* **2016**, *105*, 171–178. [CrossRef]

98. Kropp, W.; Larsson, K.; Barrelet, S. The influence of belt and tread band stiffness on the tyre noise generation mechanisms. In Proceedings of the International Congress on Acoustics (ICA) 1998, Seattle, WA, USA, 20–26 June 1998.

99. Landau, L.D.; Lifshitz, E.M. *Theory of Elasticity*, 3rd ed.; Butterworth-Heinemann: Oxford, UK, 1986; Volume 7, ISBN 978-0-7506-2633-0.

100. O'Boy, D.J.; Dowling, A.P. Tyre/road interaction noise-Numerical noise prediction of a patterned tyre on a rough road surface. *J. Sound Vib.* **2009**, *323*, 270–291. [CrossRef]

101. Watanabe, T.; Tomita, N.; Kishinami, S.; Yamaguchi, H.; Konishi, S.; Kawana, A. Noise generation mechanism of cross-bar tyres and countermeasures against it. *Int. J. Veh. Des.* **1988**, *9*, 641–653.

102. Plotkin, K.J.; Stusnick, E. *A Unified Set of Models for Tire/Road Noise Generation*; Report: WR-81-26; Environmental Protection Agency, Office of Noise Abatement and Control: Arlington, VA, USA, 1981; 63p.

103. Doan, V.Q. Influence of tire construction and tire mold profile on coast-by noise. In *Tire Technology International 1996, The Annual Review of Tire Materials and Tire Manufacturing Technology*; UKi Media & Events: Dorking, Surrey, United Kingdom, 1996.

104. Eberhardt, A.C. Investigations of the truck tire vibration sound mechanisms. In Proceedings of the International Tire Noise Conference, Stockholm, Sweden, 29–31 August 1979.

105. Sandberg, U.; Ejsmont, J.A. Influence of tyre rubber hardness on tyre/road noise emission. In *Turkish Acoustical Society—36th International Congress and Exhibition on Noise Control Engineering, INTER-NOISE 2007 ISTANBUL, Istanbul, Turkey, 28–31 August 2007*; Curran Associates, Inc.: Red Hook, NY, USA, 2007; Volume 1, pp. 394–403.

106. ISO. *Plastics and Ebonite—Determination of Indentation Hardness by Means of a Durometer (Shore Hardness)*; ISO 868; ISO: Geneva, Switzerland, 2003.

107. ASTM. *Standard Test Method for Rubber Property—Durometer Hardness*; ASTM D2240-05(2010); ASTM: West Conshohocken, PA, USA, 2005.

108. Oddershede, J.; Kragh, J. Changes in noise levels from Standard Reference Test Tyres due to increasing tyre tread hardness. In Proceedings of the Forum Acusticum, FA, Krakow, Poland, 7–12 September 2014.

109. Wullens, F.; Kropp, W. Influence of the local stiffness of the rubber layer of the tire on the generation of tire/road noise. In Proceedings of the ICA 2001, Rome, Italy, 2–7 September 2001.

110. Wullens, F. Towards an Optimisation of Tire/Road Parameters for Noise Reduction. Master's Thesis, Report F 02-01. Department of Applied Acoustics, Chalmers University of Technology, Gothenburg, Sweden, 2002.

111. Saemann, E.U. Contribution of the tyre to further lowering tyre/road noise. In Proceedings of the ParisAcoustics'08, Paris, France, 29 June–4 July 2008.

112. Ishige, T.; Furusho, H.; Aoki, Y.; Kawanage, K. Adaptive slip control using a brake torque sensor. In Proceedings of the 9th International Symposium on Advanced Vehicle Control, Kobe, Japan, 6–9 October 2008; Volume 1, pp. 417–422.

113. Rochoux, D.; Biesse, F. Tire/road noise, the tire vibration as the main noise source from road texture. In Proceedings of the 39th International Congress on Noise Control Engineering 2010, INTER-NOISE 2010, Lisbon, Portugal, 13–16 June 2010; Volume 5, pp. 3597–3606.

114. Swieczko-Zurek, B.; Ejsmont, J.; Mioduszewski, P.; Ronowski, G.; Taryma, S. The effect of tire aging on acoustic performance of CPX reference tires. In Proceedings of the 44th International Congress and Exposition on Noise Control Engineering, INTER-NOISE 2015, San Francisco, CA, USA, 9–12 August 2015.

115. Buhlmann, E.; Schulze, S.; Ziegler, T. Ageing of the new CPX reference tyres during a measurement season. In Proceedings of the 42nd International Congress and Exposition on Noise Control Engineering 2013, INTER-NOISE 2013: Noise Control for Quality of Life, Innsbruck, Austria, 15–18 September 2013; Volume 1, pp. 369–376.

116. Schubert, S.; Mannel, M.; Ertsey, M.; Hoever, C. Influence of the tyre impedance on CPX level used to evaluate tyre/road noise. In Proceedings of the INTER-NOISE 2016—45th International Congress and Exposition on Noise Control Engineering: Towards a Quieter Future, Hamburg, Germany, 21–24 August 2016; pp. 4945–4954.

117. Langwieder, K.; Lehnerer, P.; Richlowski, W.; Schneider, D.; Stankowitz, W. *Die Ergebnisse des Reifen Check und deren Bedeutung für die Verkehrssicherheit (The Results of the Tire Check and ist Significance for Traffic Safety)*; VDI-Berichte Nr. 1632, 2001; VDI: Düsseldorf, Germany, 2001.

118. Gothié, M. *Information presented at the meeting of PIARC/C1 in Copenhagen, Denmark, September 2001*; World Road Association (PIARC): La Défense, France, 2001.

119. Gothié, M. *Presentation at the meeting of PIARC/C1 in Rome, Italy, 05*; World Road Association (PIARC): La Défense, France, 2005.

120. Li, T.; Burdisso, R.; Sandu, C. The Effect of Rubber Hardness and Tire Size on Tire-Pavement Interaction Noise. In Proceedings of the 36th Annual Meeting and Conference on Tire Science and Technology, Akron, OH, USA, 12–13 September 2017.

121. ETRTO. *ETRTO Recommendations 2002*; The European Tire and Rim Technical Organization (ETRTO): Brussels, Belgium, 2002.

122. Thiriez, K.; Subramanian, R. *Tire Pressure Special Study: Tread Depth Analysis*; DOT HS 809 359; National Center for Statistics and Analysis: Washington, DC, USA, 2001.

123. Walker, J.C.; Major, D.J. Noise generated at the tire-road interface. In Proceedings of the Annual Conference Stress Analysis Group of Institute of Physics, University of Aston, Birmingham, UK, 2–4 January 1974.

124. Walker, J.C. Noise from the tire-road interface with heavy commercial vehicles. *Trans. Eng.* **1975**, *68*, 11–12.

125. Flanagan, W. Recent studies give unified picture of tire noise. *J. Autom. Eng.* **1972**, *80*, 15–19.

126. Hillquist, R.K.; Carpenter, P.C. *A Basic Study of Automobile Tire Noise*; GM Engineering Publication 5269; General Motors: Milford, MI, USA, 1973.

127. Tetlow, D. Truck Tire Noise. *Sound Vib.* **1971**, *5*, 17–23.

128. Archard, J.F. Contact and Rubbing of Flat Surfaces. *J. Appl. Phys.* **1953**, *24*, 981–988. [CrossRef]

129. Tong, G.; Wang, Q.; Yang, K.; Wang, L. Simulation on the radial tire wear noise. *Appl. Mech. Mater.* **2014**, *488*, 1121–1124. [CrossRef]

130. FEHRL (Forum of European National Highway Research Laboratories). *Tyre/Road Noise*; FEHRL Final Report SI2.408210; FEHRL: Woluwe-Saint-Lambert, Belgium, 2001.

131. Sandberg, U. Survey of noise emission from truck tires. In Proceedings of the Inter-Noise 91, Sydney, Australia, 2–4 December 1991.

132. Sandberg, U. Noise emissions of road vehicles effect of regulations: Final Report 01-1. *Noise News Int.* **2001**, *9*, 147–203. [CrossRef]

133. Johnsson, R.; Nykänen, A. Stud Noise Auralization. *Int. J. Passeng. Cars Mech. Syst.* **2013**, *6*, 1577–1585. [CrossRef]

134. Nilsson, N.-A. Principles in the control of external tire/road noise. In Proceedings of the INTER-NOISE 82, San Francisco, CA, USA, 17–19 May 1982; p. 123.

135. Sandberg, U.; Kalman, B.; Williams, A.R. The porous tread tire—The quietest pneumatic tire measured so far? In Proceedings of the International Congress on Noise Control Engineering 2005, INTERNOISE 2005, Rio de Janeiro, Brazil, 7–10 August 2005; Volume 5, pp. 3996–4005.

136. Pottinger, M.G.; Marshall, K.D.; Lawther, J.M.; Thrasher, D.B. Review Of Tire/Pavement Interaction Induced Noise And Vibration. In *ASTM Special Technical Publication*; BFGoodrich Co: Brecksville, OH, USA, 1986; pp. 183–287.

137. Wang, X.; Mohamed, Z.; Ren, H.; Liang, X.; Shu, H. A study of tyre, cavity and rim coupling resonance induced noise. *Int. J. Veh. Noise Vib.* **2014**, *10*, 25–50. [CrossRef]

138. Ejsmont, J.; Ronowski, G.; Taryma, S.; Mioduszewski, P.; Sobieszczyk, S.; Swieczko-Zurek, B. Relations between tire/road noise and tire rolling resistance on different road pavements. In Proceedings of the 41st International Congress and Exposition on Noise Control Engineering 2012, INTER-NOISE 2012, New York, NY, USA, 19–22 August 2012; Volume 11, pp. 9476–9485.

139. Stenschke, R.; Vietzke, P. Noise and use characteristics of modern car tyres (State of the art). In Proceedings of the 7th International Congress on Sound and Vibration, Garmisch-Partenkirchen, Germany, 4–7 July 2000.

140. Hoever, C.; Kropp, W. A simulation-based parameter study of car tyre rolling losses and sound generation. In Proceedings of the European Conference on Noise Control, Prague, Czech Republic, 10–13 June 2012; pp. 926–931.

141. ISO. *Passenger Car, Truck, Bus and Motorcycle Tyres—Methods of Measuring Rolling Resistance*; ISO 18164; ISO: Geneva, Switzerland, 2005.

142. ISO. *Passenger Car Tyres—Methods of Measuring Rolling Resistance*; ISO 8767; ISO: Geneva, Switzerland, 1992.

143. ISO. *Truck and bus Tyres—Methods of Measuring Rolling Resistance*; ISO 9948; ISO: Geneva, Switzerland, 1992.

144. ISO. *Motorcycle Tyres—Method of Measuring Rolling Resistance*; ISO 13327; ISO: Geneva, Switzerland, 1998.

145. ISO. *Acoustics—Specification of Test Tracks for Measuring Noise Emitted by Road Vehicles and Their Tyres*; ISO 10844; ISO: Geneva, Switzerland, 2014.

146. Rasmussen, R. Measuring and modeling tire-pavement noise on various concrete pavement textures. *Noise Control Eng. J.* **2009**, *57*, 139–147. [CrossRef]

147. ASTM. *Standard Specification for P225/60R16 97S Radial Standard Reference Test Tire*; ASTM F2493; ASTM: West Conshohocken, PA, USA, 2014.

148. Ruhala, R.J. A Study of Tire/Pavement Interaction Noise Using Near-Field Acoustical Holography. Ph.D. Thesis, Pennsylvania State University, State College, PA, USA, 1999.

149. Donavan, P.R.; Lodico, D. Parameters affecting the noise performance of ASTM standard reference test tires. In *SAE Technical Papers*; SAE International: Warrendale, PA, USA, 2013; Volume 4.

150. Pope, J.; Reynolds, W.C. Tire noise generation: The roles of tire and road. In *SAE Technical Papers*; SAE International: Warrendale, PA, USA, 1976.

151. Li, T.; Feng, J.; Burdisso, R.; Sandu, C. The effects of tread pattern on tire pavement interaction noise. In Proceedings of the INTER-NOISE 2016—45th International Congress and Exposition on Noise Control Engineering: Towards a Quieter Future, Hamburg, Germany, 21–24 August 2016.

152. Li, T.; Burdisso, R.; Sandu, C. An Artificial Neural Network Model to Predict Tread Pattern-Related Tire Noise. In Proceedings of the SAE 2017 Noise and Vibration Conference and Exhibition, Grand Rapids, MI, USA, 12–15 June 2017. SAE Technical Paper 2017-01-1904.

153. Cao, P.; Yan, X.; Xiao, W.; Chen, L. A prediction model to coupling noise of tire tread patterns and road texture. In Proceedings of the 8th International Conference of Chinese Logistics and Transportation Professionals—Logistics: The Emerging Frontiers of Transportation and Development in China, Chengdu, China, 8–10 October 2008; American Society of Civil Engineers: Chengdu, China, 2008; pp. 2332–2338.

154. Alt, N.; Wolff, K.; Eisele, G.; Pichot, F. Fahrzeug Außen Geräuschsimulation (Vehicle exterior noise simulation). *Automob. Z.* **2006**, *108*, 832–836. [CrossRef]

155. Braun, M.E.; Walsh, S.J.; Horner, J.L.; Chuter, R. Noise source characteristics in the ISO 362 vehicle pass-by noise test: Literature review. *Appl. Acoust.* **2013**, *74*, 1241–1265. [CrossRef]

156. Hanson, D.I.; James, C.R.S.; Ne Smith, C. *Tire/Pavement Noise Study*; NCAT Report 04–02; NCAT: Greensboro, NC, USA, 2004; 49p.

157. Yong, C.; Wang, X.; Li, J.; Huang, Z. GA-BP Neural Network Based Tire Noise Prediction. *Adv. Mater. Res.* **2012**, *443–444*, 65–70.

158. Ge, J.; Fan, J.; Gu, Q.; Qian, R.; Youming, L. Design method and application of low noise tire. In Proceedings of the Symposium of International Rubber Conference 2004, Beijing, China, 21–25 September 2004.

159. Saemann, E.-U. Reducing tire/road rolling noise. Presented at the Conference Intelligent Tire Technology, Frankfurt, Germany, 29–30 November 2005; PowerPoint Presentation by Dr Saemann of NVH Engineering, Continental Tyres, Hanover, Germany.

160. Xie, K.-J. Method of Developing Tread Pattern. U.S. Patent US6514366 B1, 4 February 2003.

161. Oswald, L.J. Identifying the noise mechanisms of a single element of a tire tread pattern. In Proceedings of the National Conference on Noise Control Engineering: Applied Noise Control Technology, BT—Proceedings—NOISE-CON 81, Raleigh, NC, USA, 4–6 June 1981; pp. 53–56.

162. Oswald, L.J.; Arambages, A. The noise mechanisms of cross groove tire tread pattern elements. In *BT—Surface Vehicle Noise and Vibration Conference Proceedings*; Proceedings—Society of Automotive Engineers; SAE, GM Research Lab, Engineering, Mechanics Dep: Warren, MI, USA, 1985.

163. Chiu, J.-T.; Tu, F.-Y. Application of a pattern recognition technique to the prediction of tire noise. *J. Sound Vib.* **2015**, *350*, 30–40. [CrossRef]

164. Liljegren, K. Visual and Acoustic tyre Tread Design. Master's Thesis, Chalmers University of Technology, Gothenburg, Sweden, 2008.

165. Williams, T.A. Tire tread pattern noise reduction through the application of pitch sequencing. In *SAE Technical Papers*; SAE International: Warrendale, PA, USA, 1995.

166. Bandel, P.; Bergomi, R.; Monguzzi, C. Low Noise Sequence of Tread Elements for Vehicle Tires and Related Generation Method. U.S. Patent US5371685, 16 January 1994.

167. ISO. *Acoustics—Description, Measurement and Assessment of Environmental Noise—Part 2: Determination of Environmental Noise Levels*; ISO 1996-2; ISO: Geneva, Switzerland, 2007.

168. Ewart, E.S. Pneumatic Tire. *U.S. Patent* **1935**.

169. Varterasian, J.H. Quieting noise mathematically its application to snow tires. In *BT—Mid-Year Meeting, May 19, 1969–May 23, 1969*; SAE Technical Papers; SAE International, Research Labs., General Motors Corp: Warrendale, PA, USA, 1969.

170. Buddenhagen, F.E. Tire Casing with Noiseless Tread. U.S. Patent US2612928, 7 October 1952.

171. Landers, S.P. Spreading Noise Generated by load Supporting Elements. U.S. Patent US4327792, 4 May 1982.

172. Williams, T.A. Tire Pitch Sequencing for Reduced Tire Tread Noise. U.S. Patent US5314551, 24 May 1994.

173. Wei, Y.; Feng, Q.; Wang, H.; Kaliske, M. A hybrid numerical-experimental analysis for tire air-pumping noise with application to pattern optimization. *Noise Control Eng. J.* **2016**, *64*, 56–63. [CrossRef]

174. Michelin. Michelin Primacy 3 ST Tyres—Lasts Longer & Maximum Safety on Wet Roads. 2016. Available online: http://www.michelin.in/IN/en/tyres/products/primacy-3-st.html (accessed on 10 October 2018).

175. Dong, Y.; Tan, Y.; Liu, H.; Yang, L. Noise performance of drainage asphalt pavement. *Int. J. Pavement Res. Technol.* **2010**, *2*, 280–283.

176. Oshino, Y.; Mikami, T.; Ohnishi, H.; Tachibana, H. Investigation into road vehicle noise reduction by drainage asphalt pavement. *J. Acoust. Soc. Jpn.* **1999**, *20*, 75–84. [CrossRef]

177. Wang, G.-L.; Zhou, H.-C.; Yang, J.; Liang, C.; Jin, L. Influence of Bionic Non-smooth Surface on Water Flow in Antiskid Tire Tread Pattern. *J. Donghua Univ. Engl. Ed.* **2013**, *30*, 336–342.

178. Zhou, H. Investigate into Influence of Tire tread Pattern on Noise and Hydroplaning and Synchronously Improving Methods. Ph.D. Thesis, Jiangsu University, Zhejiang, China, 2013; pp. 1–178.

179. Ejsmont, J.A.; Sandberg, U.; Taryma, S. Influence of tread pattern on tire/road noise. In *Passenger Car Meeting, October 1, 1984–October 4, 1984*; SAE Technical Papers; Technical University of Gdansk, PolandSwedish Road and Traffic Research Institute, SAE International: Linkoeping, Sweden, 1984; 9p.

180. Ih, J.-G.; Oey, A. Effect of patterns on wave propagation and sound radiation over the tire surface. In Proceedings of the 41st International Congress and Exposition on Noise Control Engineering 2012, INTER-NOISE 2012, New York, NY, USA, 19–22 August 2012; Volume 2, pp. 1436–1441.

181. Domenichini, L.; Fracassa, A.; La Torre, F.; Loprencipe, G.; Ranzo, A.; Scalamandrè, A. Relationship between road surface characteristics and noise emission. In Proceedings of the First International Colloquium on Vehicle Tyre Road Interaction, Rome, Italy, 28 May 1999; Paper 99.03. pp. 1–22.

182. NZ Transport Agency. *Guide to State Highway Road Surface Noise*; NZ Transport Agency: Wellington, New Zealand, 2014.

183. Donavan, P.R. Comparative measurements of tire/pavement noise in Europe and the United States. *Noise News Int.* **2005**, *13*, 46–53. [CrossRef]

184. Mcghee, K. Virginia Quiet Pavement Study. In Proceedings of the 7th Symposium on Pavement Surface Characteristics, Presentation at SURF 2012, Norfolk, VA, USA, 19–22 September 2012.

185. Sandberg, U.; Ejsmont, J.A.; Gustavsson, E. *Tire/Road Noise on Rubberized Asphalt and Cement Concrete Surfaces in Sweden*; Swedish National Road and Transport Research Institute: Linköping, Sweden, 1990; 60p.

186. Li, M.; Molenaar, A.; van de Ven, M.; Huurman, R.; van Keulen, W. New Approach for Modelling Tyre/Road Noise. In Proceedings of the Inter-Noise 2009, Ottawa, ON, Canada, 23–26 August 2009.

187. Klein, P.; Cesbron, J. A 3D envelopment procedure for tyre belt radiated noise level prediction. In Proceedings of the INTER-NOISE 2016—45th International Congress and Exposition on Noise Control Engineering: Towards a Quieter Future, Hamburg, Germany, 21–24 August 2016; pp. 2230–2241.

188. Li, T. Tire-Pavement Interaction Noise (TPIN) Modeling Using Artificial Neural Network (ANN). Ph.D. Thesis, Virginia Tech, Blacksburg, VA, USA, 2017.

189. ISO. *Characterization of Pavement Texture by Use of Surface Profiles—Part 1: Determination of Mean Profile Depth*; ISO 13473-1; ISO: Geneva, Switzerland, 1997.

190. Huschek, S. Characterization of pavement surface texture and its influence on tire/road noise. In Proceedings of the Third International Symposium on Pavement Surface Characteristics, Christchurch, New Zealand, 3–4 September 1996.

191. Wayson, R.L. *NCHRP Synthesis 268—Relationship between Pavement Surface Texture and Highway Traffic Noise*; Transportation Research Board, National Academy Press: Washington, DC, USA, 1998; 94p.

192. Thrasher, D.B.; Miller, R.F.; Bauman, R.G. Effect of pavement texture on tire/pavement interaction noise. In *SAE Technical Papers*; SAE International: Warrendale, PA, USA, 1976.

193. Li, M.; van Keulen, W.; Ceylan, H.; Tang, G.; van de Ven, M.; Molenaar, A. Influence of Road Surface Characteristics on Tire-Road Noise for Thin-Layer Surfacings. *J. Transp. Eng.* **2015**, *141*, 04015024. [CrossRef]

194. Biermann, J.; von Estorff, O.; Petersen, S.; Schmidt, H. Computational model to investigate the sound radiation from rolling tires. *Tire Sci. Technol.* **2007**, *35*, 209–225. [CrossRef]

195. Hamet, J.-F.; Klein, P. Road texture and tire noise. In Proceedings of the Inter-Noise 2000, Nice, France, 27–30 August 2000; pp. 178–183.

196. Hanson, D.I.; Waller, B. *Evaluation Of The Noise Characteristics Of Minnesota Pavements*; Minnesota Department of Transportation: Saint Paulc, MN, USA, 2005.

197. Pinnington, R.J. A particle-envelope surface model for road–tyre interaction. *Int. J. Solids Struct.* **2012**, *49*, 546–555. [CrossRef]

198. Pinnington, R.J. Tyre-road contact using a particle-envelope surface model. *J. Sound Vib.* **2013**, *332*, 7055–7075. [CrossRef]

199. He, D.-C.; Wang, L. Texture features based on texture spectrum. *Pattern Recognit.* **1991**, *24*, 391–399. [CrossRef]

200. Lee, Y.G.; Lee, J.H.; Hsueh, Y.C. Texture classification using fuzzy uncertainty texture spectrum. *Neurocomputing* **1998**, *20*, 115–122. [CrossRef]

201. Wang, L.; He, D.-C. Texture classification using texture spectrum. *Pattern Recognit.* **1990**, *23*, 905–910. [CrossRef]

202. ISO. *Characterization of Pavement Texture by Use of Surface Profiles—Part 4: Spectral Analysis of Surface Profiles*; ISO/TS 13473-4; ISO: Geneva, Switzerland, 2008.

203. ISO. *Characterization of Pavement Texture by Use of Surface Profiles—Part 3: Specification and Classification of Profilometers*; ISO 13473-3; ISO: Geneva, Switzerland, 2002.

204. Dubois, G.; Cesbron, J.; Yin, H.P.; Anfosso-Ledee, F.; Duhamel, D. Statistical estimation of low frequency tyre/road noise from numerical contact forces. *Appl. Acoust.* **2013**, *74*, 1085–1093. [CrossRef]

205. ASTM. *Standard Test Method for Measuring Pavement Macrotexture Properties Using the Circular Track Meter*; ASTM E2157; ASTM: West Conshohocken, PA, USA, 2009.

206. Hamet, J.-F.; Klein, P. Use of a rolling model for the study of correlation between road texture and tire noise. In Proceedings of the 2001 International Congress and Exhibition on Noise Control Engineering, The Hague, The Netherlands, 28–30 August 2001.

207. McDaniel, R.; Shah, A.; Dare, T.; Bernhard, R. *Hot Mix Asphalt Surface Characteristics Related to Ride, Texture, Friction, Noise and Durability*; Purdue University: St. Paul, MN, USA, 2014.

208. Dare, T.; Bernhard, R. Predicting tire-pavement noise on longitudinally ground pavements using a nonlinear model. In Proceedings of the 38th International Congress and Exposition on Noise Control Engineering 2009, INTER-NOISE 2009, Ottawa, ON, Canada, 23–26 August 2009; Volume 1, pp. 405–415.

209. Sandberg, U.; Ejsmont, J.A. Texturing of cement concrete pavements to reduce traffic noise. *Noise Control Eng. J.* **1998**, *46*, 231. [CrossRef]

210. Rasmussen, R.; Karamihas, S.; Mun, E.; Chang, G. Relating pavement texture to tire-pavement noise. In Proceedings of the 35th International Congress and Exposition on Noise Control Engineering, INTER-NOISE 2006, Institute of Noise Control Engineering of the USA, Honolulu, HI, USA, 3–6 December 2006; Volume 1, pp. 422–431.

211. FHWA. *Technical Advisory T 5040.36—Surface Texture for Asphalt and Concrete Pavements*; FHWA: Washington, DC, USA, 2005.

212. Henry, J.J. *Evaluation of Pavement Friction Characteristics*; Transportation Research Board: Washington, DC, USA, 2000; Volume 291.

213. Flintsch, G.W.; de Leon, E.; McGhee, K.; Al-Qadi, I. Pavement Surface Macrotexture Measurement and Application. *Transp. Res. Rec. J. Transp. Res. Board* **2003**, *1860*, 168–177. [CrossRef]

214. ASTM. *Standard Test Method for Measuring Pavement Macrotexture Depth Using a Volumetric Technique*; ASTM E965; ASTM: West Conshohocken, PA, USA, 2006.

215. ASTM. *Standard Practice for Calculating Pavement Macrotexture Mean Profile Depth*; ASTM E1845; ASTM: West Conshohocken, PA, USA, 2009.

216. ISO. *Characterization of Pavement Texture by Use of Surface Profiles—Part 5: Determination of Megatexture*; ISO 13473-5; ISO: Geneva, Switzerland, 2009.

217. ISO. *Mechanical Vibration—Road Surface Profiles—Reporting of Measured Data*; ISO 8608; ISO: Geneva, Switzerland, 1995.

218. Barbosa, R.S. Vehicle dynamic response due to pavement roughness. *J. Braz. Soc. Mech. Sci. Eng.* **2011**, *33*, 302–307.

219. Stroup-Gardiner, M.; Brown, E.R. *Segregation in Hot-Mix Asphalt Pavements*; Report No. 441; Transportation Research Board: Washington, DC, USA, 2000.

220. Zhang, Y.; McDaniel, J.G.; Wang, M.L. Pavement macrotexture estimation using principal component analysis of tire/road noise. *Proc. SPIE Int. Soc. Opt. Eng.* **2014**, *9063*, 90630K.

221. Saykin, V.V. Pavement Macrotexture Monitoring through Sound Generated by the Tire-Pavement Interaction. Master's Thesis, Northeastern University, Boston, MA, USA, 2011.

222. Reyes, C.H.; Harvey, J. A method for predicting sound intensity noise levels using laboratory pavement cores. In Proceedings of the Noise-Con 2011, Portland, OR, USA, 25–27 July 2011; pp. 522–534.

223. Kohler, E. OBSI Testing. In Proceedings of the Presentation at Pavement Evaluation 2010, Roanoke, VA, USA, 25–27 October 2010.

224. ASTM. *Standard Practice for Computing International Roughness Index of Roads from Longitudinal Profile Measurements*; ASTM E1926; ASTM: West Conshohocken, PA, USA, 2008.

225. ASTM. *Standard Test Method for Measuring Road Roughness by Static Level Method*; ASTM E1364; ASTM: West Conshohocken, PA, USA, 2012.

226. Sayers, M.W.; Gillespie, T.D.; Paterson, W.D. *Guidelines for the Conduct and Calibration of Road Roughness Measurement*; World Bank Technical Paper No. 46; The World Bank: Washington, DC, USA, 1986.

227. ASME. *Surface Texture (Surface Roughness, Waviness, and Lay)*; ASME B46.1; ASME: New York; NY, USA, 2009.

228. Wullens, F.; Kropp, W.; Jean, P. Quasi-3D versus 3D contact modelling for tyre/road interaction. In Proceedings of the INTER-NOISE 04, Prague, Czech Republic, 22–25 August 2004; p. 3318.

229. Rasmussen, R.O.; Garber, S.I.; Fick, G.J.; Ferragut, T.R.; Wiegand, P.D. *How to Reduce Tire-Pavement Noise-Interim Better Practices*; Federal Highway Administration: Washington, DC, USA, 2008.

230. Kane, A. *Concrete Pavement Joints*; FHWA Technical Advisory T 5040.30; Federal Highway Administration: Washington, DC, USA, 1990.

231. Donavan, P. Influence of PCC Surface Texture and Joint Slap on Tire/Pavement Noise Generation. In Proceedings of the Noise-Con 2004, Baltimore, MD, USA, 12–14 July 2004; pp. 251–262.

232. Meiarashi, S.; Gagarin, N.; Coppage, T. Effect of transverse tines/grooves spacing on tire/pavement noise from aspect of annoyance caused by wailing. In Proceedings of the Inter-Noise 98, Christchurch, New Zealand, 16–18 November 1998; pp. 203–208.

233. Dare, T.; Bernhard, R.; Thornton, W. Effects of contraction joint width, fill condition, faulting and beveling on wheel-slap noise. *Noise Control Eng. J.* **2011**, *59*, 228–233. [CrossRef]

234. Dare, T.; Bernhard, R. Noise generation in contraction joints in Portland cement concrete. In Proceedings of the 24th National Conference on Noise Control Engineering 2010, Noise-Con 10, Held Jointly with the 159th Meeting of the Acoustical Society of America, Baltimore, MD, USA, 19–21 April 2010; Volume 1, pp. 561–572.

235. Marriner, D.; Wakefield, C. Modular expansion joint noise in B.C. In Proceedings of the 40th International Congress and Exposition on Noise Control Engineering 2011, INTER-NOISE 2011, Osaka, Japan, 4–7 September 2011; Volume 1, pp. 763–768.

236. Behzad, M.; Hodaei, M.; Alimohammadi, I. Experimental and numerical investigation of the effect of a speed bump on car noise emission level. *Appl. Acoust.* **2007**, *68*, 1346–1356. [CrossRef]

237. Sexton, T. Controlling expansion joint noise on the Tacoma narrows bridge in Washington State, USA. In Proceedings of the 40th International Congress and Exposition on Noise Control Engineering 2011, INTER-NOISE 2011, Osaka, Japan, 4–7 September 2011; Volume 1, pp. 734–739.

238. Glaeser, K.-P.; Schwalbe, G.; Zoller, M. Mitigation the noise emissions of vehicles travelling over bridge expansion joints. In Proceedings of the 40th International Congress and Exposition on Noise Control Engineering 2011, INTER-NOISE 2011, Osaka, Japan, 4–7 September 2011; Volume 1, pp. 753–762.

239. Wakefield, C.W.; Marriner, D.E. Analysis and control of bridge expansion joint croaking noise. *Can. Acoust. Acoust. Can.* **2011**, *39*, 138–139.

240. Tournour, M.A.; Cuschieri, J.M. Contribution to the overall noise level of the vibration of an open grid bridge deck. In Proceedings of the National Conference on Noise Control Engineering, Fort Lauderdale, FL, USA, 1–4 May 1994; pp. 105–110.

241. Cuschieri, J.M.; Gregory, S.; Tournour, M. Open grid bridge noise from grid and tire vibrations. *J. Sound Vib.* **1996**, *190*, 317–343. [CrossRef]

242. Meggers, D.A. *Effectiveness of Polymer Bridge Deck Overlays in Highway Noise Reduction*; Report Number KS-15-11; Kansas. Dept. of Transportation: Topeka, KS, USA, 2016.

243. Payne, A.R.; Scott, J.R. *Engineering Design with Rubber*; Interscience Publishers Inc.: New York, NY, USA, 1960.

244. Donavan, P.R. Effect of porous pavement on wayside traffic noise levels. *Trans. Res. Rec.* **2014**, *2403*, 28–36. [CrossRef]

245. Bérengier, M.C.; Stinson, M.R.; Daigle, G.A.; Hamet, J.F. Porous road pavements: Acoustical characterization and propagation effects. *J. Acoust. Soc. Am.* **1997**, *101*, 155. [CrossRef]

246. ASTM. *Standard Test Method for Effective Porosity and Effective Air Voids of Compacted Bituminous Paving Mixture Samples*; ASTM D7063/D7063M; ASTM: West Conshohocken, PA, USA, 2011.

247. AASHTO. *Theoretical Maximum Specific Gravity and Density of Hot Mix Asphalt (HMA)*; AASHTO T 209; AASHTO: Washington, DC, USA, 2011.

248. AASHTO. *Bulk Specific Gravity and Density of Compacted Hot Mix Asphalt (HMA) Using Automatic Vacuum Sealing Method*; AASHTO T 331; AASHTO: Washington, DC, USA, 2010.

249. Ongel, A.; Harvey, J. Pavement characteristics affecting the frequency content of tire/pavement noise. *Noise Control Eng. J.* **2010**, *58*, 563–571. [CrossRef]

250. Neithalath, N.; Weiss, J.; Olek, J. *Reducing the Noise Generated in Concrete Pavements through Modification of the Surface Characteristics*; R&D Serial No. 2878; Portland Cement Association: Skokie, IN, USA, 2005; 71p.

251. De Roo, F.; Gerretsen, E. TRIAS—Tyre road interaction acoustic simulation model. In Proceedings of the 29th International Congress and Exhibition on Noise Control Engineering, InterNoise 2000, Nice, France, 27–30 August 2000; Volume 4, pp. 2488–2496.

252. Olek, J.; Weiss, W.J.; Neithalath, N.; Marolf, A.; Sell, E.; Thornton, W.D. *Development of Quiet and Durable Porous Portland Cement Concrete Paving Materials*; University Transportation Centers Program, Report: SQDH-2003-5; Department of Transportation: Washington, DC, USA, 2003; 181p.

253. ISO. *Acoustics—Determination of Sound Absorption Coefficient and Impedance in Impedance Tubes—Part 1: Method Using Standing Wave Ratio*; ISO 10534-1; ISO: Geneva, Switzerland, 1996.

254. ISO. *Acoustics—Determination of Sound Absorption Coefficient and Impedance in Impedance Tubes—Part 2: Transfer-Function Method*; ISO 10534-2; ISO: Geneva, Switzerland, 1998.

255. ASTM. *Standard Test Method for Impedance and Absorption of Acoustical Materials Using a Tube, Two Microphones and a Digital Frequency Analysis System*; ASTM E1050; ASTM: West Conshohocken, PA, USA, 2012.

256. ISO. *Acoustics—Measurement of Sound Absorption Properties of Road Surfaces In Situ—Part 1: Extended Surface Method*; ISO 13472-1; ISO: Geneva, Switzerland, 2002.

257. ISO. *Acoustics—Measurement of Sound Absorption Properties of road Surfaces In Situ—Part 2: Spot Method for Reflective Surfaces*; ISO 13472-2; ISO: Geneva, Switzerland, 2010.

258. Rasmussen, R.O.; Bernhard, R.J.; Sandberg, U.; Mun, E.P. *The Little Book of Quieter Pavements*; Report No. FHWA-IF-08-004; The Transtec Group: Austin, TX, USA, 2007.

259. ISO. *Acoustics—Materials for Acoustical Applications—Determination of Airflow Resistance*; ISO 9053; ISO: Geneva, Switzerland, 1991.

260. ANSI/ASA. *American National Standard Method for Determining the Acoustic Impedance of Ground Surfaces*; ANSI/ASA S1.18; ASA: Melville, NY, USA, 2010.

261. Ren, R.; Gao, C. Improved porous noise reducing asphalt mixture design method. *Int. J. Pavement Res. Technol.* **2009**, *2*, 275–279.

262. Mogrovejo, D.E.; Flintsch, G.W.; De Leon Izeppi, E.D.; McGhee, K.K.; Burdisso, R.A. Short-term effect of pavement surface aging on tire-pavement noise measured with onboard sound intensity methodology. *Transp. Res. Rec.* **2014**, 17–27. [CrossRef]

263. Berge, T.; Storeheier, S.A. Low noise pavements in a Nordic climate. Results from a four year project in Norway. In Proceedings of the Inter-Noise 2009, Ottawa, ON, Canada, 23–26 August 2009; p. 1936.

264. Li, M.; Molenaar, A.A.A.; van de Ven, M.F.C.; van Keulen, W. Mechanical impedance measurement on thin layer surface with impedance hammer device. *J. Test. Eval.* **2012**, *40*, 860–865. [CrossRef]

265. Sandberg, U.; Goubert, L. PERSUADE—A European project for exceptional noise reduction by means of poroelastic road surfaces. In Proceedings of the 40th International Congress and Exposition on Noise Control Engineering 2011, INTER-NOISE 2011, Osaka, Japan, 4–7 September 2011; Volume 1, pp. 673–683.

266. Storeheier, S.A. *Preliminary Investigation on a Poroelastic Material Used as a Low Noise Road Surface*; SINTEF Foundation Ofscient and Industrial Research; Norwegian Institute of Technology: Trondheim, Norway, 1987; 41p.

267. Nilsson, N.-A.; Sylwan, O. New vibro-acoustical measurement tools for characterization of poroelastic road surfaces with respect to tire/road noise. In Proceedings of the Tenth International Congress on Sound and Vibration, Stockholm, Sweden, 7–10 July 2003; pp. 4343–4350.

268. Sandberg, U.; Goubert, L. Poroelastic road surface (PERS): A review of 30 years of R&D work. In Proceedings of the Inter-Noise 2011, Osaka, Japan, 4–7 September 2011.

269. Swieczko-Zurek, B. Biological hazards in low noise, poroelastic road surfaces. In Proceedings of the 20th International Congress on Sound and Vibration 2013, ICSV 2013, Bangkok, Thailand, 7–11 July 2013; Volume 4, pp. 2813–2818.

270. Bilawchuk, S. Tire noise assessment of asphalt rubber crumb pavement. *Can. Acoust.* **2005**, *33*, 37–41.

271. Ponniah, J.; Tabib, S.; Lane, B.; Raymond, C. Evaluation of the effectiveness of different mix types to reduce noise level at the tire/pavement interface. In Proceedings of the 2010 Annual Conference and Exhibition of the Transportation Association of Canada: Adjusting to New Realities, TAC/ATC 2010, Halifax, NS, Canada, 26–29 September 2010.

272. Beckenbauer, T. Akustische Eigenschaften von Fahrbahnoberflaechen. *Strasse+Autobahn* **2001**, *54*, 553–561.

273. Stenschke, R. Activities of the German Federal Environmental Agency to reduce tire/road noise. In Proceedings of the International Tire/Road Noise Conference 1990, Gothenburg, Sweden, 8–10 August 1990.

274. Liao, G.; Heitzman, M.; West, R.; Wang, S.; Ai, C. Temperature Effects on the Correlations between Tire-Pavement Noises and Pavement Surface Characteristics. *New Front. Road Airpt. Eng.* **2015**, 219–232.

275. AASHTO. *Standard Method of Test for Determining Dynamic Modulus of Hot-Mix Asphalt Concrete Mixtures*; AASHTO T 342; AASHTO: Washington, DC, USA, 2011.

276. Rao, C.; Von Quintus, H.L. *Determination of In Place Elastic Layer Modulus–Selection and Demonstration of Backcalculation Methodology and Practice: Phase I Interim Report, Long Term Pavement Performance Program*; Federal Highway Administration: Washington, DC, USA, 2012.

277. ASTM. *Standard Test Method for Measuring the P-Wave Speed and the Thickness of Concrete Plates Using the Impact-Echo Method*; ASTM C1383; ASTM: West Conshohocken, PA, USA, 2010.

278. Biligiri, K.P. Effect of pavement materials' damping properties on tyre/road noise characteristics. *Constr. Build. Mater.* **2013**, *49*, 223–232. [CrossRef]

279. Oshino, Y.; Mikami, T.; Tachibana, H. Study of road surface indices for the assessment of tire/road noise. In Proceedings of the Inter-Noise 2001, The Haag, The Netherlands, 28–30 August 2001.

280. ASTM. *Standard Test Method for Skid Resistance of Paved Surfaces Using a Full-Scale Tire*; ASTM E274/E274M; ASTM: West Conshohocken, PA, USA, 2011.

281. ASTM. *Standard Specification for Standard Rib Tire for Pavement Skid-Resistance Tests*; ASTM E501; ASTM: West Conshohocken, PA, USA, 2008.

282. ASTM. *Standard Specification for Standard Smooth Tire for Pavement Skid-Resistance Tests*; ASTM E524; ASTM: West Conshohocken, PA, USA, 2008.

283. ASTM. *Standard Test Method for Measuring Paved Surface Frictional Properties Using the Dynamic Friction Tester*; ASTM E1911; ASTM: West Conshohocken, PA, USA, 2009.

284. ASTM. *Standard Practice for Calculating International Friction Index of a Pavement Surface*; ASTM E1960; ASTM: West Conshohocken, PA, USA, 2011.

285. ASTM. *Standard Test Method for Measuring Surface Frictional Properties Using the British Pendulum Tester*; ASTM E303; ASTM: West Conshohocken, PA, USA, 2013.

286. Khaki, A.M.; Forouhid, A.E.; Zare, M. Comparison of the noise level and the skid resistance of asphalt pavement mixtures on road surface. *J. Meas. Eng.* **2015**, *3*, 71–76.

287. McDaniel, R.S.; Kowalski, K.J.; Shah, A.; Olek, J.; Bernhard, R.J. *Long-Term Performance of a Porous Friction Course*; FHWA/IN/JTRP-2009/22, Joint Transportation Research Program; Indiana Department of Transportation and Purdue University: West Lafayette, IN, USA, 2010.

288. Kowalski, K.J.; McDaniel, R.S.; Olek, J. *Identification of Laboratory Technique to Optimize Superpave HMA Surface Friction Characteristics*; FHWA/IN/JTRP-2010/06, Joint Transportation Research Program; Indiana Department of Transportation and Purdue University: West Lafayette, IN, USA, 2010.

289. Paje, S.E.; Bueno, M.; Teran, F.; Vinuela, U. Monitoring road surfaces by close proximity noise of the tire/road interaction. *J. Acoust. Soc. Am.* **2007**, *122*, 2636–2641. [CrossRef] [PubMed]

290. Ng, W.K.; Ng, P.S.; Hung, W.T. Measurement of tyre/road surface noise with close-proximity method in Hong Kong. In Proceedings of the INTER-NOISE 09, Ottawa, ON, Canada, 23–26 August 2009; p. 1178.

291. Chalupnik, J.D. Predicting Roadside Noise Levels from Near Field Trailer Measurements. In Proceedings of the Noise-Con 1996, Bellevue, WA, USA, 29 September–2 October 1996; Volume 1, pp. 61–66.

292. Dare, T.; Wulf, T.; Thornton, W.; Bernhard, R.J. *Acoustical Effects of Grinding and Grooving on Portland Cement Concrete Pavements*; Technical Report; The Institute for Safe, Quiet and Durable Highways: West Lafayette, IN, USA, 2009.

293. Bendsten, H.; Kohler, E.; Lu, Q. *Acoustic Aging of Asphalt Pavements—A California Danish Comparison*; Report 171; Road Directate, Danish Road Institute: Roskilde, Denmark, 2009.

294. Anderson, K.W.; Uhlmeyer, J.S.; Sexton, T.; Russell, M.; Weston, J. *Evaluation of Long-Term Pavement Performance and Noise Characteristics of the Next Generation Concrete Surface: Final Report*; Washington (State) Dept. of Transportation, WA-RD 767.2; Washington (State) Dept. of Transportatio: Olympia, WA, USA, 2014; 52p.

295. Hencken, J.; Haas, E.; Bennert, T. Using Tire/Pavement Interface Noise Results to Define Statistically Similar Bituminous Pavements in Massachusetts. In Proceedings of the Presented at 7th Symposium on Pavement Surface Characteristics: SURF 2012, Norfolk, VA, USA, 19–22 September 2012.

296. Kay, R.K. *Pavement Surface Condition Rating Manual*; Washington State Department of Transportation Report; Washington State Department of Transportation: Olympia, WA, USA, 1992.

297. MNDOT. *MnDOT Distress Identification Manual*; Report; Minnesota Department of Transportation, Office of Materials and Road Research: St. Paul, MN, USA, 2003.

298. Miller, J.S.; Bellinger, W.Y. *Distress Identification Manual for the Long-Term Pavement Performance Program*; FHWA Report No. FHWA-RD-03-031; FHWA: Washington, DC, USA, 2003.

299. Boullosa, R.R.; Lopez, A.P. Tra. *Noise Control Eng. J.* **1987**, *29*, 54. [CrossRef]

300. Descornet, G. Vehicle noise emission on wet road surfaces. In Proceedings of the INTER-NOISE 00, Nice, France, 27–30 August 2000; p. 4968.

301. Bergmann, M. Noise generation by tire vibrations. In Proceedings of the INTER- NOISE 80, Miami, FL, USA, 8–10 December 1980; p. 239.

302. Kongrattanaprasert, W.; Nomura, H.; Kamamura, T.; Ueda, K. Automatic detection of road surface states from tire noise using neural network analysis. *IEEJ Trans. Ind. Appl.* **2010**, *130*, 920–925. [CrossRef]

303. Kocak, S.; Kutay, M.E. Relationship between Material Characteristics of Asphalt Mixtures and Highway Noise. In *TRB 91st Annual Meeting Compendium of Papers*; Compendium of Papers, Paper No. 12–4309; National Research Council: Washington, DC, USA, 2012.

304. Biligiri, K.P. Asphalt Mixtures' Properties Indicative of Tire/Pavement Noise. Ph.D. Thesis, Arizona State University, Tempe, AZ, USA, 2008.

305. Sohaney, R.; Rasmussen, R.; Seybert, A.; Donavan, P. New ISO test track specification for measuring tire and vehicle noise. *Sound Vib.* **2012**, *46*, 9–14.

306. Moore, D. Revised ISO 10844 Test Surface: Technical Principles. *SAE Int. J. Passeng. Cars Mech. Syst.* **2011**, *4*, 1126–1131. [CrossRef]

307. Van Blokland, G.; Van Leeuwen, M. Efficiency of the combined application of silent tyres and silent road surfaces. In Proceedings of the 39th International Congress on Noise Control Engineering 2010, INTER-NOISE 2010, Lisbon, Portugal, 13–16 June 2010; Volume 5, pp. 3469–3478.

308. Sandberg, U. Semi-generic temperature corrections for tyre/road noise. In Proceedings of the INTER-NOISE 04, Prague, Czech Republic, 22–25 August 2004; p. 3302.

309. Kuijpers, A.H.W.M. *Further Analysis of the Sperenberg Data—Towards a Better Understanding of the Processes Influencing Tire/Road Noise*; Report No. M+P.MVM.99.3.1 rev. 1; MP Consulting Engineers: Hertogenbosch, The Netherlands, 2001.

310. Konishi, S.; Fujino, T.; Tomita, N.; Sakamoto, M. Temperature effect on tire/road noise. In Proceedings of the International Conference on Noise Control Engineering, Newport Beach, CA, USA, 10–12 July 1995; Volume 1, p. 147.

311. Anfosso-LédéE, F.; Pichaud, Y. Temperature effect on tyre-road noise. *Appl. Acoust.* **2007**, *68*, 1–16. [CrossRef]

312. Nilsson, N.-A.; Bennerhult, O.; Soderqvist, S. External tire/road noise: its generation and reduction. In *Proceedings of the Inter-Noise 80. Noise Control for the 80's. Proceedings of the 1980 International Conference on Noise Control Engineering*; Miami, FL, USA, 8–10 December 1980, pp. 245–252.

313. EEC. *Tyre Noise: Legal Requirements*; EC Directive (2001/43/EC); United Nations Economic Commission for Europe: Geneva, Switzerland, 2001.

314. SAE. Sound Level Of Highway Truck Tires. *SAE J.* **2014**, *57*. [CrossRef]

315. AASHTO. *Standard Method of Test for Measurement of Tire/Pavement Noise Using the On-Board Sound Intensity (OBSI) Method*; AASHTO TP 76; AASHTO: Washington, DC, USA, 2013.

316. Jabben, J. Temperature effects on road traffic noise measurements. In Proceedings of the 40th International Congress and Exposition on Noise Control Engineering 2011, INTER-NOISE 2011, Osaka, Japan, 4–7 September 2011; Volume 1, pp. 552–556.

317. Bae, A.; Stoffels, S.M.; Lee, S.W. Observed Effects of Subgrade Moisture on Longitudinal Profile. In *TRB 85th Annual Meeting Compendium of Papers CD-ROM*; Paper No. 06-2312; National Research Council: Washington, DC, USA, 2006.

318. Donavan, P.R. Investigations of the influence of lower frequency aerodynamic noise on interior cruise and exterior pass-By sound levels. In *SAE Technical Papers*; SAE International: Warrendale, PA, USA, 2012; Volume 5.

319. Cantrell, D. *Airborne Tire Noise Generation—The Effects of Axle Weight, Tire Inflation Pressure, and Suspension Alignment*; Noise & Vibration Laboratory, General Motors Proving Ground: São Paulo, Brazil, 1988.

320. Graham, W.R. Influence of tire geometry on the horn effect. In Proceedings of the 41st International Congress and Exposition on Noise Control Engineering 2012, INTER-NOISE 2012, New York, NY, USA, 19–22 August 2012; Volume 8, pp. 6995–7008.

321. Oldenettel, H.; Koster, H.J. Test procedure for the quantification of rolling tire belt vibrations. *Veh. Syst. Dyn.* **1997**, *27*, 37–49. [CrossRef]

322. Hung, W.-T.; Lam, Y.-K.; Ng, C.-F.; Leung, R.C.-K. The impacts of tyre hardness and tread depth on tyre/road noise. In Proceedings of the 20th International Congress on Sound and Vibration 2013, ICSV 2013, Bangkok, Thailand, 7–11 July 2013; Volume 4, pp. 2846–2852.

323. Thrasher, D.B. Effect of tread wear on tire/pavement interaction noise. In Proceedings of the Inter-Noise 80. Noise Control for the 80's. Proceedings of the 1980 International Conference on Noise Control Engineering, Miami, FL, USA, 8–10 December 1980; pp. 277–280.

324. Spelman, R.H. Truck tires—Effects of design and construction on wear and noise. In *SAE Technical Papers*; SAE International: Warrendale, PA, USA, 1963.

325. Sandberg, U.; Glaeser, K.-P. Effect of tyre wear on noise emission and rolling resistance. In Proceedings of the INTER-NOISE 08, Shanghai, China, 26–29 October 2008; p. 4066.

326. Raabe, R.C.; Burche, I. Retreaded truck tire noise tests. In *BT—Truck Meeting, November 4, 1974–November 7, 1974*; SAE Technical Papers; Bandag, Inc.: Muscatine, IA, USA, 1974.

327. Hasebe, M. Experimental study of the noise generated by a passenger automobile equipped with studded and regular snow tyres. *Appl. Acoust.* **1984**, *17*, 247–254. [CrossRef]

328. AASHTO. *Effects of Studded Tires*; TRB/NCHRP/SYN-32; Transportation Research Board: Washington, DC, USA, Federal Highway Administration: Washington, DC, USA; American Association of State Highway and Transportation Officials: Washington, DC, USA; 1975; 58p.

329. Liu, Y.; Li, T.; Liu, Y.; Su, Y. Optimize the Structure Parameters of Tread Pattern Based on the Fuzzy Genetic Arithmetic. In Proceedings of the 2010 International Conference on Measuring Technology and Mechatronics Automation (ICMTMA 2010), Piscataway, NJ, USA, 13–14 March 2010; Volume 2, pp. 860–863.

330. Sandberg, U.; Mioduszewski, P. Gaining extra noise reduction and lower rolling resistance by grinding a porous asphalt pavement. In Proceedings of the 41st International Congress and Exposition on Noise Control Engineering 2012, INTER-NOISE 2012, New York, NY, USA, 19–22 August 2012; Volume 8, pp. 6958–6969.

331. Van Blokland, G.-J.; Von Meier, A. Reducing tyre/road noise with porous road surfaces and the effect of tyre choice. In *SAE Technical Papers*; SAE International: Warrendale, PA, USA, 1993.

332. Sachakamol, P.; Dai, L. Impact of porous pavement characteristics on tire/pavement noise emission from ARC roads. In Proceedings of the 17th International Congress on Sound and Vibration 2010, ICSV 2010, Cairo, Egypt, 18–22 July 2010; Volume 4, pp. 2464–2473.

333. Crocker, M.J.; Hanson, D.; Li, Z.; Karjatkar, R.; Vissamraju, K.S. Measurement of acoustical and mechanical properties of porous road surfaces and tire and road noise. *Transp. Res. Rec.* **2004**, *1891*, 16–22. [CrossRef]

334. Rochat, J.L.; Donavan, P.; Seybert, A.; Dare, T. Pavement sound absorption measurements in the U.S. In Proceedings of the 41st International Congress and Exposition on Noise Control Engineering 2012, INTER-NOISE 2012, New York, NY, USA, 19–22 August 2012; Volume 3, pp. 2612–2626.

335. Seybert, A.F.; Han, J. Measurement of pavement absorption using ISO 13472-2. In Proceedings of the European Conference on Noise Control, Paris, France, 29 June–4 July 2008; pp. 4907–4911.

336. Hubelt, J.; Bartolomaeus, W.; Wellner, F. On the correlation between motor vehicle noise levels and in situ measurement data of airflow resistance, water permeability and sound absorption coefficient of open porous asphalts. In Proceedings of the 35th International Congress and Exposition on Noise Control Engineering, INTER-NOISE 2006, Institute of Noise Control Engineering of the USA, Honolulu, HI, USA, 3–6 December 2006; Volume 2, pp. 1119–1123.

337. Altreuther, B.; Beckenbauer, T. Dynamic measurement of air flow resistance. In Proceedings of the EURONOISE 2006—The 6th European Conference on Noise Control: Advanced Solutions for Noise Control, Tampere, Finland, 30 May–1 June 2006.